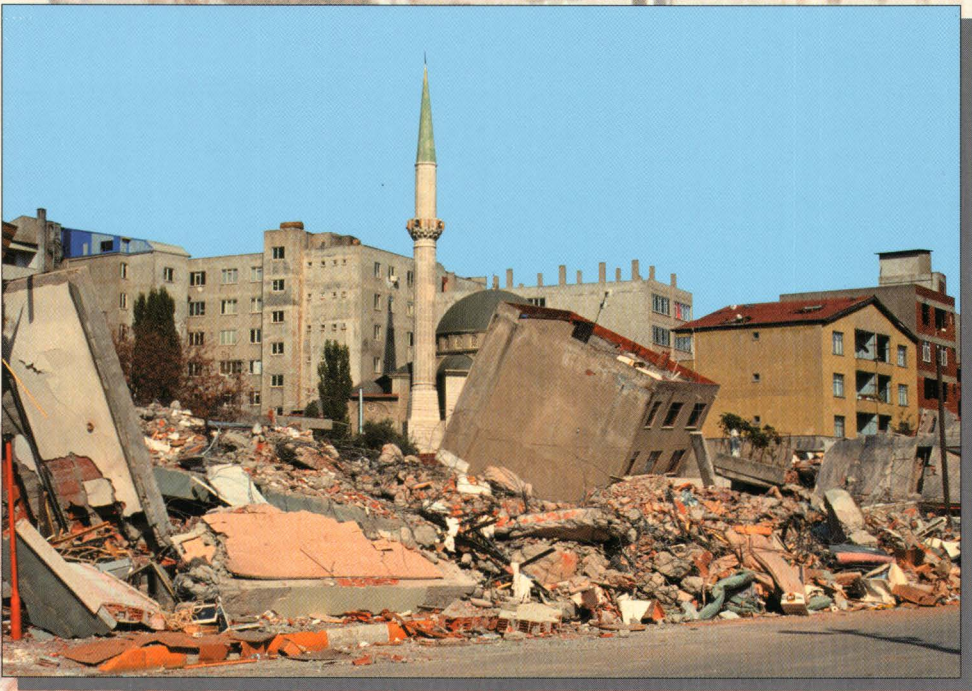


Implications for Earthquake Risk Reduction in the United States from the Kocaeli, Turkey, Earthquake of August 17, 1999



U.S. Geological Survey Circular 1193

U.S. Department of the Interior
U.S. Geological Survey

Cover: Damage in Korfez, Turkey, following the August 17 Kocaeli earthquake.

Photograph by Charles Mueller

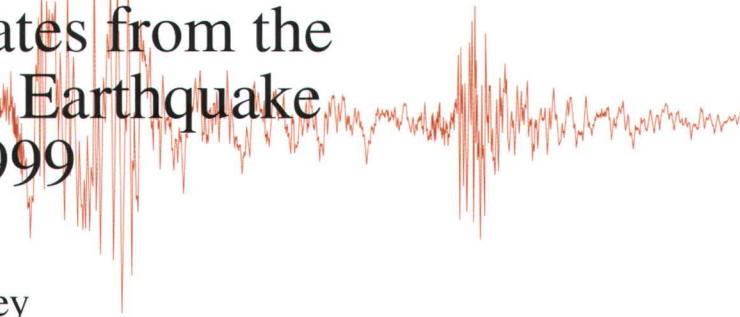
Cover design by Carol A. Quesenberry



NIST

Field investigations were coordinated with the U.S. Army Corps of Engineers and National Institute of Standards and Technology

Implications for Earthquake Risk Reduction in the United States from the Kocaeli, Turkey, Earthquake of August 17, 1999

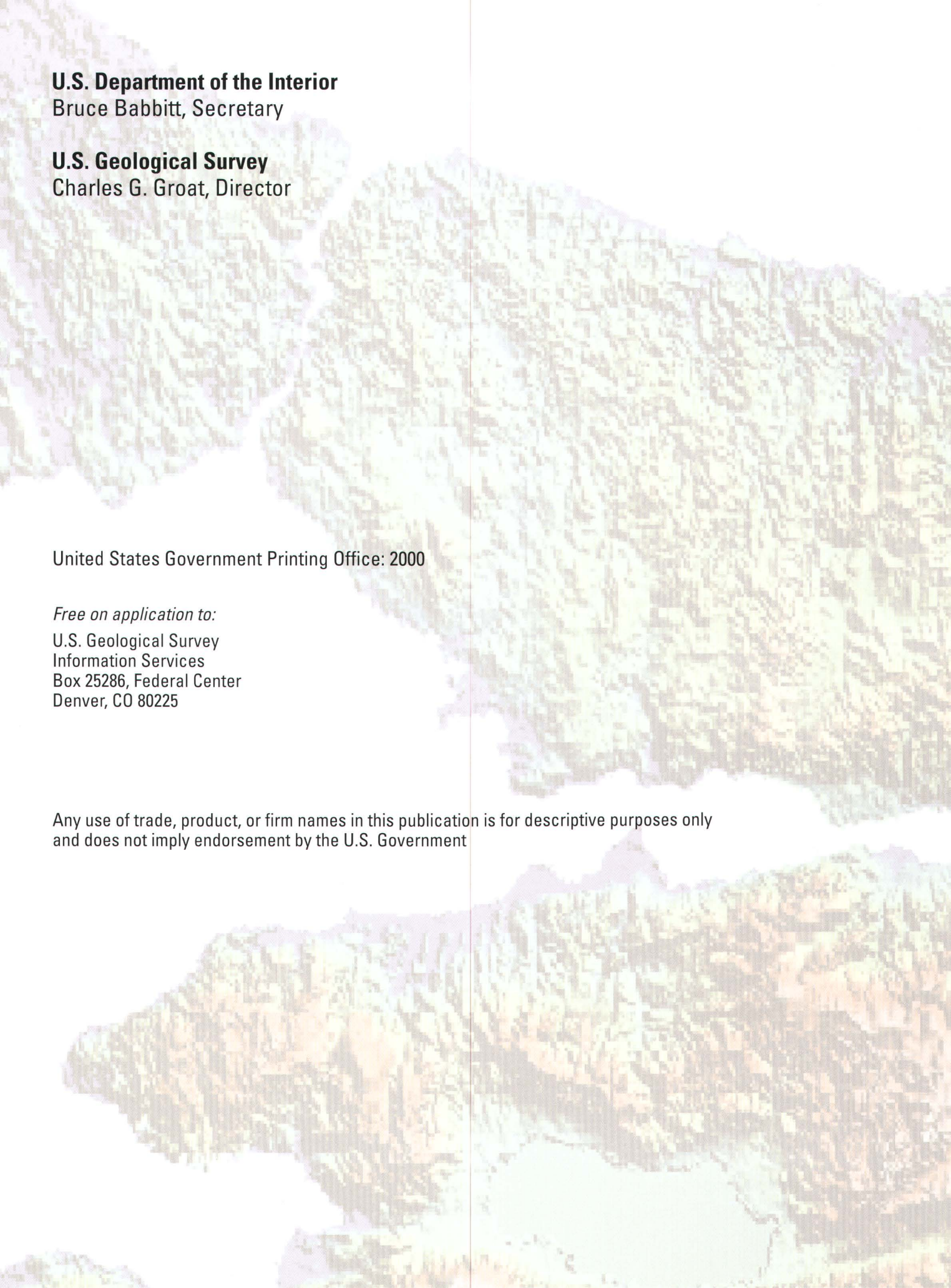


By U.S. Geological Survey



U.S. Geological Survey Circular 1193

U.S. Department of the Interior
U.S. Geological Survey



U.S. Department of the Interior

Bruce Babbitt, Secretary

U.S. Geological Survey

Charles G. Groat, Director

United States Government Printing Office: 2000

Free on application to:

U.S. Geological Survey
Information Services
Box 25286, Federal Center
Denver, CO 80225

Any use of trade, product, or firm names in this publication is for descriptive purposes only and does not imply endorsement by the U.S. Government

Contributors

Thomas L. Holzer, Scientific Editor, U.S. Geological Survey

Aykut A. Barka, Istanbul Technical University, Turkey

David Carver, U.S. Geological Survey

Mehmet Çelebi, U.S. Geological Survey

Edward Cranswick, U.S. Geological Survey

Timothy Dawson, San Diego State University and Southern California Earthquake Center

James H. Dieterich, U.S. Geological Survey

William L. Ellsworth, U.S. Geological Survey

Thomas Fumal, U.S. Geological Survey

John L. Gross, National Institute of Standards and Technology

Robert Langridge, U.S. Geological Survey

William R. Lettis, William Lettis & Associates

Mark Meremonte, U.S. Geological Survey

Charles Mueller, U.S. Geological Survey

Richard S. Olsen, Engineer Research and Development Center, U.S. Army Corps of Engineers

Oguz Ozel, Kandilli Observatory and Earthquake Research Institute, Bogazici University, Turkey

Tom Parsons, U.S. Geological Survey

Long T. Phan, National Institute of Standards and Technology

Thomas Rockwell, San Diego State University and Southern California Earthquake Center

Erdal Safak, U.S. Geological Survey

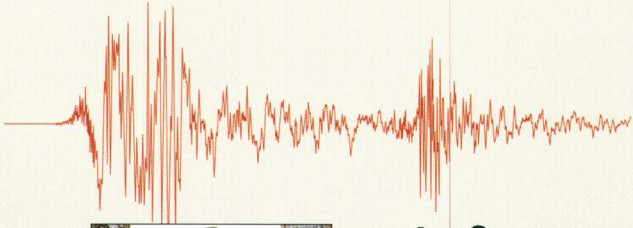
Ross S. Stein, U.S. Geological Survey

Heidi Stenner, U.S. Geological Survey

Shinji Toda, Earthquake Research Institute, University of Tokyo, Japan

Selcuk Toprak, U.S. Geological Survey

Contents



1 Summary



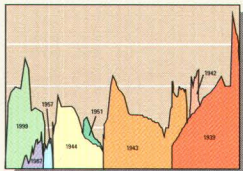
3 Introduction



5 The Earthquake



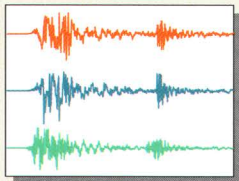
9 Geologic Setting and Earthquake History



11 Earthquake Forecasts



13 Surface Faulting



21 Ground Shaking

21 Main-Shock Observations



31 Implications of Aftershock Observations



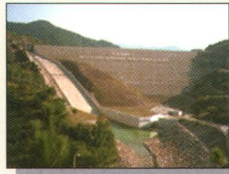
37 Liquefaction

41 Performance of the Built Environment

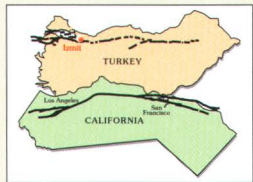
41 Buildings



47 Trans European Motorway (TEM)



51 Earth Dams



55 Implications for the United States



61 Acknowledgments



63 References

Summary



The moment magnitude (M_W) 7.4 Kocaeli, Turkey, earthquake struck the Kocaeli province of northwestern Turkey on Tuesday, August 17, 1999, at 3:02 a.m. local time. The cause of the earthquake was the sudden breakage, or rupture, of the Earth's crust along a western branch of the 1,500-km-long North Anatolian fault system. The total length of the fault rupture was about 110 km. The region hit by the earthquake is the industrial heartland and the most densely populated section of Turkey. According to official Turkish government estimates, the earthquake caused 17,127 deaths and 43,953 injuries, and displaced more than 250,000 people. Approximately 121 tent cities were required for emergency housing. Approximately 214,000 residential units and 30,500 business units were lightly to heavily damaged.

Most of the collapsed and damaged buildings were of reinforced concrete construction. Their poor performance was due primarily to the poor quality of construction and failure to enforce the local building code. Peak ground accelerations recorded close to the fault were below average for a M_W 7.4 event. The earthquake's strong velocity pulse and long duration, however, were important factors in the collapse of and damage to residences.

Immediately following the earthquake, the USGS was invited by the Kandilli Observatory and Earthquake Research Institute of Bogazici University in Istanbul, Turkey, to assist in its post-earthquake investigations. Teaming up with representatives from the National Institute of Standards and Technology and the U.S. Army Corps of Engineers, the reconnaissance teams documented the following implications for earthquake risk reduction in the United States.

- *Large-scale human disaster:* Of all natural disasters, large-magnitude earthquakes in urban areas are almost unique in their ability to cause large-scale human suffering and property loss. The Kocaeli earthquake damaged many homes and displaced more than a quarter of a million people. Earthquake loss models predict that tragedies of comparable scope are possible here in the United States.
- *Building collapse hazard:* More than 20,000 reinforced concrete buildings with little or no ductility are estimated to have collapsed in the Kocaeli earthquake. Much of the building stock in the United States was constructed before the importance of ductility, the ability to deform without catastrophic loss of strength, was fully appreciated. In the Eastern United States most reinforced concrete structures, including both buildings and bridges, have little or no ductility. This leaves the United States vulnerable to the catastrophic collapse of large numbers of buildings and bridges when they are shaken by the oscillatory motion of large earthquakes.
- *Earthquake monitoring systems:* A delayed reaction by government emergency response officials in Turkey to the earthquake disaster may have been due in part to the inability of the local seismic monitoring network to determine a reliable seismic magnitude and shaking intensities for the Kocaeli earthquake. Near real-time warnings using modern digital technology are now available and can identify precisely both the size and location of a large earthquake within minutes of its occurrence as well as the distribution of shaking intensity.

- *Earthquake forecasting:* The North Anatolian fault system is a close analog of the San Andreas fault system in California. The Kocaeli earthquake was the tenth in a systematic westward progression of earthquakes along 1000 km of the North Anatolian fault since 1939. Understanding how these earthquakes interacted may be useful for improving probabilistic earthquake forecasts in the United States. The November 12, 1999, M_W 7.1 earthquake, which was near Düzce at the eastern end of the August surface rupture, occurred in an area where the Kocaeli earthquake is estimated to have increased the earthquake potential by increasing stress on the fault.
- *Permanent ground deformation hazards:* Although earthquake shaking typically causes more than 90 percent of the loss associated with earthquakes directly, earthquake-induced permanent deformation or shifting of the ground can be more devastating to structures locally. Three types of permanent ground deformation were noteworthy in the Kocaeli earthquake: liquefaction, surface faulting, and densification of dry approach fills on the Trans European Motorway. Liquefaction, the transformation of solid material into liquidlike material, caused many buildings to sink into the ground. The sinking of buildings suggests a failure mechanism that may be very important to river levee systems in the United States, which are typically built in areas susceptible to liquefaction. This hazard compounds the already formidable challenge of dealing with the extensive potential for static failures of levee systems in the United States. Liquefaction of silts in Turkey has important implications for earth dams founded on alluvial foundations around the world. Although earth dams in Turkey performed well, the bearing capacity failures of buildings indicates low-strength silt foundations beneath earth dams can liquefy and cause the embankment to sink or rotate into the foundation. Surface faulting damaged many buildings as well as the modern Trans European Motorway, which was built to the same standard as American highway systems. Densification of dry approach fills was extensive along the Trans European Motorway and required its closing to resurface much of the roadway surface. Permanent ground deformation is not considered by the current code for highway and bridge design in the United States.



Introduction



The Kocaeli, Turkey, earthquake struck near the city of Izmit on August 17, 1999. According to official government estimates (as of October 19, 1999), it killed 17,127, and injured more than 43,953 people. Estimates of property losses (as of September 14, 1999) according to the World Bank range from \$3 to \$6.5 billion, which is equivalent to 1.5 to 3.3 percent of the Gross National Product of Turkey. It was the most devastating earthquake to strike Turkey since the 1939 Erzincan earthquake killed 30,000 people. Immediately following the Kocaeli earthquake, the Kandilli Observatory and Earthquake Research Institute of Bogazici University in Istanbul, Turkey, invited the U.S. Geological Survey (USGS) to assist in its post-earthquake investigation. In addition to assisting Turkish colleagues, the invitation provided an opportunity to learn lessons for reducing the risk of earthquakes in the United States. The USGS team coordinated its efforts in Turkey with representatives from the Engineer Research and Development Center of the U.S. Army Corps of Engineers and the National Institute of Standards and Technology.

It was immediately recognized that the Kocaeli earthquake, which occurred on the North Anatolian fault system, might provide useful insight into the seismic implications of the geologic record preserved along the San Andreas fault system in California. Thorough mapping of the surface faulting in Turkey, thus, had high priority. Predicting where and how frequently faults

Ductility: *The property of a material to deform without catastrophic loss of strength.*

Liquefaction: *The process by which sandy wet earth materials become fluidlike when shaken by earthquakes.*

will rupture is at the core of earthquake risk reduction. The similarity of these two major fault systems had prompted joint scientific studies for more than 30 years. Members of the USGS team also concentrated on documenting ground shaking and analyzing how local geology controlled the patterns of damage. Representatives from the National Institute of Standards and Technology documented

construction damage and drew implications for engineering design practice. While it quickly became apparent that construction quality and the failure to enforce local building codes were major contributors to damage, aspects of the damage are important to the United States. These include the collapse of reinforced concrete buildings with little or no ductility and liquefaction failures of building foundations. Representatives from the U.S. Army Corps of Engineers visited major earth dams in the epicentral region, all of which performed excellently.

The Kocaeli earthquake struck ten years after the Loma Prieta, California, earthquake, and five and four years, respectively, after the devastating urban earthquakes in Northridge, California, and Kobe, Japan. Each of these earthquakes has affected how we mitigate the risk of earthquakes. The Loma Prieta, California, earthquake, striking at the south edge of the San Francisco Bay region, was the first earthquake to cause significant damage in a major urban region in the United States since the enactment of the National Earthquake Hazards Reduction Program in 1977 (U.S. Geological Survey, 1989). It prompted intense scientific scrutiny and reinvigorated mitigation efforts in California; approximately \$2.5 billion was spent to retrofit bridges in the State highway system. The 1994 Northridge, California, earthquake, on the north edge of the Los Angeles metropolitan area (U.S. Geological Survey, 1996), cost more than \$12.5 billion in insured property loss and prompted a revolution in the earthquake insurance industry in the United States. In California, a public-private corporation, the California Earthquake Authority, was established to provide most of the residential earthquake insurance in California. Nationally, the insurance sector was prompted to base insurance premiums on more rigorous estimates of nationwide seismic risk using models developed by earthquake scientists and engineers. The 1995 Hyogoken-Nambu, Japan, earthquake caused \$100 billion in total property loss in the Kobe area. It further demonstrated the potential of urban earthquakes to cause extraordinary property losses (National Institute of Standards and Technology, 1996).

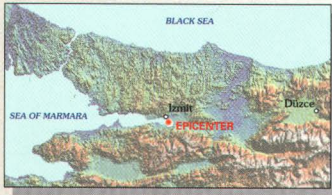


Figure 1. The heavy damage to residences required the use of 113,869 tents in 121 tent cities for temporary shelter. *Photographs by Thomas L. Holzer.*

Now, ten years after the Loma Prieta earthquake, the Kocaeli earthquake has again demonstrated the awesome potential of large earthquakes and particularly the immense human suffering that can occur when an earthquake strikes in an urban area. In Turkey, more than 250,000 people were forced out of their damaged homes and into huge tent encampments. Tent cities were established both next to collapsed and damaged homes and in open fields outside of the cities (fig. 1). Long lines of people waiting for food were a constant reminder of their dependency on urban infrastructure.

Tragedy, however, can be an opportunity if we learn from it. The challenge now is to learn from the Kocaeli earthquake. The contributors to this report hope that the memory of the people who died in the Kocaeli earthquake will inspire renewed efforts to mitigate efforts from future earthquakes. This report summarizes implications for the United States drawn from findings by teams from the U.S. Geological Survey, National Institute of Standards and Technology, and U.S. Army Corps of Engineers Engineer Research and Development Center.

The Earthquake



The moment magnitude (M_W) 7.4 Kocaeli, Turkey, earthquake struck the Kocaeli province of northwestern Turkey on Tuesday, August 17, 1999, at 3:02 a.m. local time. The cause of the earthquake was the sudden breakage, or rupture, of the Earth's crust along a western branch of the 1,500-km-long North Anatolian fault system. The epicenter of the earthquake, the location on the ground surface above where the faulting began, was at lat 40.70° N., long 29.91° E. according to the Earthquake Research Department of the Directorate for Disaster Affairs of the Ministry of Public Works and Settlement. This is about 7 km southeast of the city of Izmit and 15 km east of the town of Gölçük. The earthquake nucleated at a depth of about 15.9 km beneath the ground surface. From the point at which faulting began, the fault rupture extended upward to the ground surface and for many tens of kilometers both east and west, producing strong ground shaking along its entire length. The total length of the fault rupture is about 110 km.

The region hit by the earthquake is the industrial heartland and the most densely populated section of Turkey. According to official government figures (as of October 19, 1999) the earthquake caused 17,127 deaths and 43,953 injuries, and left more than 250,000 people homeless. An estimated 214,000 residential units and 30,500 business units either collapsed or were lightly to heavily damaged. Figure 2 shows fatalities and damaged residential units on a map of northwest Turkey. The heavy damage to residences required the use of 113,869 tents in 121 tent cities for temporary shelter. The region of heaviest damage extended from Yalova and Korfez to the town of Düzce, which is 100 km east of the epicenter. Most of the damage and fatalities were in towns located on the narrow flat shorelines of the Sea of Marmara. There also was heavy damage and loss of life in Adapazari, which is in the Sakarya valley. Anomalous damage, because it was isolated, occurred in the Avcilar district of Istanbul, west of the epicenter about 80 km from the end of the causative fault rupture.

Maximum amplitudes of accelerations recorded by the three strong motion stations closest to the fault rupture, which were within 7.5 km of the rupture, were smaller than is usually generated by a M_W 7.4 event. Recordings of the earthquake at two stations close to the fault indicate it had a strong velocity pulse and was of long duration, which were important factors in the damage to buildings. Recorded accelerations and computed velocities and displacements from the two strong motion stations are shown on figures 3 and 4. The velocity and the displacement records show the impulsive character of the ground shaking.

Strong motion: Earthquake shaking of sufficient intensity to cause damage to buildings and other structures.

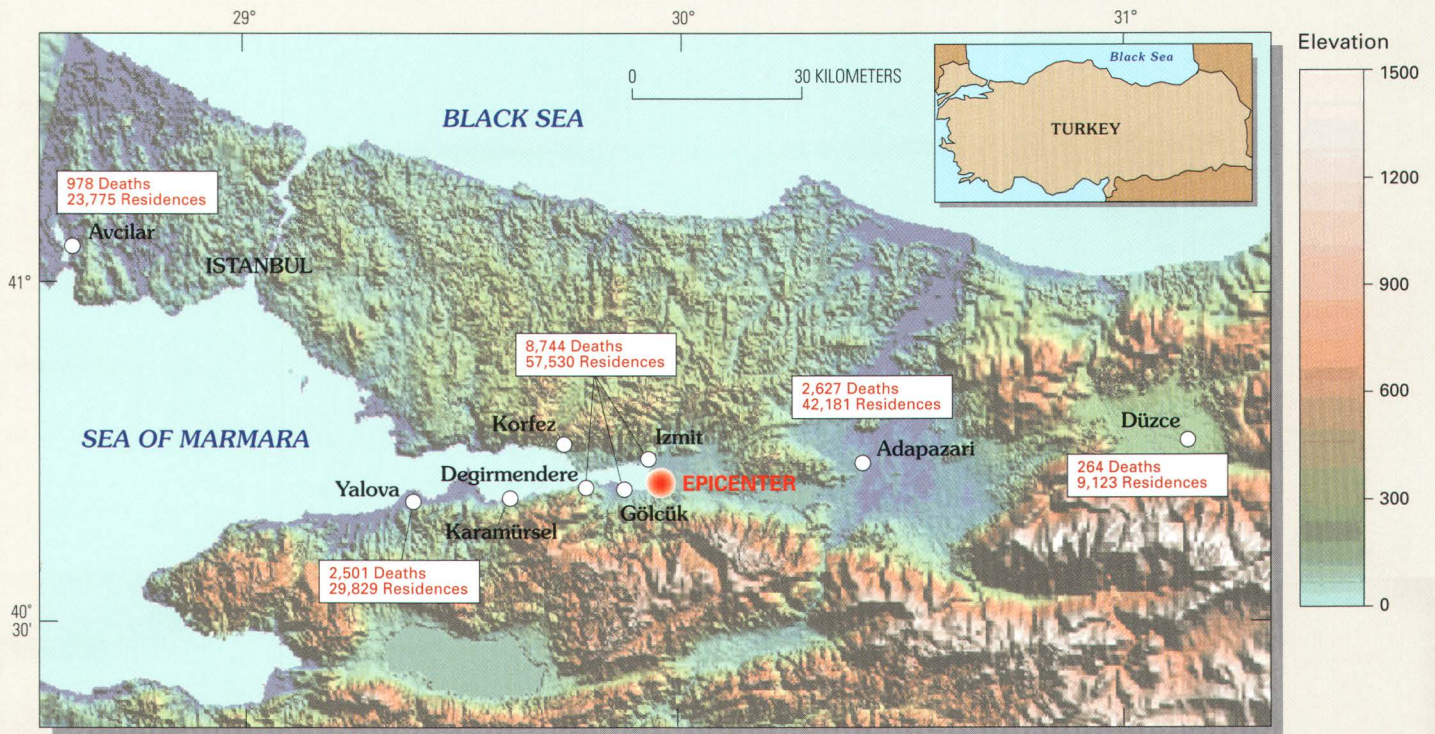


Figure 2. Major cities and towns in Turkey that experienced significant damage to residential units and loss of life during the Kocaeli earthquake. Upper number is fatalities; lower number is lightly to heavily damaged residential units. (Statistics from the Prime Ministry of Turkey, Crisis Management Center, September 12, 1999).

Although the M_W 7.4 was the magnitude finally adopted by all parties involved in the earthquake investigation, the wide range in magnitudes initially reported for the earthquake played a role in the controversy in Turkey that arose over the Turkish government's handling of the August 17, 1999, disaster. The magnitudes were used by the Turkish press to symbolize perceived government ineptitude in its postearthquake response. The USGS National Earthquake Information Center reported a surface wave magnitude (M_S) of 7.8 in the hours after the earthquake, during a time period when Kandilli Observatory, the Turkish institution that monitors the epicentral region, was reporting that the earthquake had a duration magnitude (M_d) of 6.7. In general, the M_S of an earthquake, which is based on the amplitudes of long-period seismic waves, would be a more reliable measure of the destructive potential of an earthquake than would the M_d , which is based on the duration of shaking. However, Kandilli Observatory personnel were forced to rely on the M_d , because many of the seismometers in the Kandilli network had gone off scale, and the

amplitudes of seismic waves could not be accurately read. Although a magnitude 6.7 earthquake is still recognized by seismologists as having high destructive potential, there was speculation in the press that reporting of the seemingly low duration magnitude delayed recognition of the seriousness of the disaster in the epicentral region, which had lost most of its telecommunication capability. The delay highlights the utility of digital seismic monitoring networks that transmit near real time announcements of potentially devastating earthquakes.

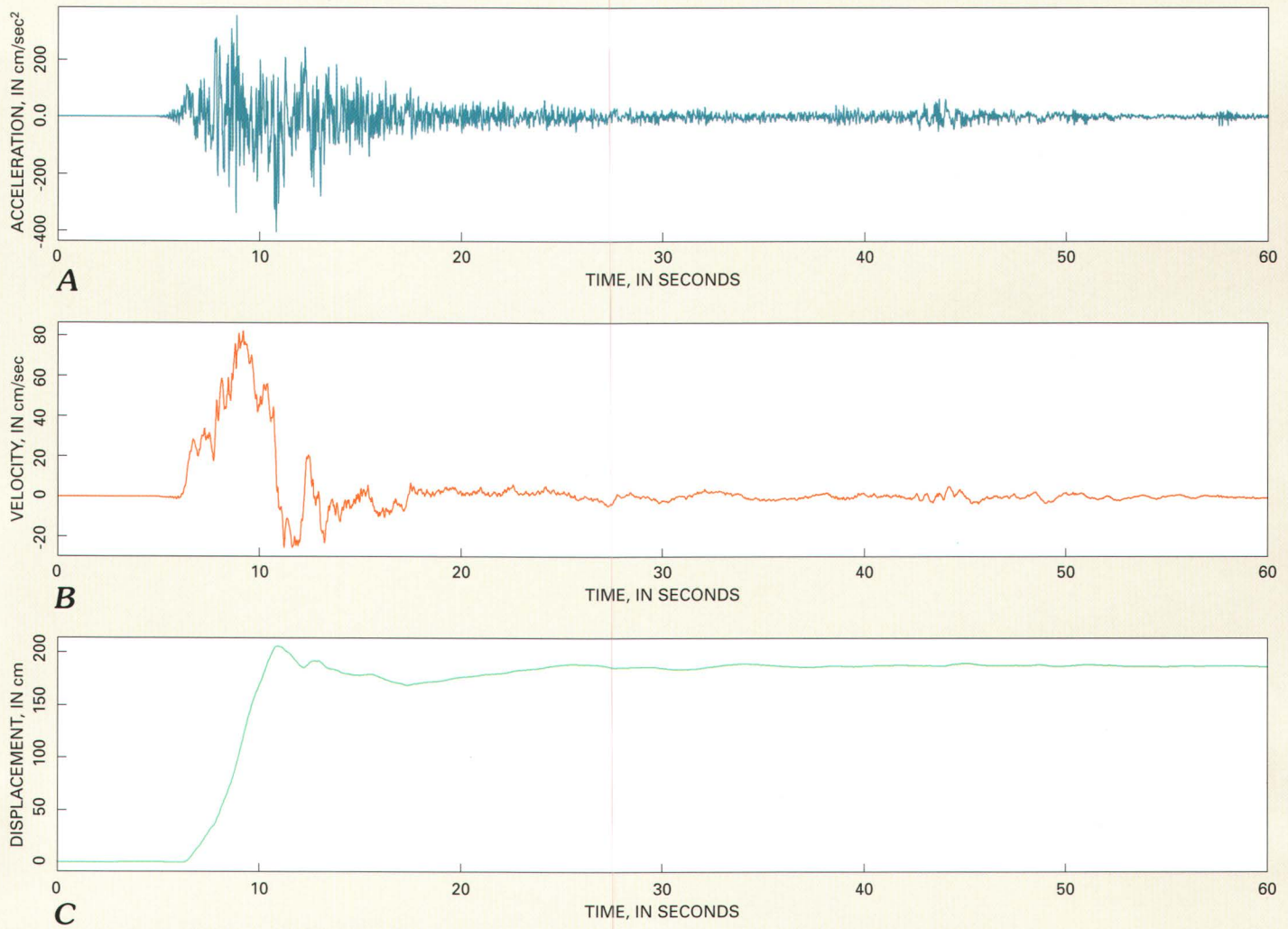


Figure 3. *A*, Recorded accelerations at the Turkish National Strong Motion Network station, SKR, in Adapazari during the August 17, 1999, main shock. Station is about 3.5 km from the surface rupture. *B*, Velocities computed from acceleration time history showing large velocity pulse. *C*, Displacements computed for acceleration time history showing large displacement pulse. *Illustration by William L. Ellsworth.*

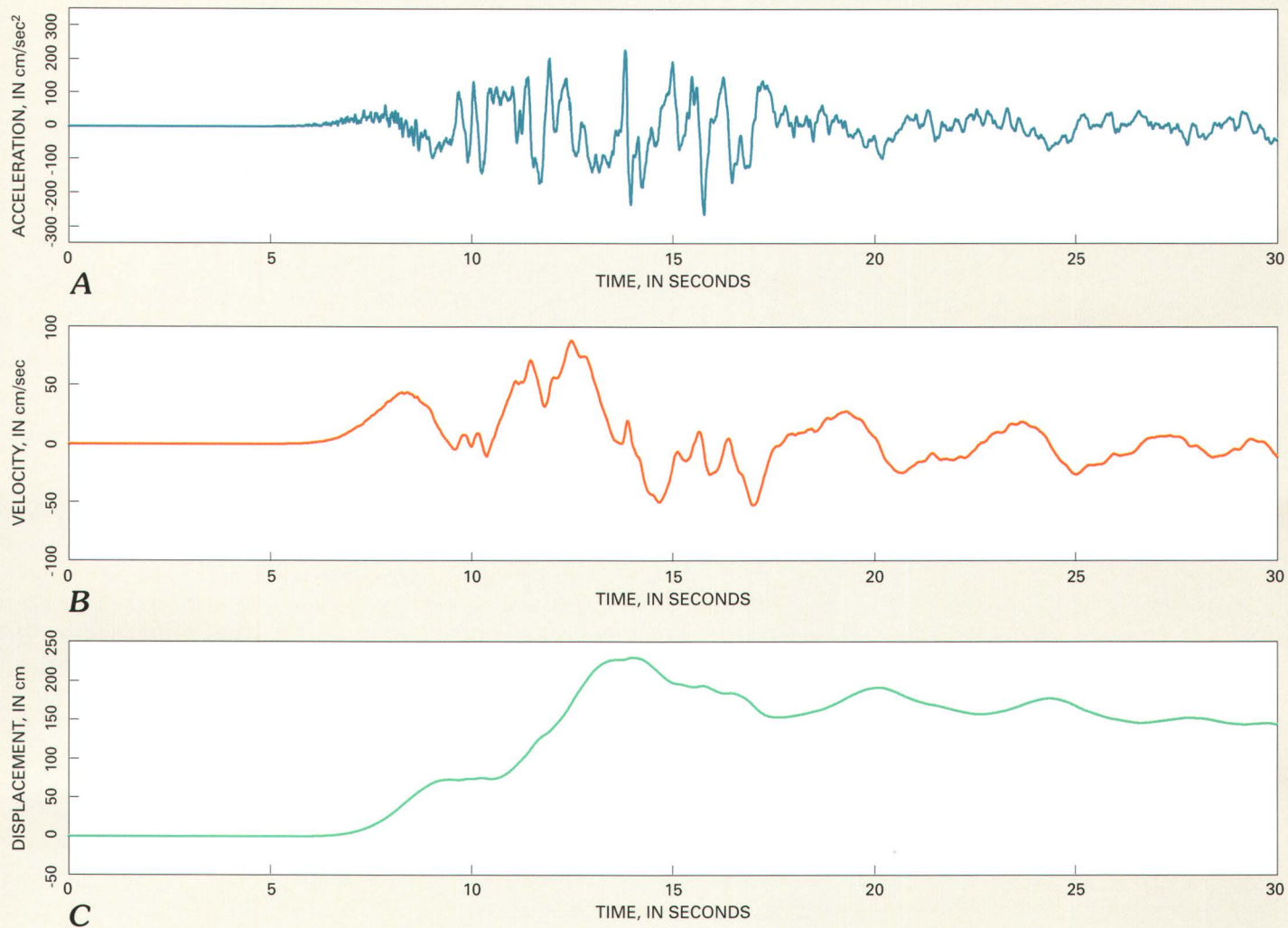
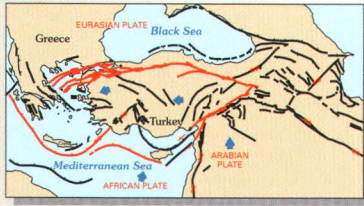


Figure 4. *A*, Recorded accelerations at the Kandilli Observatory and Earthquake Research Institute strong motion station, YPT, at the Petro-Chemical Plant in Korfez during the August 17, 1999, main shock. Station is about 4 km from the surface rupture. *B*, Velocities computed from acceleration time history showing large velocity pulse. *C*, Displacements computed for acceleration time history showing large displacement pulse. *Illustration by William L. Ellsworth.*

Geologic Setting and Earthquake History



Turkey is geologically active and frequently experiences large earthquakes. The activity is a consequence of the country being squeezed between the northward-moving Arabian and African tectonic plates and the relatively stable Eurasian plate (fig. 5). A wedge of continental crust, which is known as the Anatolian block and incorporates much of Turkey, is being squeezed westward away from the collision zone between the Arabian and Eurasian plates. Movement of the wedge is accommodated along two major strike-slip faults: the 1500-km-long North Anatolian fault on the wedge's north side and the 550-km-long East Anatolian fault on the southeast side. The August 17, 1999, Kocaeli earthquake was caused by slip along the western end of the North Anatolian fault. This major right-lateral strike-slip fault allows the region south of the fault to move to the west relative to the region north of the fault, at a rate of 10-20 mm/yr (Barka, 1992; Straub and Kahle, 1995). The fault is predominantly a single strand for much of its length with a few shorter, subparallel faults; however, it branches into three strands in the western 650 km where the 1999 earthquake occurred (fig. 6A). The northernmost, and most active, of these strands traverses in part the Sea of Marmara and includes the section that slipped on August 17, 1999. Surface rupture from the 1999 Kocaeli earthquake was mainly confined to Pliocene and Quaternary sedimentary basins and valley fill. Some of these basins appear to be formed between offset segments of the fault due to repeated slip of these segments.

The long written history of Turkey includes descriptions of many destructive earthquakes during the past thousand years. Although these historical accounts do not include descriptions of surface faulting, rupturing segments commonly can be inferred from descriptions of damage and how far away the earthquake was felt. It is important to know where and when the fault ruptured because scientists can use this information to evaluate the regularity and magnitude of earthquakes that can be expected on a specific fault segment. Furthermore, if the rate of strain accumulation on the fault is known from either geologic or geodetic studies, scientists can roughly estimate the time to the next earthquake on the same fault segment.

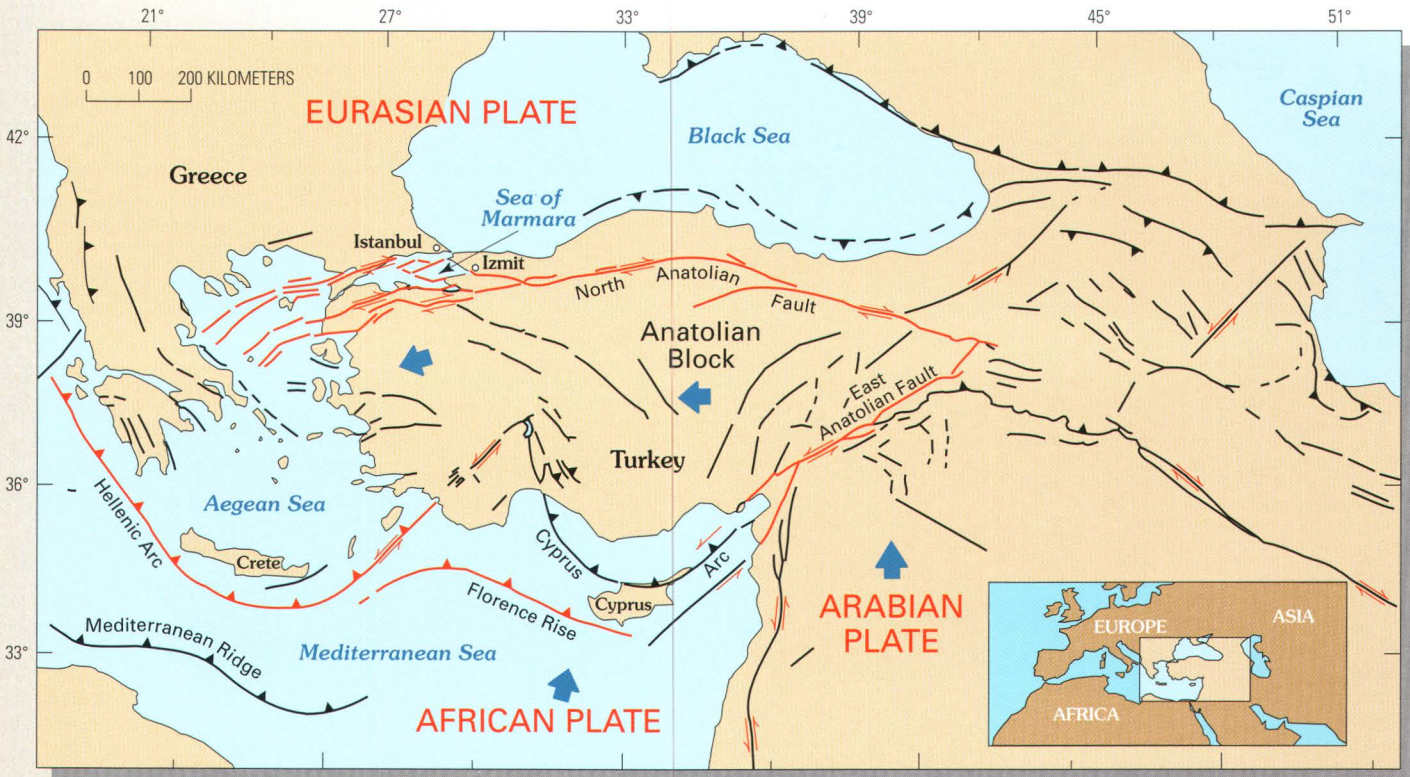


Figure 5. The tectonic map of Turkey includes the North Anatolian fault, East Anatolian fault, and Hellenic and Florence trenches. The westward movement of the Anatolian block results from (1) differences in rates of motion between the Arabian and African plates, (2) different directions of motion between the Anatolian block and Eurasian plate to the north, and (3) subduction of the African plate beneath the Anatolian block at the Hellenic and Florence trenches. The Arabian plate is moving to the north faster than the African plate, both relative to a stable Eurasian plate. The result is a westward moving wedge incorporating most of Turkey. *Modified from Barka (1992) and Rockwell and others (in press).*

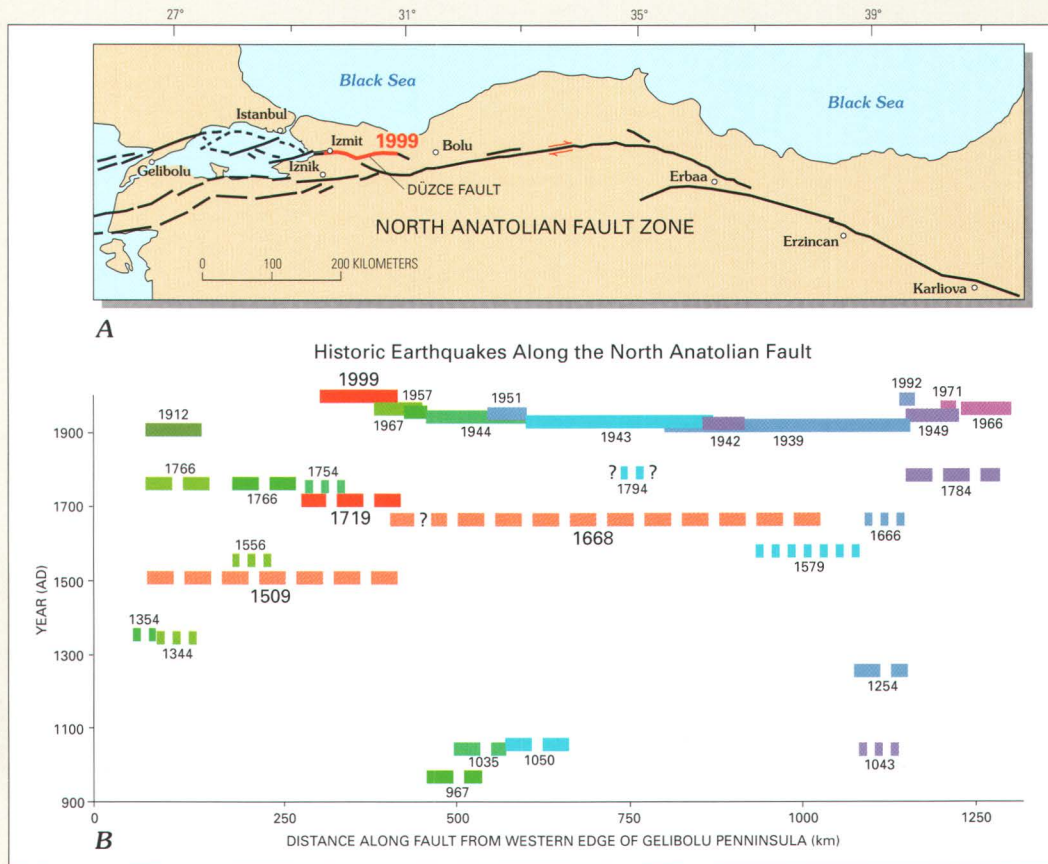
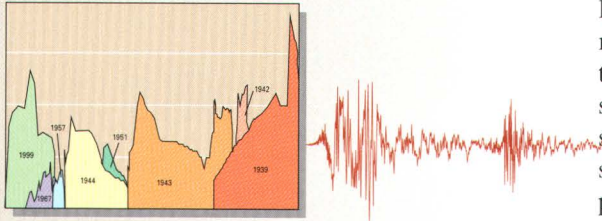


Figure 6. **A**, Strip map showing the 1500-km-long North Anatolian fault. Relatively straight, the fault has several short, minor strands associated with it along its eastern half and breaks into three strands to the west. The section of the fault that ruptured to the surface during the 1999 Kocaeli earthquake is shown in red. In 1999, the fault ruptured along the northernmost, generally east-west main strand, as well as along a northerly strand called the Düzce fault. Modified from Barka (1992) and Rockwell and others (in press). **B**, Historical earthquakes located along the fault where they are believed to have ruptured the ground surface. The 1999 rupture appears to be similar to the 1719 rupture. Solid lines indicate an earthquake known to have ruptured the ground, long-dashed lines indicate highly probable surface-rupturing events, and short-dashed lines are shown when the earthquake is believed to have ruptured the ground but that interpretation of the historic record has less certainty. Before 1719, the same section of the fault slipped as part of a longer rupture. There is no record in the 20th century of the kind of event that produced the long rupture in 1668. Gaps in the historic record of earthquakes may indicate no seismic activity or simply that there is no record of the seismicity. Because few population centers are in the central portion of the fault, the lack of seismic record may be accentuated. Compiled from Ambraseys (1970), Ikeda and others (1991), Ambraseys and Finkel (1995), Barka (1996), Stein and others (1997), and Rockwell and others (in press).

Based on comparisons of reported damage and how far away they were felt, the 1999 Kocaeli earthquake appears to be similar to an earthquake that damaged communities in 1719. Reports of shaking and descriptions of damage from the 1719 earthquake are remarkably similar to those observed in 1999 (Ambraseys and Finkel, 1995). There were also two earthquakes in 1766 and one in 1754 that probably resulted from fault rupture closer to Istanbul. These earthquakes are similar in size to those felt during the 20th century. In the more remote past, however, there have been earthquakes that appear to have ruptured more of the fault than has ruptured in any single earthquake during the past three centuries. In 1509, for example, an earthquake occurred that probably resulted from the rupture of faults from Gelibolu on the west to Bolu on the east (fig. 6B). Rupture of a long section of the fault is also inferred along the eastern section during the great earthquake of 1668. Faulting during this earthquake is thought to have occurred over 600 km, from west of Bolu to Erzincan (fig. 6B). The long ruptures inferred for the 1509 and 1668 shocks would be larger than any during the 20th century. Studying the Kocaeli earthquake is important because it can provide insight into faulting processes responsible for the variable behavior.

During the past 60 years, the North Anatolian fault has produced earthquakes along different sections of the fault in a systematic manner that is atypical of long faults. Beginning with the 1939 M 7.9 earthquake, which produced about 350 km of ground rupture along the eastern North Anatolian fault, the 20th century has seen ten additional moderate to large earthquakes along the fault (fig. 6B). Most of the earthquakes occurred sequentially in a westward progression. The 1999 Kocaeli earthquake is now the westernmost large earthquake (on the northern strand of the fault), breaking a section that appears, on the basis of historical reports of damage, not to have slipped for at least 250 years. The historical record does not support a theory that seismic behavior of the North Anatolian fault in the 20th century is a repetition of the pattern of earlier centuries. The record does show that several ground-rupturing earthquakes had occurred in close succession in the past, as with the sequences of events in the mid-eighteenth, fourteenth, and eleventh centuries. An incomplete historical record may hide evidence of other, longer sequential earthquake ruptures.

Earthquake Forecasts



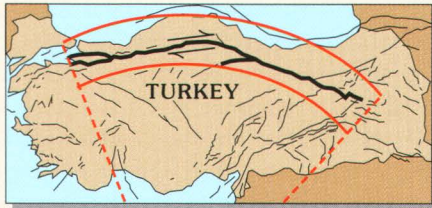
The sequential westward progression of $M_W > 6.7$ earthquakes along the North Anatolian fault during the 20th century has prompted study of how one large earthquake in Turkey may set up the next one (fig. 7) (Stein and others, 1997; Nalbant and others, 1998). One recent investigation consisted of calculations of the earthquake-induced changes in stress on adjacent fault segments (Stein and others, 1997). Stein and others (1997) showed that 9 out of the 10 observed ruptures were brought closer to failure by the preceding shocks; they estimated that the shocks are equivalent to about 20 years of stress that would typically build up along the North Anatolian fault. The stress change also affects the change in the probability of future events. The permanent change in probability occurs because increasing (or decreasing) the stress on a fault shortens (or lengthens) the time to bring a segment to failure. There is also a transient change in probability that strongly amplifies the effect of the stress change for periods of about a decade. For the North Anatolian fault, the computed stress change yielded an average threefold gain in the ensuing earthquake probability. Before the Kocaeli earthquake, Stein and others (1997) calculated that stresses at several isolated sites along the fault had been increased by prior events. They estimated a 15 percent probability of a $M_W > 6.7$ earthquake east of Erzincan and a 12 percent probability for a large event south of the city of Izmit during the interval from 1997 to 2027 on the Izmit segment of the North Anatolian fault. The August 17, 1999, Kocaeli earthquake ruptured the Izmit segment.

Application of this modeling technique to evaluate the effect of the Kocaeli earthquake on other faults indicates that stress was transferred to nearby fault segments both to the east and west (fig. 8). To the east, the area of increased stress included the Düzce fault on which the November 12, 1999, M_W 7.1 earthquake occurred. To the west, both the 80-km-long Yalova segment, southeast of Istanbul, and the North Boundary fault, immediately south of Istanbul, are closer to failure. A cluster of aftershocks of the 1999 Kocaeli earthquake are located 50 km west of the end of the Kocaeli rupture on the Yalova fault segment, suggesting that the calculated stress changes have increased the rate of seismicity on the Yalova fault. There also have been scattered aftershocks on the North Boundary fault.

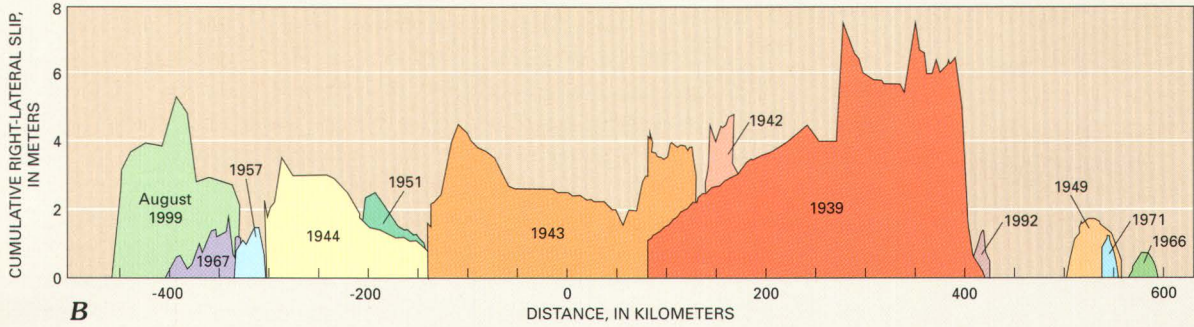
The November 12, 1999, earthquake also occurred at a location along the North Anatolian fault system where strain appears to have been aseismically accumulating. Fault slip during earthquakes located between and including the 1939 Erzincan and 1999 Kocaeli events was at a minimum along the interval that includes the Düzce fault (fig. 7B, C), where the November 12 event produced as much as about 5 m of slip. The ongoing relative movement between the Eurasian plate and Anatolian block of about 20 mm/yr causes strain to accumulate steadily along the North Anatolian fault.

Figure 7 (facing page, top). The North Anatolian fault, Turkey. **A**, Location of main fault and related strands; **B-D** are projected relative to its pole of rotation (where the dashed lines converge). **B, C**, The westward progression of earthquake ruptures is associated with fault slip of 2-6 m in each event, with 4 m as average. The August 1999 event is seen to be typical in extent along strike and in slip, although the 1967 and 1999 events significantly overlap on roughly parallel fault strands of the North Anatolian system. **D**, Stress build-up on the North Anatolian faults associated with the 1939-1967 westward progression of earthquakes and the contribution of steady stress accumulation. Although the stress dropped along 750 km of the North Anatolian fault, it was calculated to have been increased at the site of the Kocaeli earthquake (Stein and others, 1997). The August 17, 1999, ground rupture is shown in red. *Modified from Stein and others (1997).*

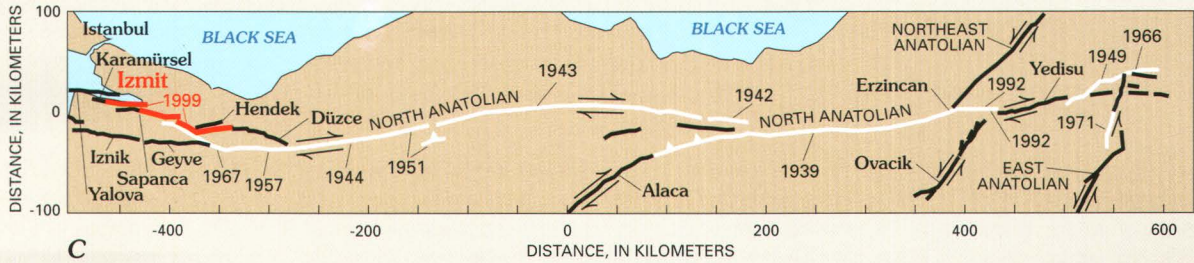
Figure 8 (facing page, bottom). Map showing stress transferred to all known or suspected faults in the Sea of Marmara by the 1999 Kocaeli earthquake. Note that off-fault aftershocks tend to locate where the Coulomb stress is calculated to have risen as a result of the 1999 Kocaeli earthquake rupture. The November 12, 1999, M_W 7.1 occurred in the area of increased stress east of the August surface rupture. The Yalova segment and the North Boundary fault, B, a probable site of a 1963 M_W 6.3 earthquake are identified. Sites of other large shocks in the Sea of Marmara are also identified. *Prepared by Ross Stein.*



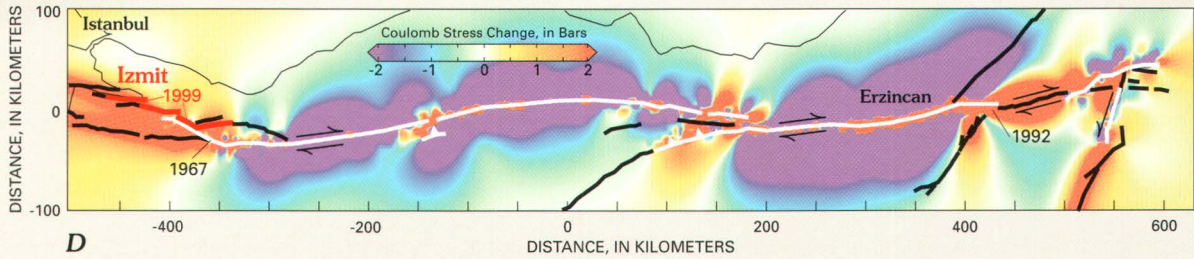
A



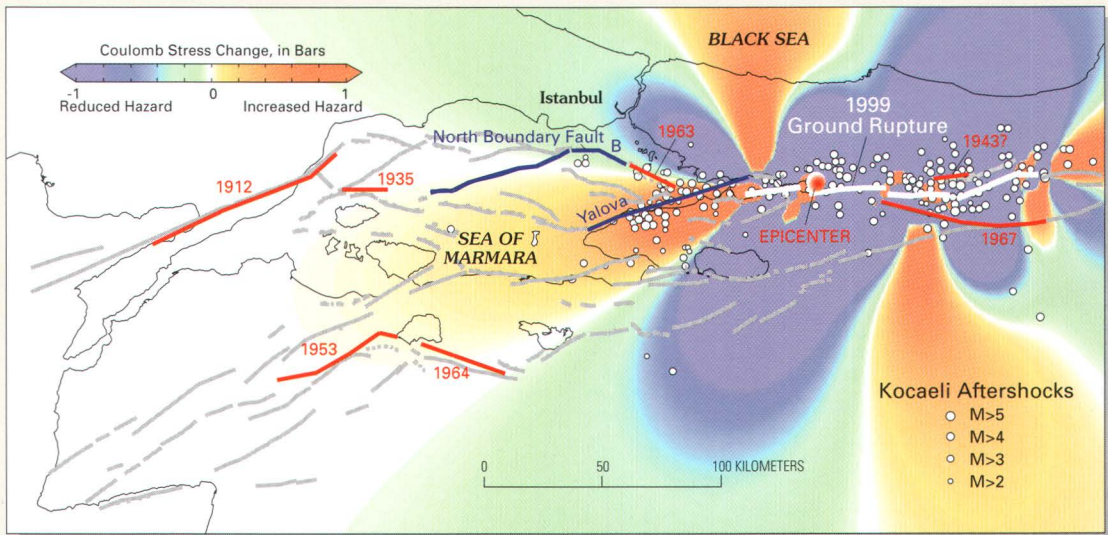
B



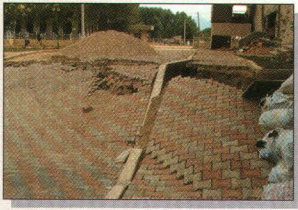
C



D



Surface Faulting



The August 17, 1999, Kocaeli earthquake produced right-lateral displacements or slip on surface ruptures over a distance of at least 110 km onshore in western Turkey (fig. 9). Rupture occurred along the North Anatolian fault to the west of the epicenter near Izmit, as well as to the east toward Akyazi, and along a northeast-trending fault toward Düzce. Thus, the fault ruptured in both east and west directions from the epicenter. The August 1999 surface rupture is characterized by an east-west trending zone of right-stepping fault strands, which express a component of extension at the western end of the northern strand of the North Anatolian fault system (Armijo and others, 1999). Maximum slip of approximately 5 m was mapped 31 km to the east of the epicenter; slip was typically 2.5 to 4.5 m right lateral at the surface. Slip decreased gradually from the maximum to the east, but more abruptly to the west and at locations where the surface trace was stepping over to a new trace (for example, at Lake Sapanca (fig. 9)). The slip also diminished abruptly to the east where it paralleled the ground rupture caused by the 1967 Mudurnu Valley earthquake. The fault zone was typically a narrow zone of cracks (5 to 25 m wide) that either followed or formed parallel sets of faults oblique to the trend of faulting. The surface expression of faulting included tension cracks and fissures with localized positive relief. The August 1999 surface rupture appeared to be located in the general vicinity of previous surface faulting events, as a pre-existing scarp was present at several locations where displacement across the rupture had a vertical component.

Figure 9. Preliminary map showing surface rupture along the North Anatolian fault zone during the Kocaeli earthquake. The rupture is marked in red with selected values of offset (in meters) along the fault. The western end of the ground rupture associated with 1967 Mudurnu Valley earthquake is also shown where it parallels the 1999 surface rupture. Surface rupture and offsets was mapped in detail by four groups of geologists from the USGS, the Southern California Earthquake Center (SCEC), the Institut de Physique du Globe (IPGP), France, and Istanbul Technical University (İTÜ). Each group focused on one of the four sections of the fault that ruptured (Barka and others, 1999).

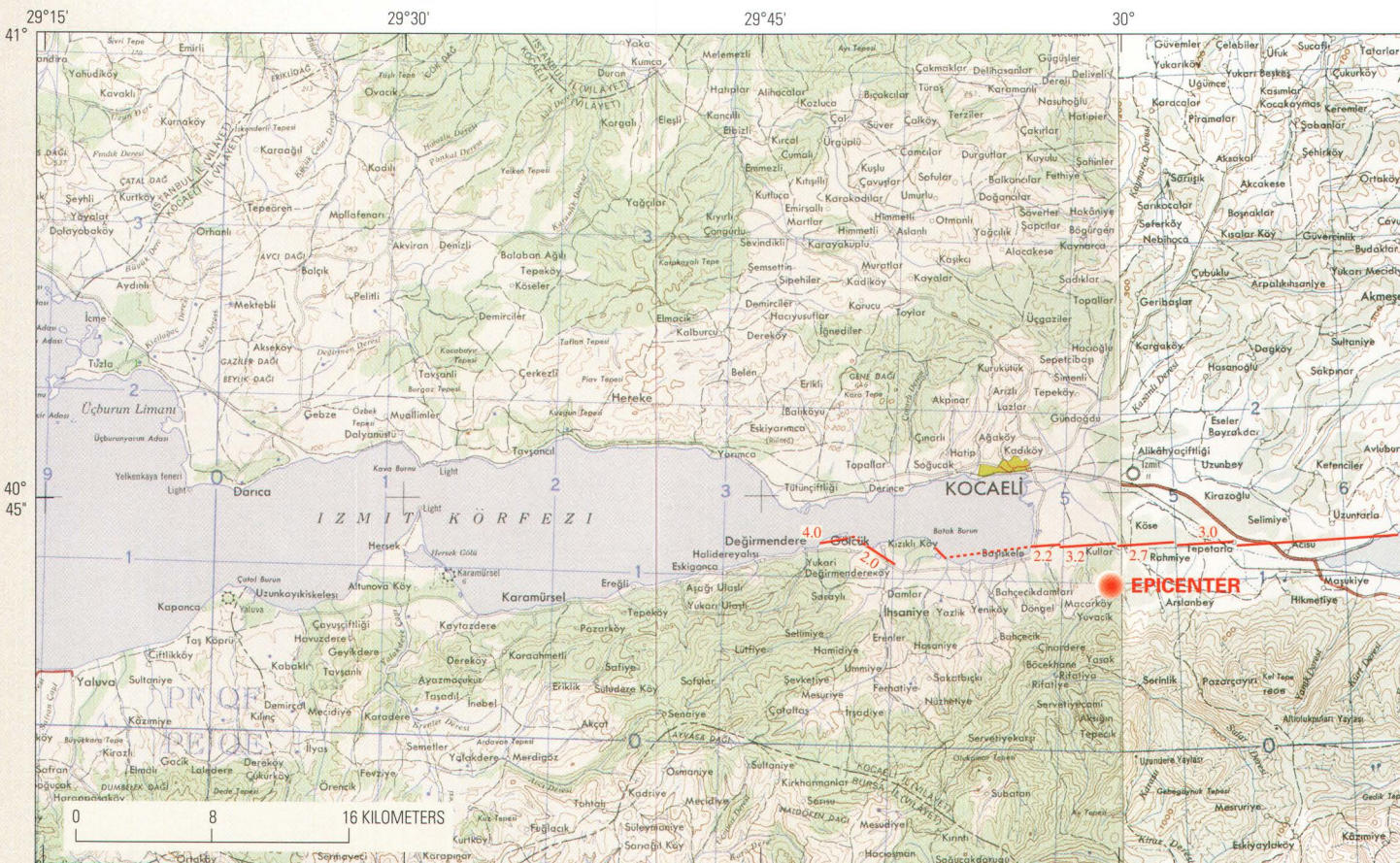
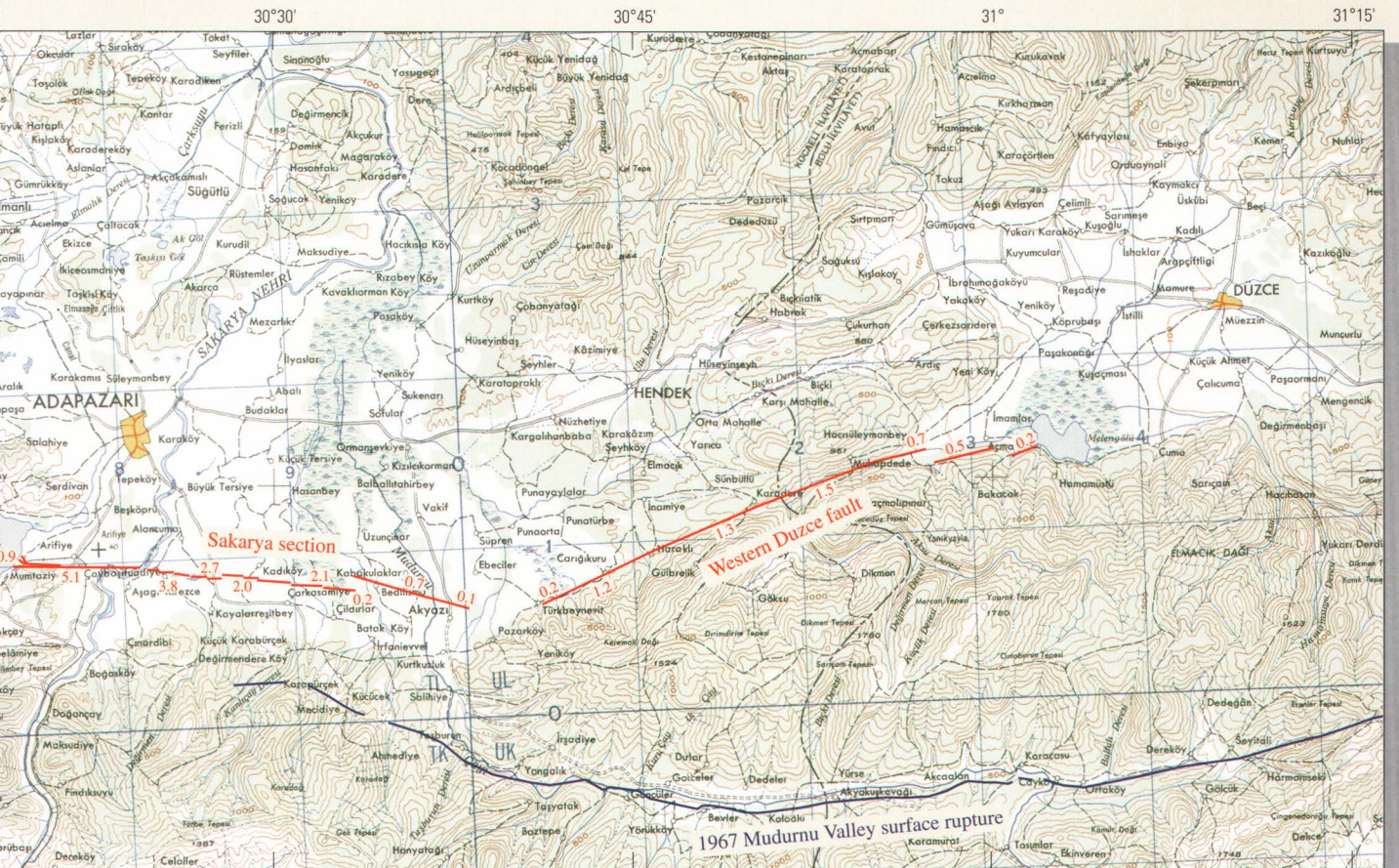




Figure 10. Tectonic scarp along the normal fault in Gölcük in a cobblestone pavement with both vertical (~1 m) and horizontal (~0.3 m) components of offset. *Photograph by Robert Langridge.*



Coastal Changes Due to Kocaeli Earthquake

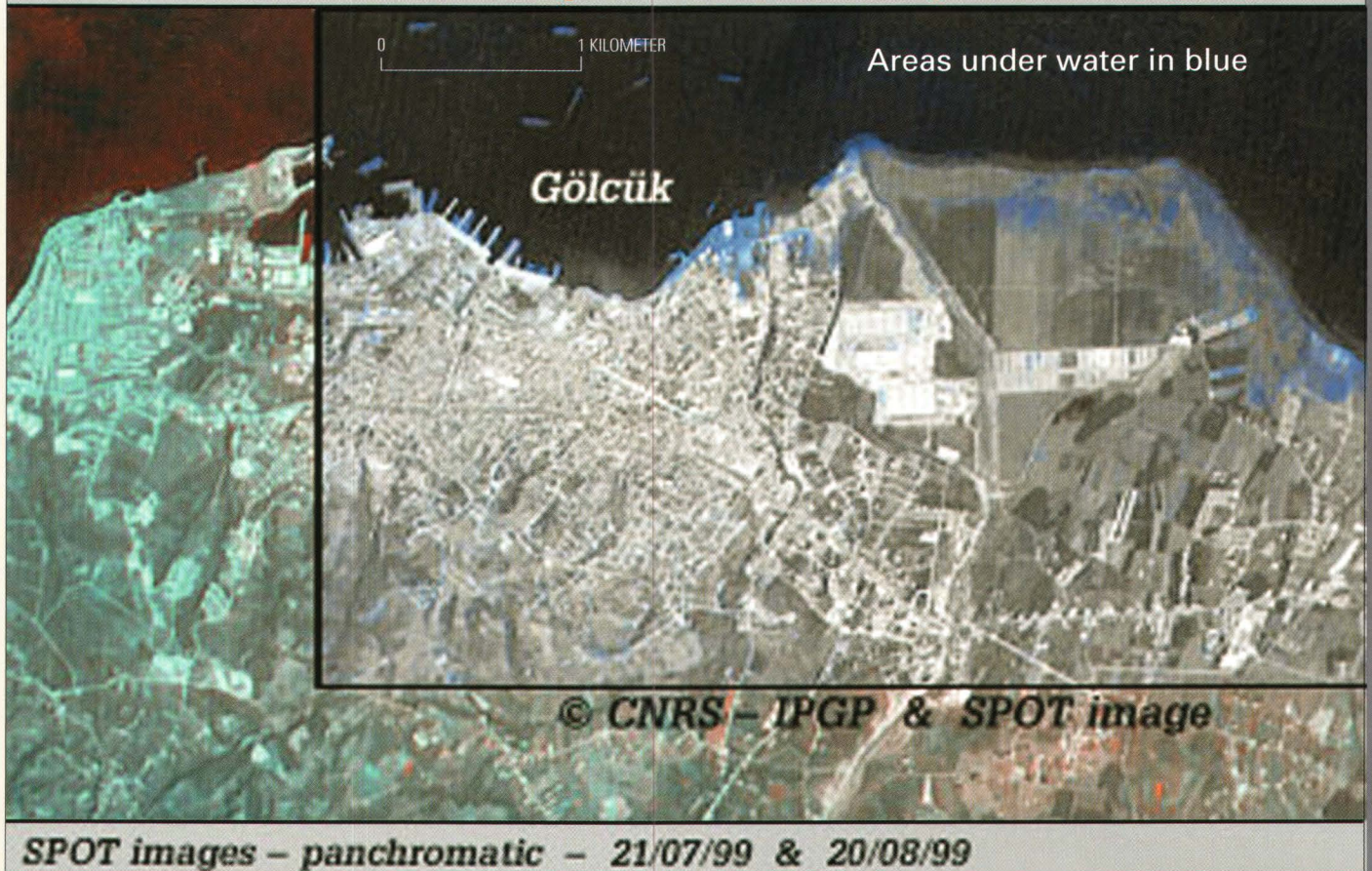


Figure 11. Satellite image of Gölcük area showing zones of coastal submergence (blue). Strike-slip faulting occurred through the port area (upper left) and oblique faulting occurred on the Gölcük (normal) fault. Copyrighted image by CNRS-IPGP and SPOT image; used with permission.

The westernmost extent of faulting found on land was in Gölcük where a seawall was offset approximately 4 m. To the west, the rupture crossed a small bay at Degirmendere and the nearby shore had subsided. Surface rupture was not reported on the Hersek Peninsula, and it is likely that offshore rupture of the sea floor stopped west of Degirmendere. A south-facing scarp near the tip of the Hersek Peninsula may be part of the next east-west trending segment of the North Anatolian fault to the west.

In Gölcük, east-west trending strike-slip faulting, with offsets of as much as 4.5 m, extended through the waterfront and port region. Part of the strike-slip faulting transfers eastward into a N. 70° W. trending zone of predominantly normal faulting. Vertical displacements of as much as 2.4 m were recorded on the normal fault in Gölcük. The fault also had a modest right-lateral strike-slip component, 1.2 m at maximum, 0.5 m on average (fig. 10). The structural relationship, the 4-km-long scarp with pre-existing geomorphology along the fault trace, and subdued topography around the bay suggest that this scarp is related to tectonic faulting rather than landsliding or delta-front collapse. Trenching of the normal fault conducted immediately after the Kocaeli earthquake revealed four previous seismic events, two dated at A.D. 1509 and A.D. 1719 and two undated older events. Another shorter normal fault lies to the east of and parallel to the

normal fault in Gölcük. Additional strike-slip faulting was not observed on the south side of Izmit Bay (B. Meyer, oral commun., 1999). The normal faulting in the Gölcük area caused regional subsidence that submerged part of the coast (fig. 11). Approximately 4 km of coastline on the south shore of Izmit Bay subsided about 2 to 3 m. Many structures built near the shore were inundated by the sea (fig. 12).

The rupture continued onshore east of Izmit Bay where it was characterized by an impressive mole track and caused damage to buildings and other cultural features (figs. 13, 14, 15). The fault right laterally offset the Trans European Motorway (TEM) near Tepetarla by about 3 m and extended to the northwest corner of Lake Sapanca. The lake fills a pull-apart basin created by long-term motion on the North Anatolian fault. The fault probably follows the north side of Lake Sapanca to near Esme, which suffered extensive damage from liquefaction. Projection of the fault trace through Lake Sapanca requires a right stepover of as much as 2 km to where the fault is next seen to the east onshore.

The 26-km-long Sakarya section of the ground rupture from Lake Sapanca to Akyazi was the focus of mapping efforts by the team of USGS geologists and is shown in detail on figure 16 (Fumal and others, 1999). Southeast-trending tensional cracks near the lakeshore connected to an east-west trending mole track



Figure 12. Submergence of shoreline in Gölcük caused by tectonic subsidence associated with normal faulting. *Upper photograph by Robert Langridge; lower photograph by Thomas L. Holzer.*

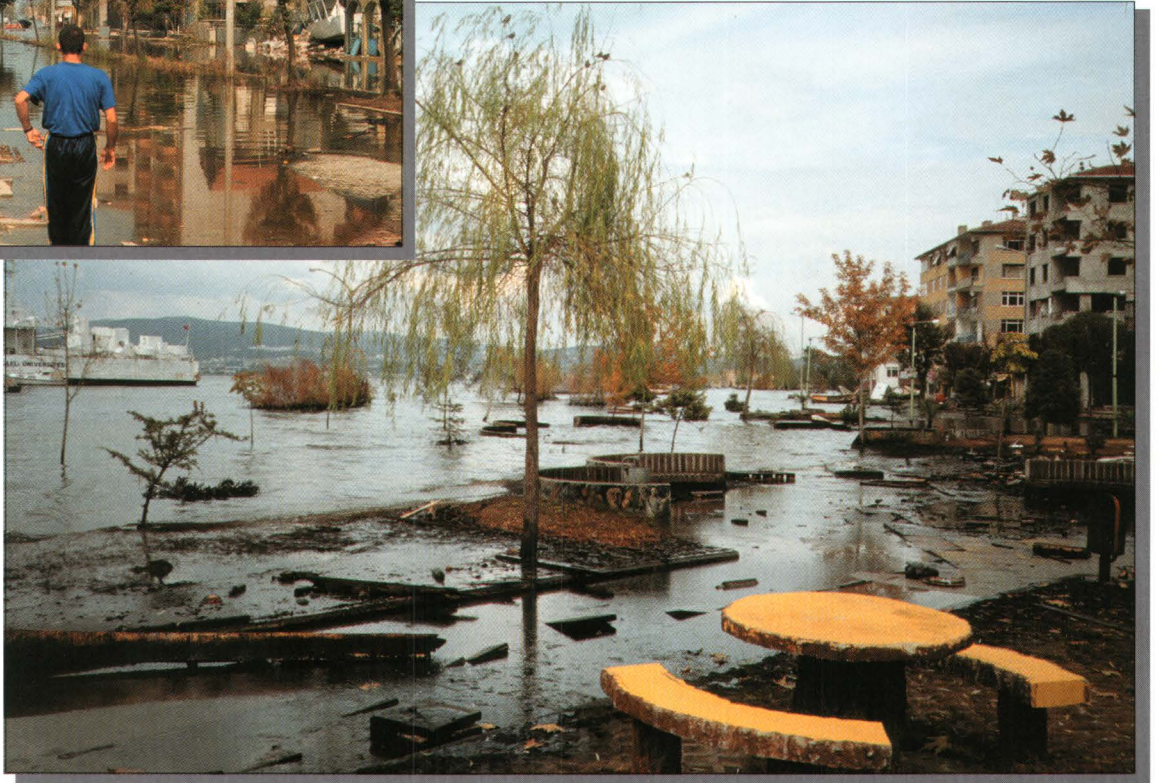


Figure 13. Mole track along ground rupture near Izmit. Right-lateral strike-slip displacement was about 3 m. Positive topographic relief of the mole track was localized and did not represent a component of the motion. *Photograph by Heidi Stenner.*



Figure 14. Offset canal near Izmit. Strike-slip displacement across the whole zone here was more than 2.5 m and included a vertical component (middle left). *Photograph by Heidi Stenner.*

Figure 16. The Sakarya section of the 1999 surface rupture mapped by USGS geologists. Site localities where measurements were taken shown as dots; data are unpublished but available by request from R.M Langridge or Heidi Stenner, USGS.





Figure 15. Surface rupture extending through boundary wall and collapsed apartments, to the east of Izmit. Strike-slip displacement here was about 3 m. *Photograph by Heidi Stenner.*



Figure 17. Offset poplar trees (2.7 m right lateral) along the surface rupture near Resitbey. The rupture traversed many poplar groves, cornfields, and arable land along the Sakarya River plain. *Photograph by Heidi Stenner.*

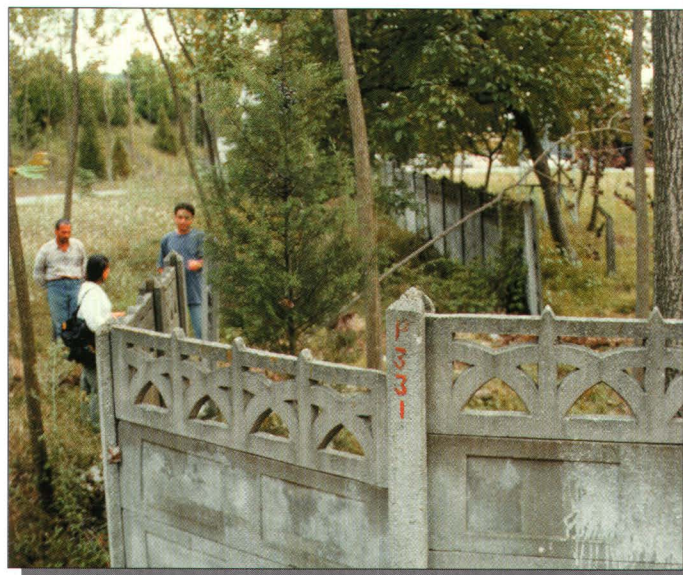
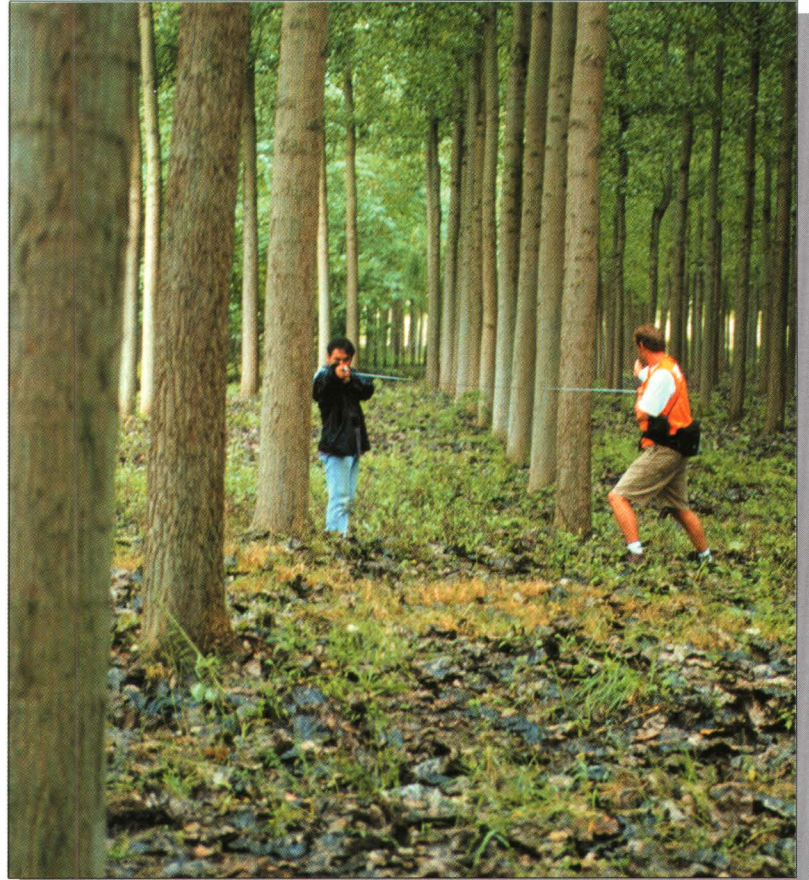


Figure 18. Offset wall near Arifiye. The right-lateral displacement is 4.58 m. *Photograph by Heidi Stenner.*

with less than 0.5 m of right-lateral displacement. The rupture continued eastward crossing the TEM and railway tracks. Right-lateral offset increased from less than 0.5 to 4.3 m over a distance of 1.5 km. A secondary trace was found that followed the southern range front of the lake from the southeast edge and exhibited as much as 0.5 m of right-lateral displacement before it merged into the main zone of faulting. The maximum right-lateral slip measurement of 5.1 ± 0.2 m was recorded near Arifiye in a grove of offset poplar trees (fig. 17). Offsets on other cultural features nearby confirm that there was a large amount of slip in this region (figs. 18, 19). Slip decreased uniformly to the east; right-lateral slip at the Sakarya River was 3.3 ± 0.2 m.

Stepover zones between east-west trending fault strands were characterized by a change in strike of the ground rupture, widening of the fault zone with an increase in the number of strands, a vertical component of offset, and a decrease in the total slip recorded. Along the Sakarya section, stepovers between fault strands, greater than 1 km in length, were typically 100 m wide (fig. 16). East of the Sakarya River, right-lateral slip decreased to approximately 2 m along the section of the rupture that parallels



Figure 19. Road offset right laterally 4.66 m near Arifiye. *Photograph by Robert Langridge.*

the surface rupture associated with the 1967 Mudurnu Valley earthquake (fig. 9). At Kanlıçay, 76 cm of total slip was recorded near the west end of the 1967 rupture (Ambraseys and Zatopec, 1969); at the same longitude, 7.5 km to the north, 2.3 to 2.9 m was measured along the 1999 rupture (fig. 20). Evidence was found for slip on the 1967 fault trace that was triggered by the 1999 earthquake. East of Kanlıçay on the 1999 rupture, slip decreased to less than 0.5 m and the rupture stepped to the left. Surface rupture was recognized again at Kazancı. From Kazancı, the rupture trended N. 75° W. toward Akyazi, and was characterized by right-stepping N. 37° W. to N. 55° W. trending tension gashes; slip increased from 0.04 m to 0.7 m on this strand, and died out to the east of Akyazi.

A 6-km gap in the surface rupture occurred from Akyazi to Türkbeynevit where surface rupture was observed again along the N. 65° E. trending western Düzce fault (fig. 9). The Düzce fault follows the northwest-edge of an uplifted bedrock block into a fault-strike valley toward Gölyaka. Despite the change in strike, this segment had predominantly right-lateral displacements along its 30 km length. Slip increased from less than 0.5 m to a maximum of 1.5 m near the east end of the valley. Slip then decreased toward the town of Gölyaka. The surface rupture terminated along the southern margin of a small pull-apart called Eften Gölü or Lake Eften. East of Gölyaka, the western Düzce fault steps to the right twice to form two short fault segments that bound the range front of Eften Gölü, and marks the termination of faulting (Hartleb and others, 1999). The final strand had right-lateral slip of as much as 0.2 m. From north to south, the western Düzce fault also parallels the ground rupture during the 1967 Mudurnu Valley earthquake.

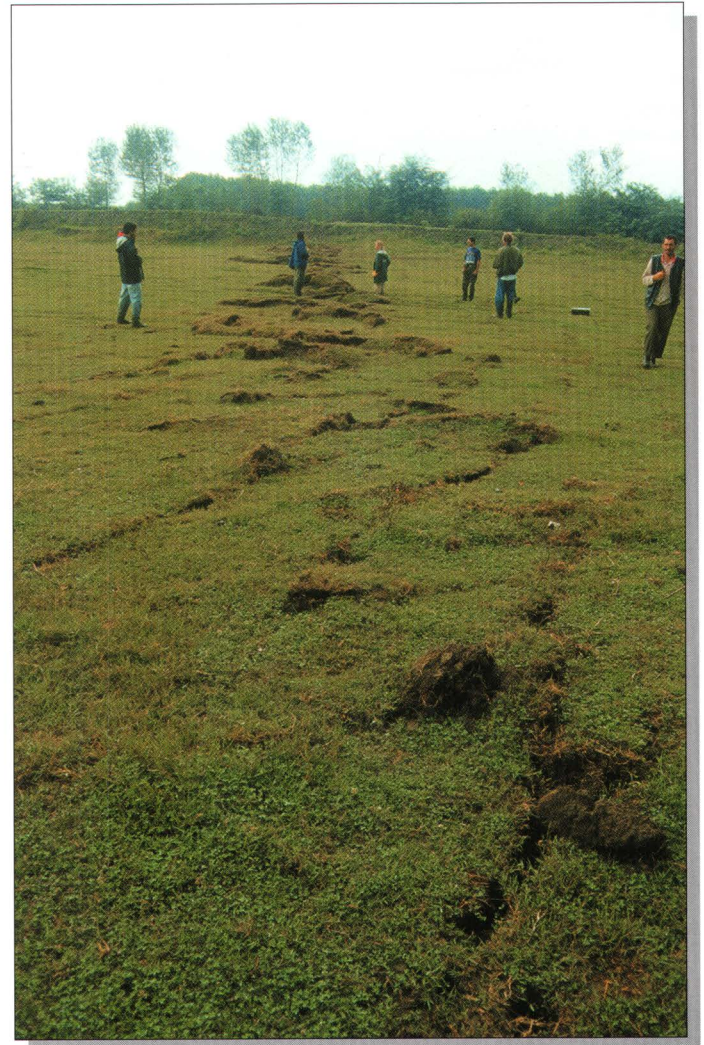
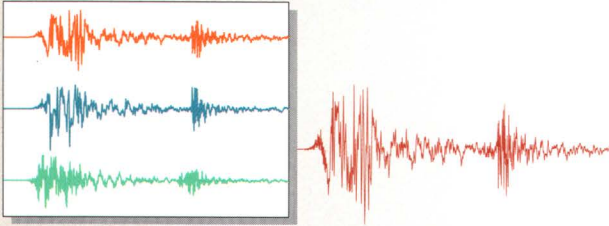


Figure 20. Complex surface rupture pattern with linking en echelon cracks seen near the Açmalık canal site. Right-lateral strike-slip displacement here amounted to 2.26 m and was 2.40 m in the dike of the canal, seen in the distance. *Photograph by Robert Langridge.*

Ground Shaking

Main-Shock Observations



On-scale recordings of strong ground shaking close to the fault rupture are important for both understanding causes of earthquake damage and the physics of fault rupture. Approximately 38 recordings of strong motion were made of the August 17, 1999, Kocaeli earthquake main shock. The recordings were made by four of the five institutions in Turkey that operate either strong motion networks or small arrays. Much of the strong motion data that was collected are available on the Internet. The five institutions, which are arranged in order of the size of their networks, and their Internet sites are as follows:

1. National Strong Motion Network (NSMP), operated by the Earthquake Research Department, Directorate for Disaster Affairs of the Ministry of Public Works and Settlement (ERD) <<http://angora.deprem.gov.tr/>>
2. Kandilli Observatory and Earthquake Research Institute (KOERI) <<http://www.koeri.boun.edu.tr/earthqk/earthqk.html>>
3. Istanbul Technical University (ITÜ) <<http://www.itu.edu.tr/>>
4. Public Water Works (DSI) <<http://www.dsi.gov.tr/>>
5. Middle East Technical University (METU) <<http://www.metu.edu.tr/home/wwweerc/>> and <<http://www.metu.edu.tr/home/wwwdmc/>>

Implications of Aftershock Observations

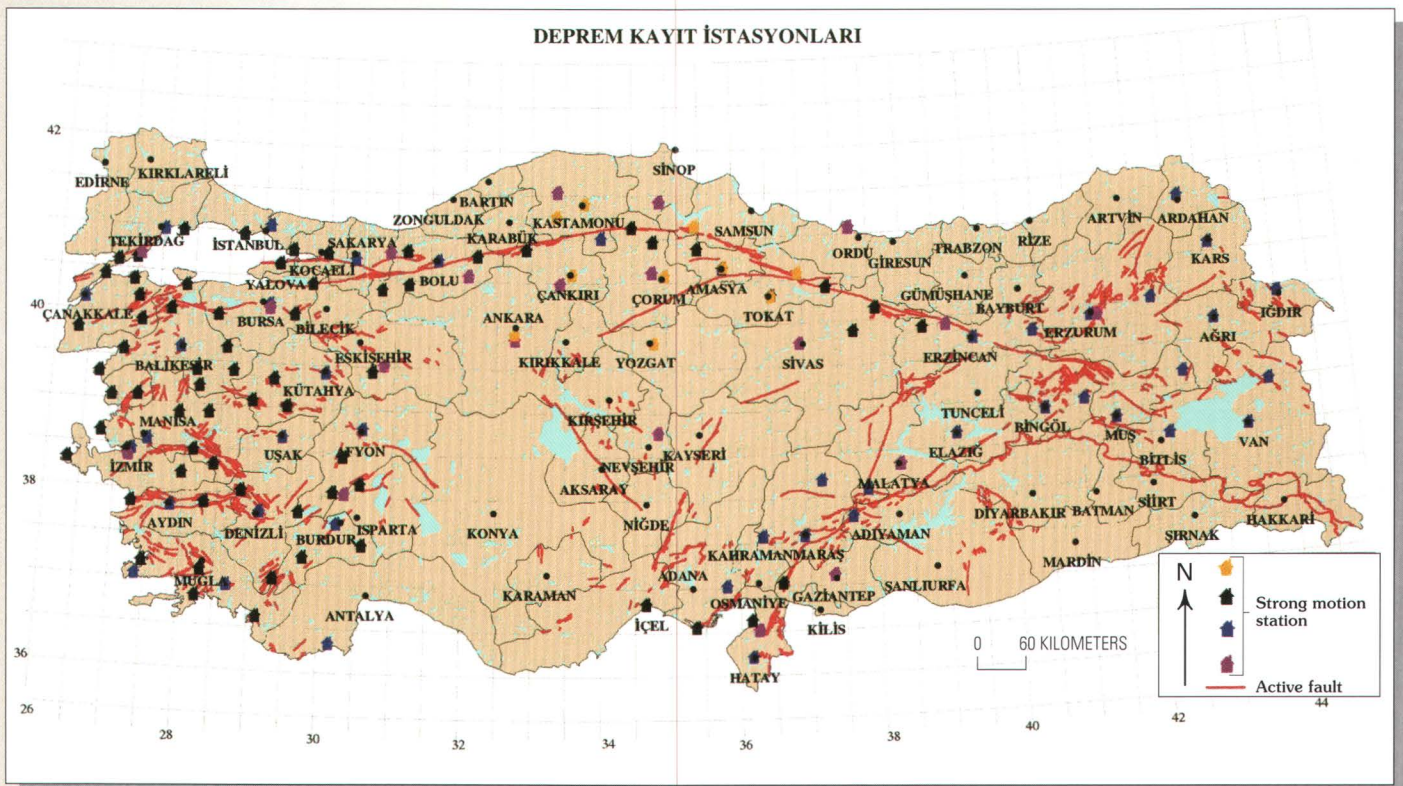


Figure 21. Modified map showing the National Strong Motion Network of Turkey and major active faults, including the North Anatolian fault. Modified from Earthquake Research Department, Directorate for Disaster Affairs, Ministry of Public Works and Settlement.

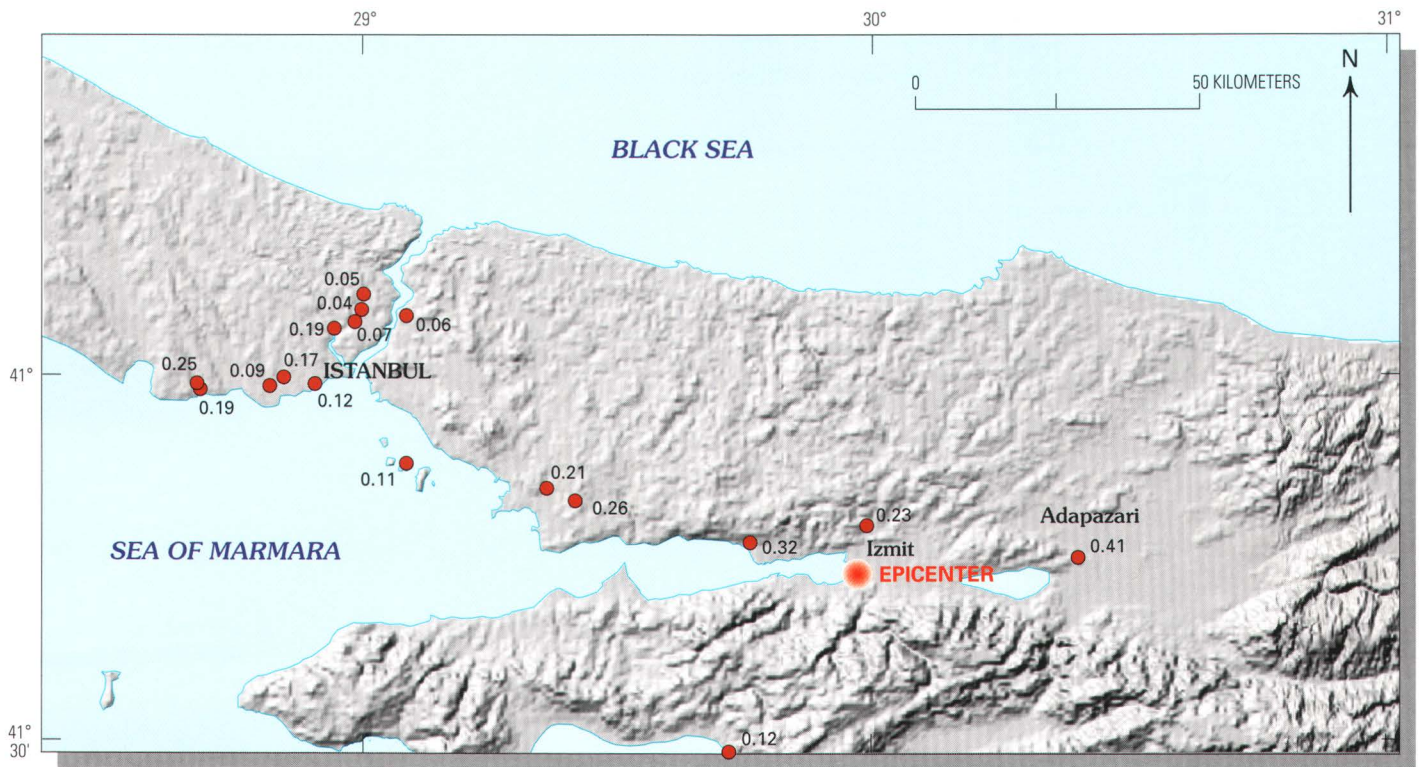


Figure 22. Map showing locations of peak horizontal accelerations recorded at strong motion stations in and near the epicentral area. The network stations included are from ERD, ITÜ, and KOERI. Base map courtesy of BKS Surveys Ltd., N. Ireland.

Station	L, in g	T, in g	L (+)	T (+)	V, in g	Lat N.	Long E.	Network operator
IZT	0.171	0.225	S	E	0.146	40.790	29.960	ERD
SKR	*	0.407	S	E	0.259	40.737	30.384	ERD
DZC	0.374	0.315	W	S	0.480**	40.850	31.170	ERD
IST	0.061	0.043	S	E	0.036	41.080	29.090	ERD
GBZ	0.264	0.142	N	W	0.199	40.820	29.440	ERD
CEK	0.118	0.190	N	W	0.050	40.970	28.700	ERD
IZN	0.092	0.123	S	E	0.082	40.440	29.750	ERD
BRS	0.054	0.046	S	E	0.025	40.183	29.131	ERD
YPT	0.230	0.322	W	N	0.241	40.763	29.761	KOERI
ATS	0.252	0.180	N	W	0.081	40.980	28.692	KOERI
DHM	0.090	0.084	S	W	0.055	40.982	28.820	KOERI
YKP	0.041	0.036	S	W	0.027	41.081	29.007	KOERI
FAT	0.189	0.162	S	E	0.131	41.054	28.950	KOERI
ARC	0.211	0.134	N	W	0.083	40.83	29.36	KOERI
HAS	0.056	0.110	S	E	0.048	40.869	29.090	KOERI
MCK	0.054	0.070	N	W	0.038	41.065	28.990	ITÜ
ZYT	0.120	0.109	N	W	0.051	40.986	28.908	ITÜ
MSK	0.054	0.038	N	W	0.031	41.104	29.010	ITÜ
ATK	0.103	0.168	N	W	0.068	40.989	28.849	ITÜ

Table 1. Coordinates and peak accelerations recorded during the 1999 Kocaeli, Turkey, earthquake at strong motion stations that recorded significant shaking.

[L, longitudinal, T, transverse, V, vertical; the components L and T are instrument components and do not correspond to north-south and east-west automatically. Refer to each network for the correct orientation of each horizontal component. * L, component did not function; **, based on a single spike (actual value may be smaller)]

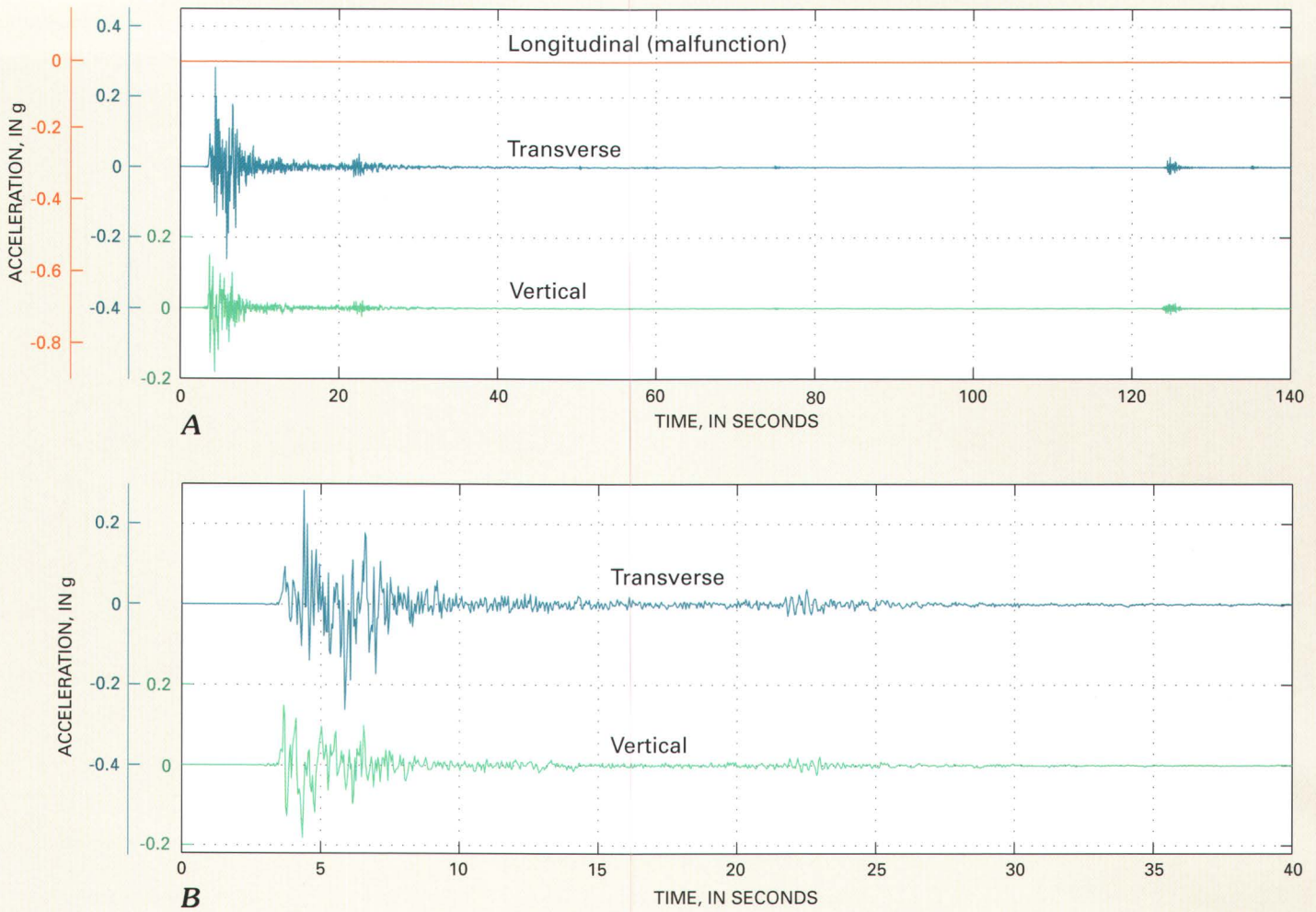
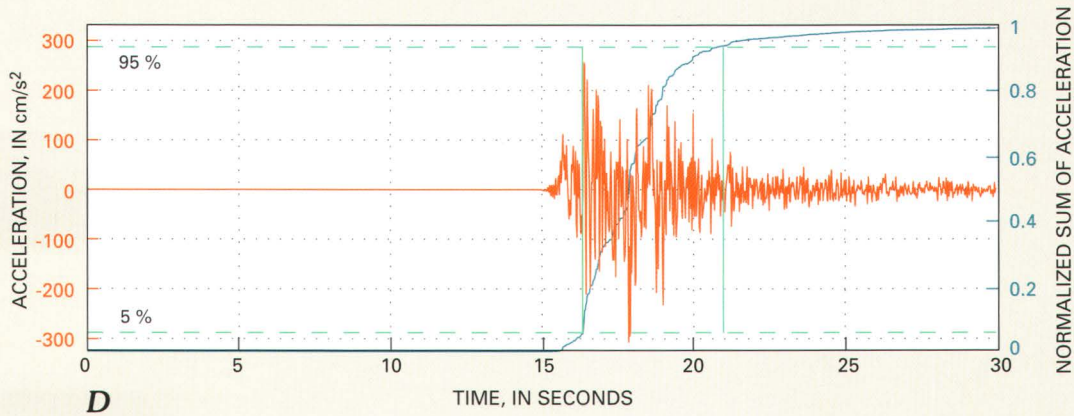
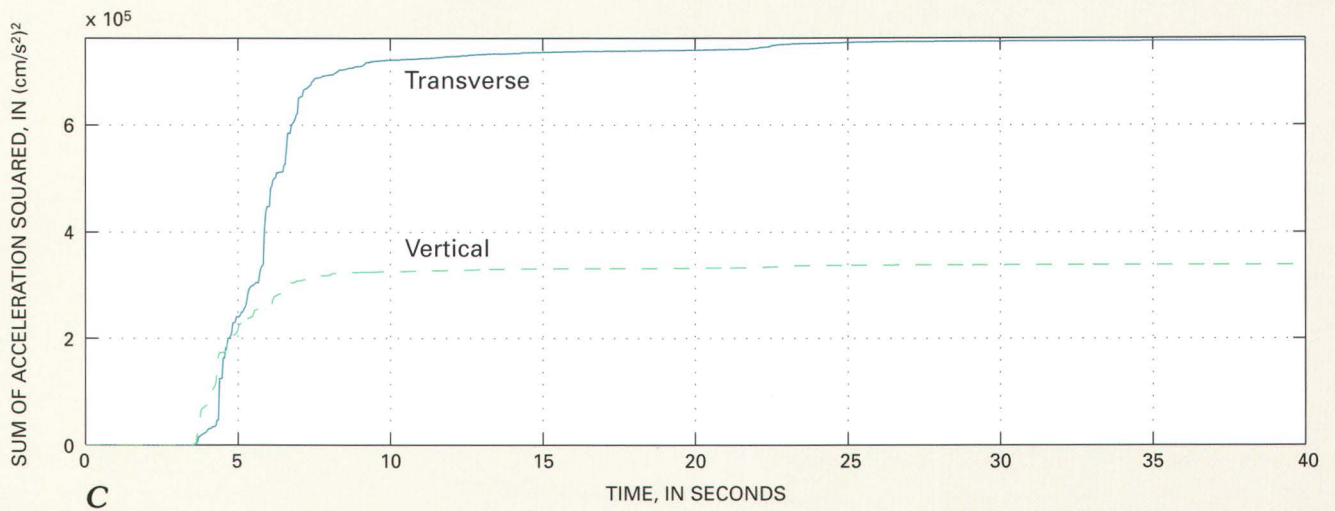


Figure 23. A, Time histories of acceleration for 140 s at SKR; note that longitudinal component malfunctioned. The plot shows several events: B, time history with first 40 s of the acceleration record; C, the cumulative sum of the squared acceleration values; and D, effective duration of significant strong motion during the main shock, based on time between 5 and 95 percentiles of the cumulative sum, is 4.5 s. *Illustration by Mehmet Çelebi.*

The 38 main-shock recordings included 24 from ERD, 10 from KOERI, 4 from ITÜ, and 3 sets of structural response records, 2 from KOERI and 1 from METU. DSI did not retrieve any records from its dams in the earthquake region. The structural records retrieved by KOERI include the structural response arrays at Süleymaniye Mosque and Aya Sofya (Hagia Sophia) Museum <<http://www.koeri.boun.edu.tr/earthqk/earthqk.html>>. Partial records were obtained by METU from an instrumented six-story building in Gerede (P. Gülkan, written commun., 1999). The largest peak acceleration at the basement of the six-story building was 0.035 g.

Although the number of instruments deployed in the epicentral area may seem sparse, the number is in part limited by a broader effort by ERD to include every major town in Turkey in the network. Figure 21 shows the NSMP network operated by ERD, which is the largest network operation in Turkey.

Table 1 compiles peak accelerations for each of the three components of accelerometers at 19 strong motion stations located in or near the epicentral region. Figure 22 is a map of the peak horizontal acceleration recorded at these stations. Most of the stations are housed in buildings, some of which are more than two stories high. Standard practice in the United States when compiling free field recordings is to ignore recordings from buildings that are more than two stories high because it is believed that the structural response of these buildings may modify the recording from free field conditions. Soil conditions beneath the stations in Turkey also have not been systematically documented.



The time history of acceleration recorded at SKR (Adapazari in Sakarya Province), a ERD station, is shown in figure 23A. The station is on soft rock and about 3.5 km from the surface trace of the fault. The record reveals at least two aftershocks immediately followed the main shock. Figures 23B, C show only 40 s of the record and figure 23D shows the cumulative sum of the square of the acceleration superimposed on the acceleration time history. This sum has been used by Trifunac and Brady (1975) to define an effective earthquake duration. The effective duration is the time between the 5 and 95 percentile values of the cumulative sum. This yields an effective duration of the main shock at SKR of approximately 4.5 s. This duration is different than the duration felt and reported by humans. People typically can sense ground shaking at levels of less than 0.01 g. The main shock contributes approximately 97 percent of the significant ground shaking of the two shocks within the 40 s of the record as inferred from the cumulative sum of the square of the acceleration.

The time history of acceleration recorded at YPT (Petro-Chemical Plant in Korfez), a KOERI station, is shown in figure 24A. The station is located on alluvium. The time history reveals two distinct earthquake pulses. Figure 24B shows the cumulative sum of the square of acceleration, indicating an effective duration of approximately 15 s for the main shock. The main shock contributes approximately 85 percent of the significant ground shaking caused by the two events. The YPT instrument is housed on the first floor of a three-story building (fig. 23C).

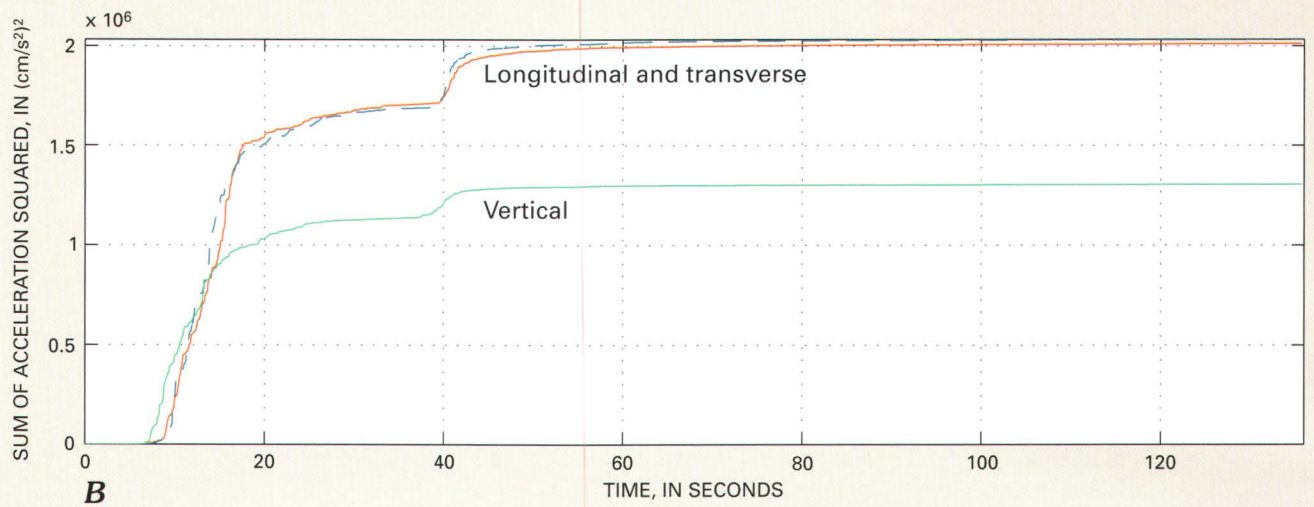
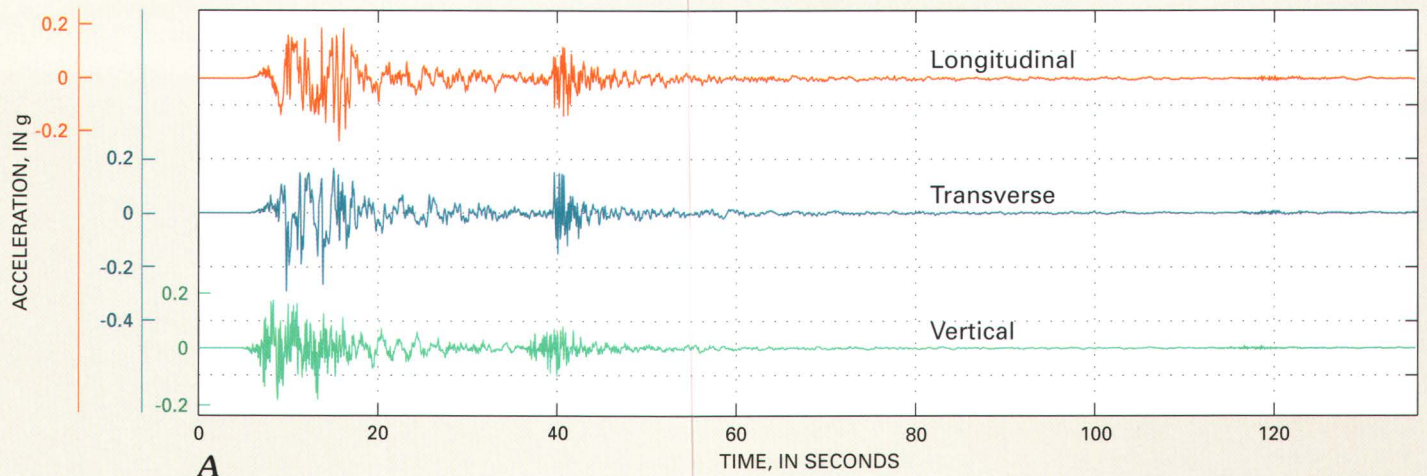


Figure 24. A, Time histories of acceleration at YPT showing a second event approximately 33 s after the main shock. B, The main shock contributes approximately 85 percent of the total significant strong motion and its effective duration was about 15 s. Illustration by Mehmet Çelebi. C, Three-story building that houses the YPT accelerograph. Instrument is inside on first floor next to entrance. Upper photograph by Mehmet Çelebi, lower photograph by Thomas L. Holzer.

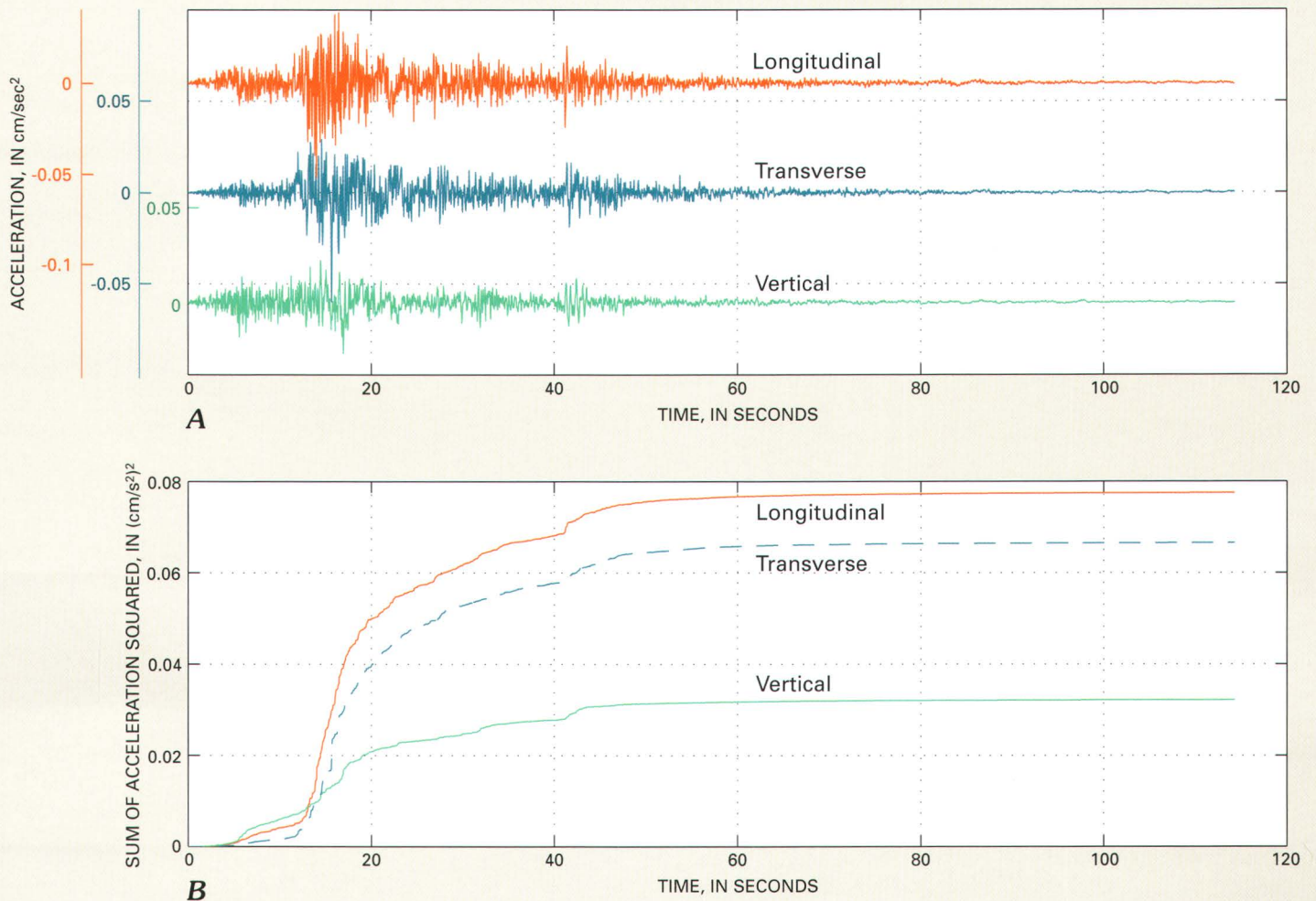


Figure 25. A, Time histories of acceleration at MCK in Istanbul. The plot shows several events. B, the cumulative sum of the squared acceleration values indicates the main shock contributed at least 90 percent of the total significant strong motion and the effective duration of strong motion was 36 s. Illustration by Mehmet Çelebi.

Figures 25A, B show the acceleration time history and the cumulative sum of the squared accelerations of the Mecidiyeköy (Istanbul) record (MCK), an ITÜ station. This station is located on rock.

Figure 26 shows actual and normalized (with respect to zero-period accelerations) pseudo-acceleration response spectra, for north-south and east-west directions, respectively, for 5 stations, DZC, IZT, MCK, SKR, and YPT. Four of the stations (DZC, IZT, SKR, YPT) are in the epicentral area, two of which, (DZC, SKR) are near areas with heavy damage in the eastern part of the epicentral area. The fifth station (MCK) is in Istanbul. Three stations (DZC, IZT, YPT) are on alluvium whereas two stations (SKR, MCK) are on either stiff soil or soft rock. The response spectra reveal different resonant periods at each station. The normalized response spectra indicate that both YPT

and DZC have long resonant periods or low-frequency responses. For comparison, the design spectra for the current Turkish Building Code for soil and alluvial site conditions are also shown in figures 26C, D (Aydinoglu, 1998). For periods between 0.1 and 1 s, the design spectra, which are similar to those used in the United States, were either nearly or actually exceeded during the Kocaeli earthquake. The majority of the structures in the epicentral area were built to a lower design spectra before the 1998 code was implemented. Thus, the strength of many structures would have been insufficient to resist the forces generated by the Kocaeli earthquake even if the structures had been constructed according to existing codes.

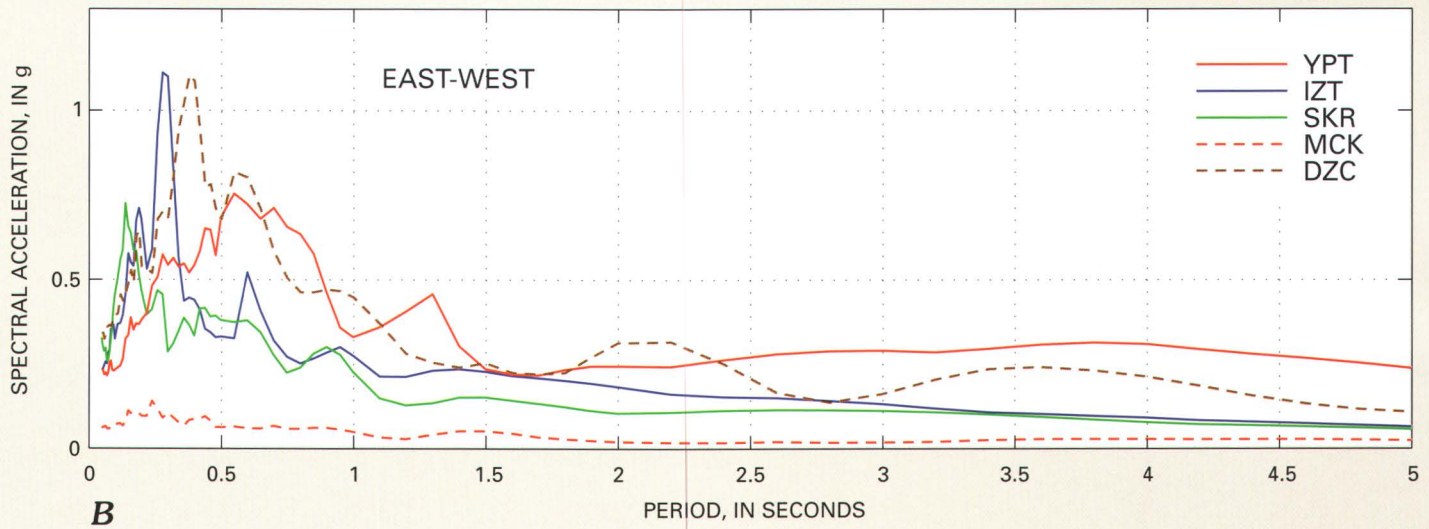
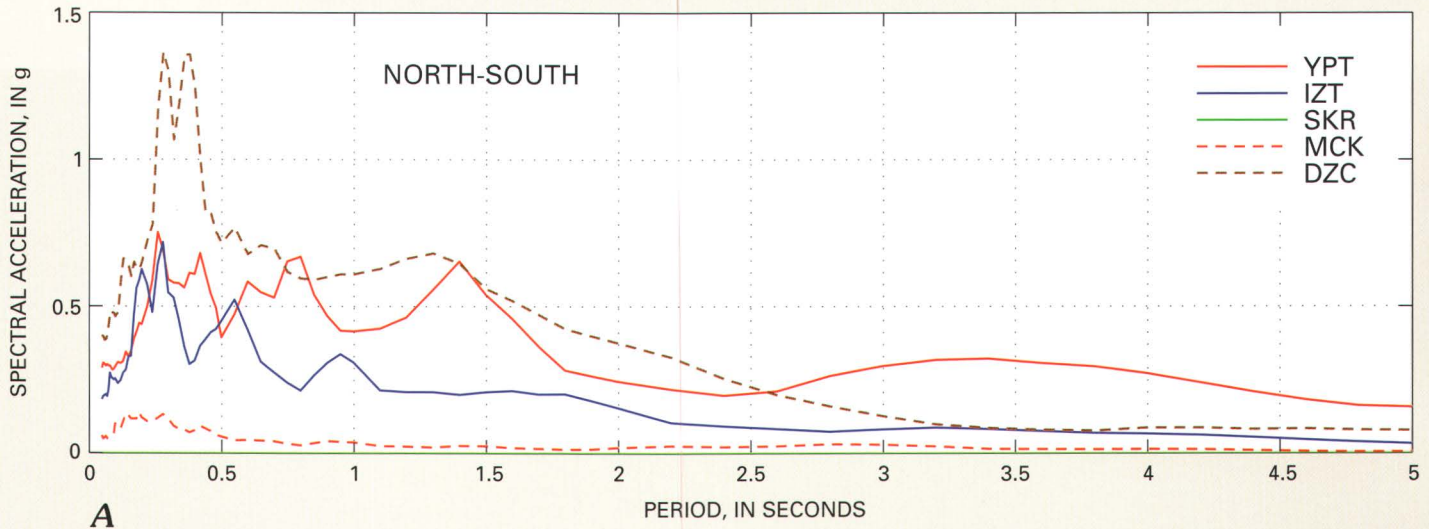
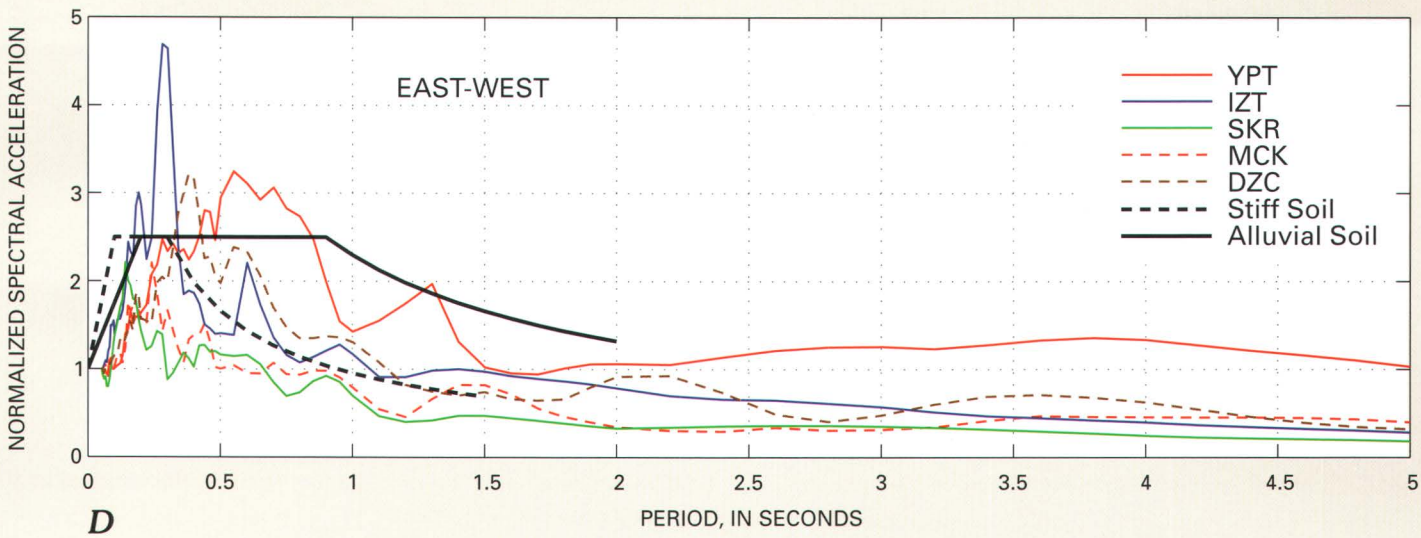
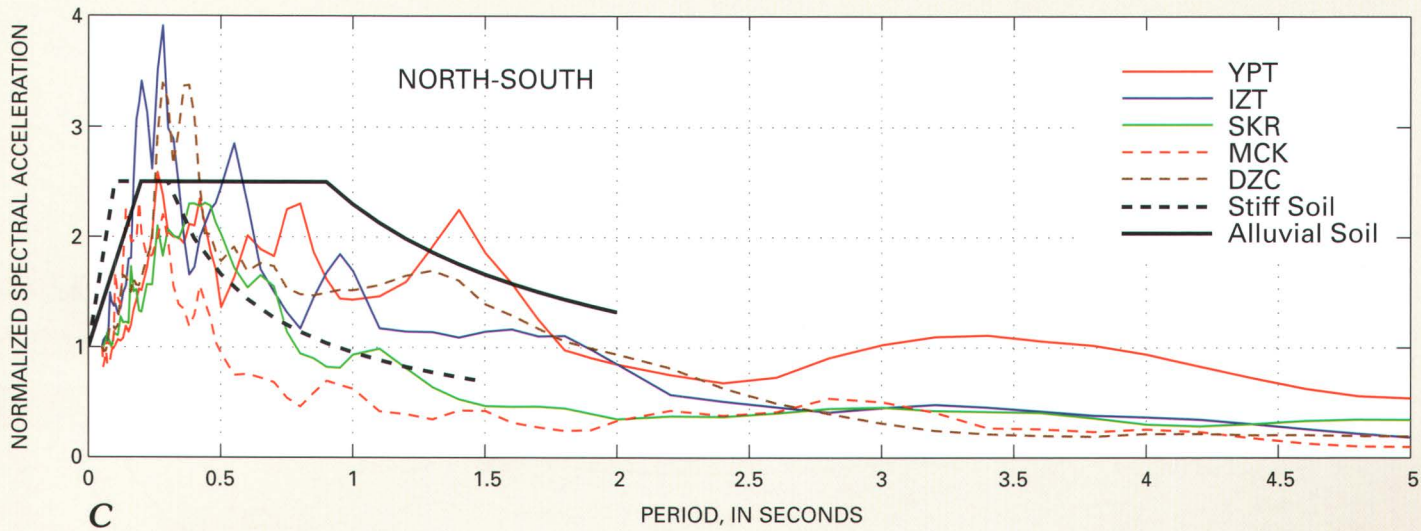


Figure 26. Actual pseudo-acceleration response spectra (A, B) and normalized (with respect to zero-period acceleration) response spectra (C, D) for 5 stations. The normalized response spectra also show the response spectra of the 1998 Turkish Building Code for stiff and alluvial soil site conditions. *Illustration by Mehmet Çelebi.*



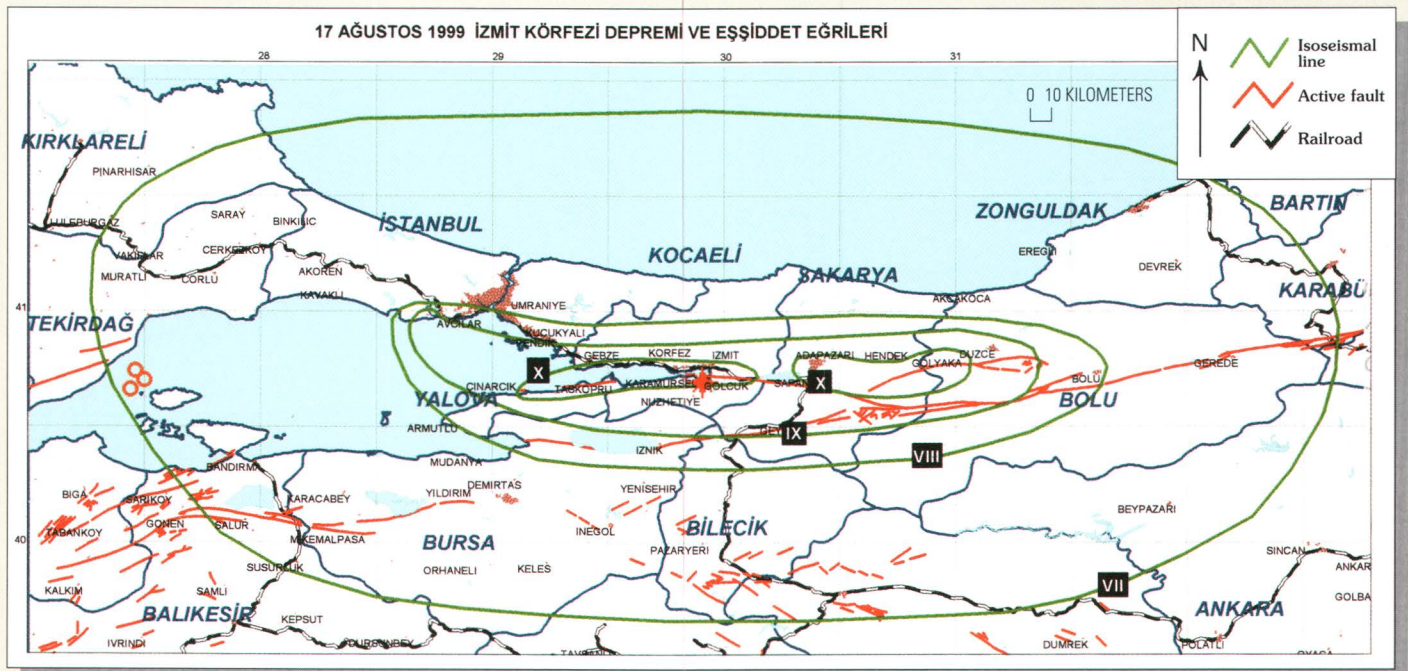


Figure 27. Preliminary isoseismal map of Modified Mercalli intensities (Roman numerals) of the August 17, 1999, Kocaeli earthquake. *Modified from Earthquake Research Department, Directorate for Disaster affairs, Ministry of Public Works and Settlement.*

The small number of strong-motion stations in the epicentral region that recorded the main shock precludes a detailed mapping of ground motions. However, the areal extent of strong shaking can be inferred from mapping damage and reports of felt shaking. The ERD of the Ministry of Public Works and Settlement issued a preliminary Modified Mercalli intensity map in late September 1999, a month after the main event (fig. 27). The Modified Mercalli scale uses observations of damage to infer the intensity of shaking (Wood and Neumann, 1931). About 150,000 km² was shaken at Modified Mercalli intensity VII or greater, intensities that prompt people to run outdoors.

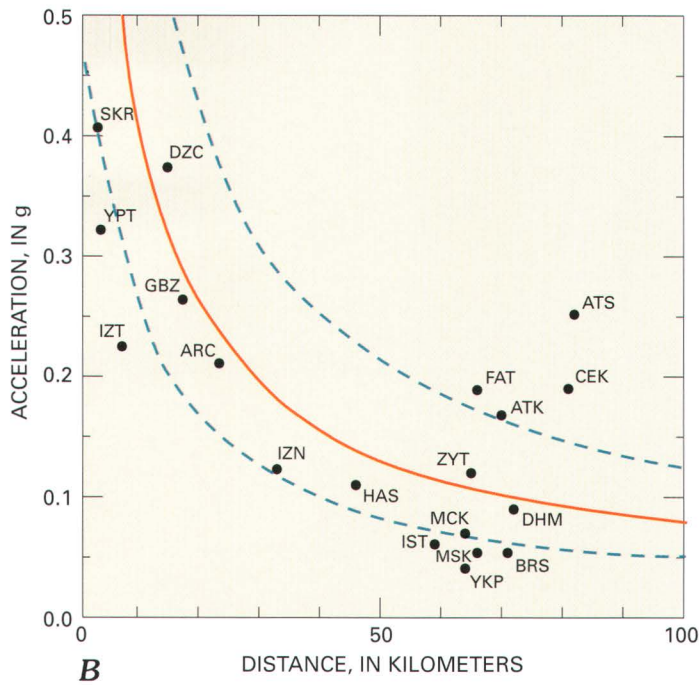
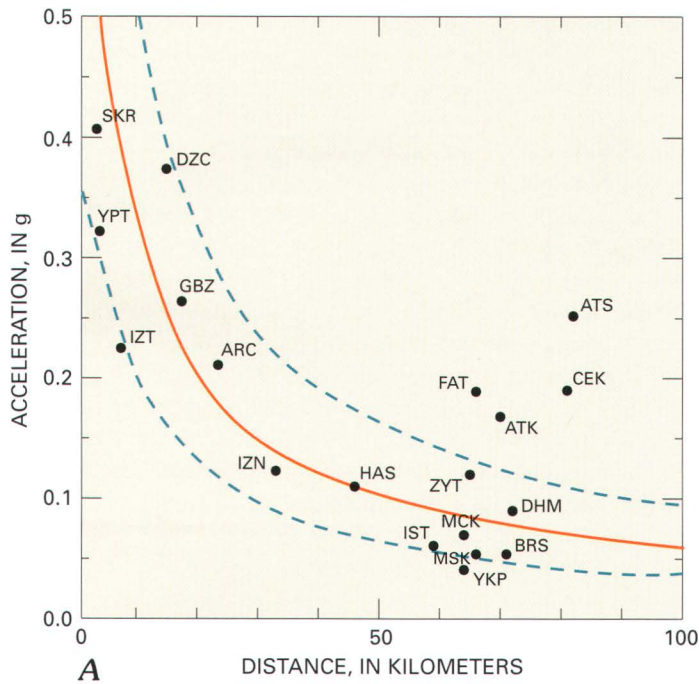
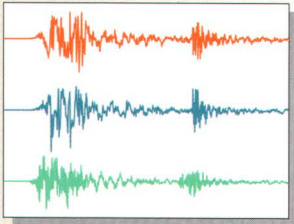


Figure 28. Values of peak horizontal acceleration recorded during the Kocaeli earthquake as a function of distance from the fault compared to values predicted by Boore and others (1994) for a M_W 7.4 earthquake in Western North America. **A**, Values predicted for sites with average shear wave velocities of 760 m/s. **B**, Values predicted for sites with average shear wave velocities of 360 m/s. Uncertainty is shown by the one standard deviation curves (dashed lines). *Illustration by Selcuk Toprak.*

Peak horizontal accelerations from the Kocaeli earthquake for the 19 stations compiled in table 1 are compared to values predicted by the empirical attenuation relation proposed by Boore and others (1994) in figure 28. Their attenuation relation, which predicts how peak accelerations decrease with distance from the surface rupture, is based on regression analyses of peak accelerations recorded in western North America. The comparison suggests that observed peak horizontal accelerations were below average within at least 7.5 km of the fault rupture for an M_W 7.4 earthquake. At greater distances from the fault, the values were more typical of those to be expected for an M_W 7.4 earthquake although values from recorded at distances from 10 to 50 km from surface rupture also are slightly on the low side. One of the factors in the regression is the soil condition at each recording site. Peak ground motions are generally higher at soil sites than rock sites. Because site conditions are poorly documented at most of the strong motion stations in Turkey, values are compared to attenuation curves for two different site conditions. Figure 28A compares the observed values to an attenuation curve for sites underlain by materials with an average shear wave velocity of 760 m/s in the upper 30 m. Figure 28B compares observed values to an attenuation curve for site conditions with an average shear wave velocity of 360 m/s in the upper 30 m beneath the station. The 760 m/s velocity is the boundary between rock and very dense soil/soft rock; the 360 m/s velocity is the boundary between very dense soil/soft rock and stiff soil (Federal Emergency Management Agency, 1998). Based on field inspection of the three stations that are closest to the surface rupture, one (SKR) is estimated to be near the 760 m/s boundary and two (IZT and YPT) are estimated to be near the 360 m/s boundary.

Ground Shaking

Main-Shock Observations



Implications of Aftershock Observations



As was also the case in Turkey, the number of on-scale recordings of the main shock for most large earthquakes is insufficient to evaluate fully the role of geology in localizing damage. Large earthquakes, however, are usually followed by abundant aftershocks and the Kocaeli earthquake was typical in this regard. Because seismic waves from aftershocks and main shocks travel similar paths from source to site, recordings of aftershocks can be used to understand better how geologic conditions impacted local variations in ground shaking and damage during the main shock at sites where the main shock was not recorded. Thus, one of the goals of the team of USGS scientists that went to Turkey immediately following the August 17 earthquake was to use 16 portable, digital seismographs and supporting equipment to help assess how the local geology related to selected damaged areas (fig. 29). Data from the initial visit, from August 24 to September 2, are discussed here. The main objectives of USGS scientists were to study both (1) site effects by comparing aftershock ground motions recorded at sites inside and outside the damage areas, and (2) propagation of the seismic wavefield recorded on small arrays.



Figure 29. USGS scientists deploy an antenna for a portable seismic recording system at Dilovasi. Antenna receives time signals from a satellite and allows the timing on the portable seismographs to be synchronized with each other. *Photograph by Thomas L. Holzer.*

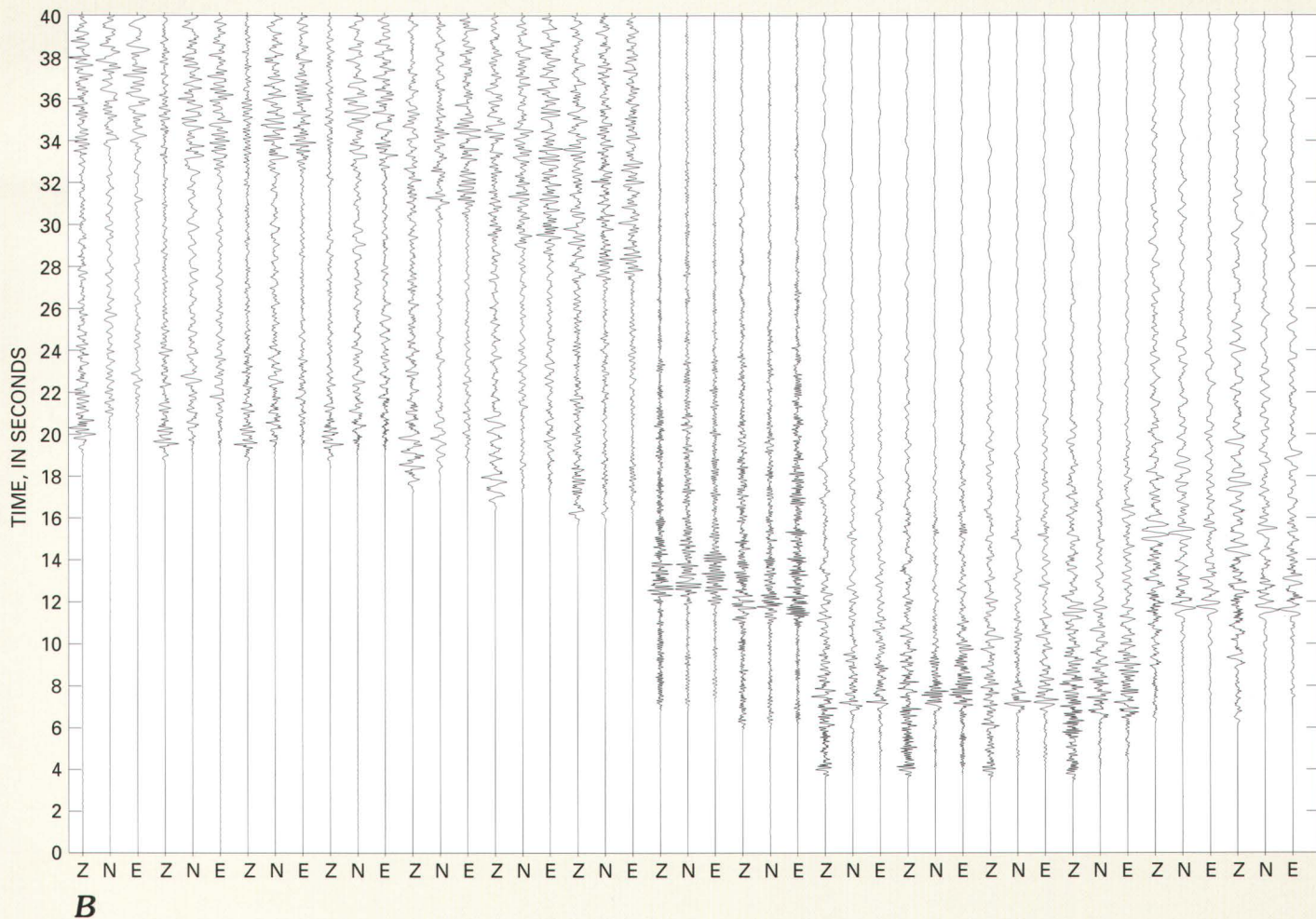
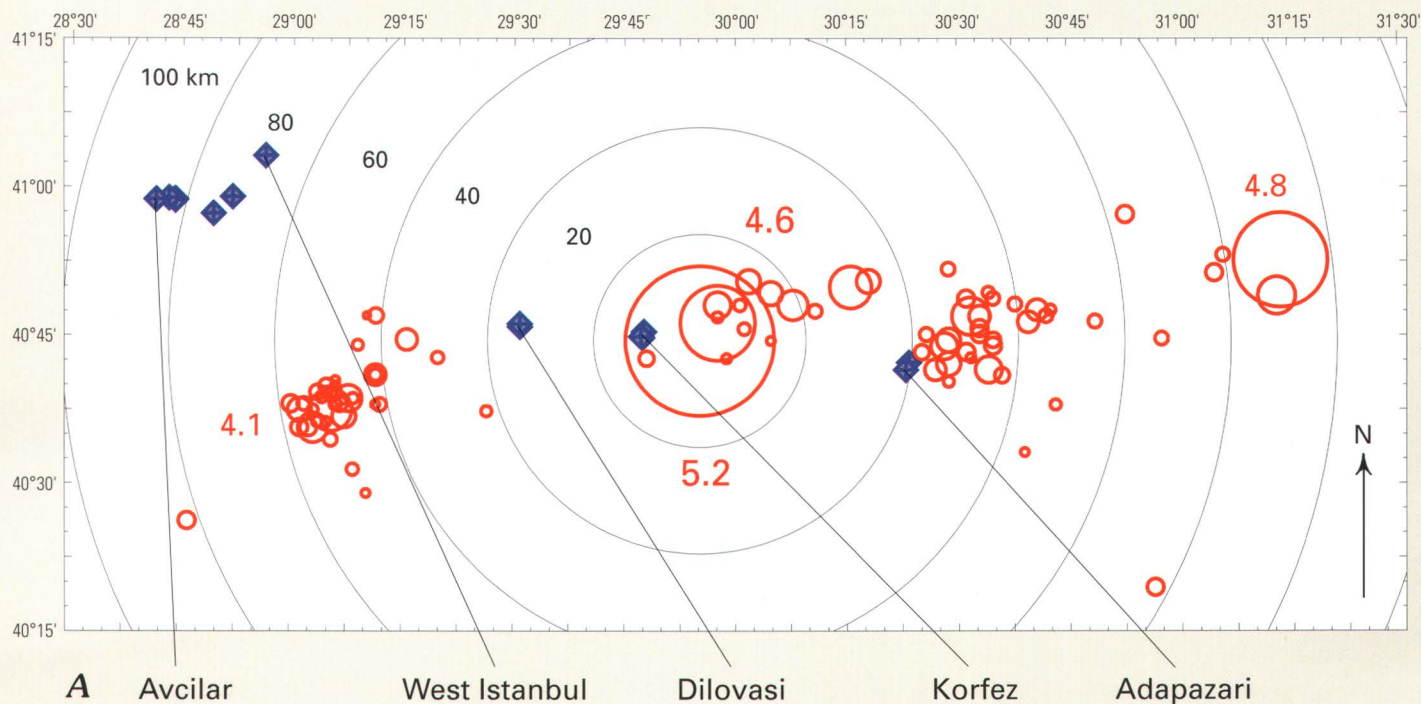


Figure 30. **A**, Map of Kocaeli earthquake aftershock zone and sites of USGS portable, digital seismographs (blue diamonds). Black concentric circles centered on the M 5.2 aftershock epicenter are in 20-km increments. Red circles are aftershock locations and their radii are proportional to their size; the magnitudes of the four largest events are annotated. **B**, The corresponding three components of ground motion for the M 5.2 aftershock recorded at the USGS sites are shown as a pseudo-record section of 40-s duration; Z, vertical, N, north-south, E, east-west. The amplitudes of each trace are normalized to the peak value of that trace. *Illustration by Edward Cranswick.*





Figure 31. Rescue effort 4 days after the main shock at a collapsed building in area of concentrated damage in Avcilar. *Photograph by Thomas L. Holzer.*

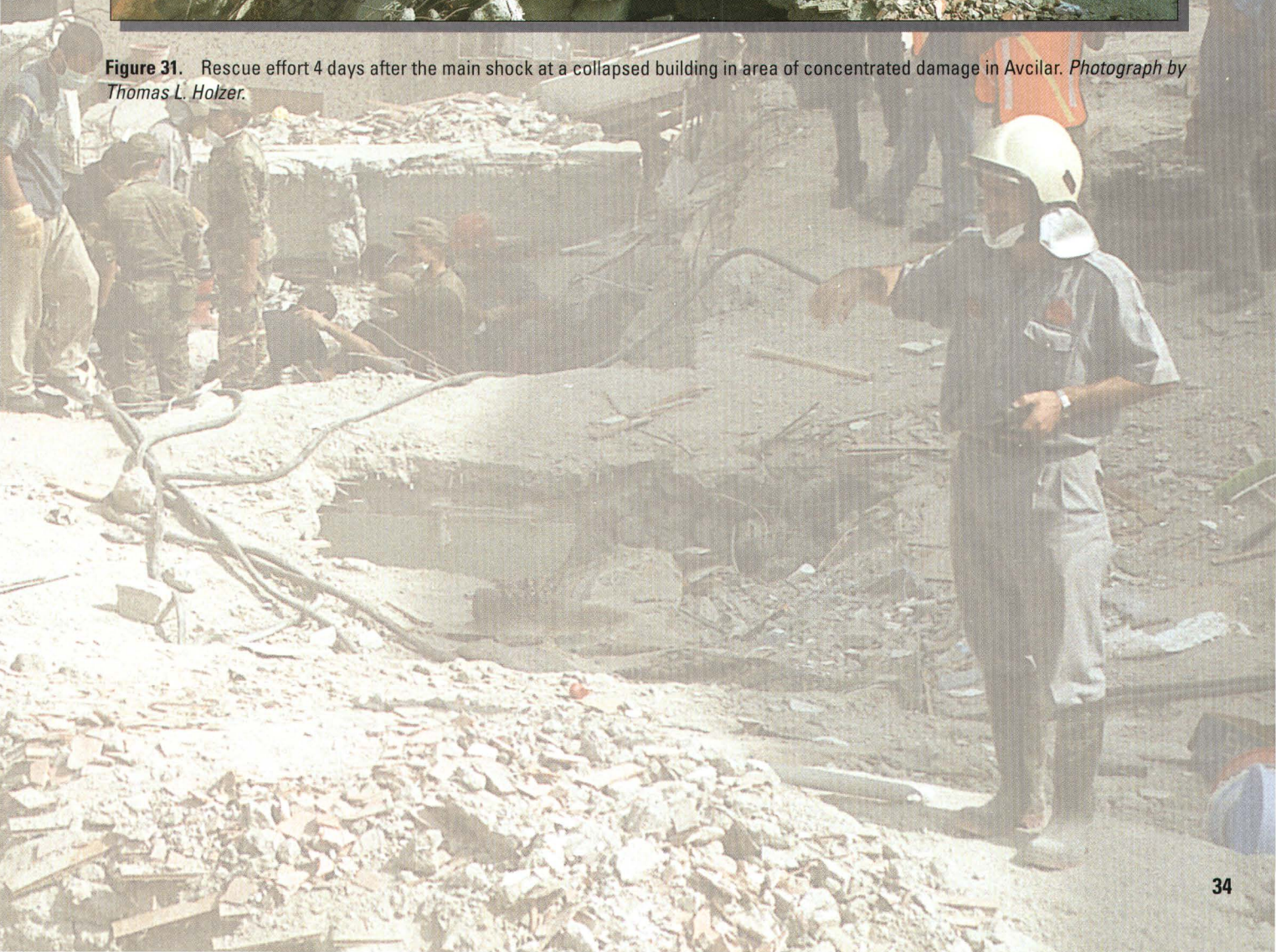


Figure 30A shows the locations of USGS instruments and epicenters of aftershocks recorded by at least one station during the initial visit. The Avcilar district, an area of severe damage, is located west of the Istanbul airport and about 80 km from the end of the main-shock seismic source zone. The damage in Avcilar (fig. 31) was surprising, given its distance from the main shock and the fact that it is surrounded by areas that sustained little damage. Three instruments were located inside the zone of severe damage and four instruments were located in the surrounding area west of Istanbul. Dilovasi, 35 km west of the main-shock epicenter, is the site of planned port facilities and the northern abutment of a planned suspension bridge across the Gulf of Izmit. Two instruments were located in Dilovasi, one on rock and one on artificial fill. Korfez, 10 km west of the main-shock epicenter, suffered severe damage and four instruments were set up, three in a triangle-shaped array on young deposits near the city center (at the TUPRAS campus), and one on older deposits several kilometers away. Adapazari, 40 km east of the main-shock epicenter, was also heavily damaged and three instruments were located in a triangular array in an alluvial valley south of the city center (at the Toyota assembly plant).

Figure 30B illustrates the breadth and quality of the USGS ground-motion data. The plot shows three-component seismograms recorded at selected sites during a magnitude 5.2 aftershock (fig. 30A) on August 31. Figure 32A shows three-component seismograms (low-pass filtered at 4 Hz) recorded at the Dilovasi and Toyota sites recorded during a magnitude 4.1 aftershock (fig. 30A) on August 31. Plotted on a common amplitude scale, these seismograms illustrate two site effects. First, horizontal shaking at Dilovasi is clearly amplified at the seismograph located on fill when compared to the shaking at the seismograph located nearby on rock. Second, shaking is much stronger at the two Toyota plant sites in the alluvial valley south of Adapazari than at Dilovasi, even though the Toyota plant sites are located farther from the epicenter of the aftershock. Figure 32B shows the coherence of low-frequency ground motion (from the magnitude-5.2 aftershock, low-pass filtered at 0.25 Hz) recorded at each station in the triangular array in Korfez. Figure 33A is a map of the Avcilar area showing units of surface geology categorized according to geotechnical properties. Low-frequency ground motion (from the magnitude-5.2 aftershock, low-pass filtered at 0.25 Hz) is strongly amplified at sites in the damage area at Avcilar compared to nearby sites outside the damage area (fig. 33B).

The USGS portable instruments were placed to confirm the importance of local geologic conditions as a mechanism for concentrating damage from shaking. The instruments at Avcilar, Dilovasi, and Adapazari all revealed local amplification of ground motion. The geologic control in Avcilar is of particular concern because, as discussed previously, the earthquake potential south of Istanbul may have been increased by the Kocaeli earthquake. In addition, understanding the specific geologic controls that contributed to damage in Avcilar during the Kocaeli earthquake may provide insight about what can be expected elsewhere in the world. For example, there is a striking resemblance between ground-motion and damage patterns in the Avcilar district in Istanbul in 1999 and the Marina district in San Francisco in 1989 (O'Rourke, 1992). Worldwide, many cities are situated in similar geologic and geotechnical settings.

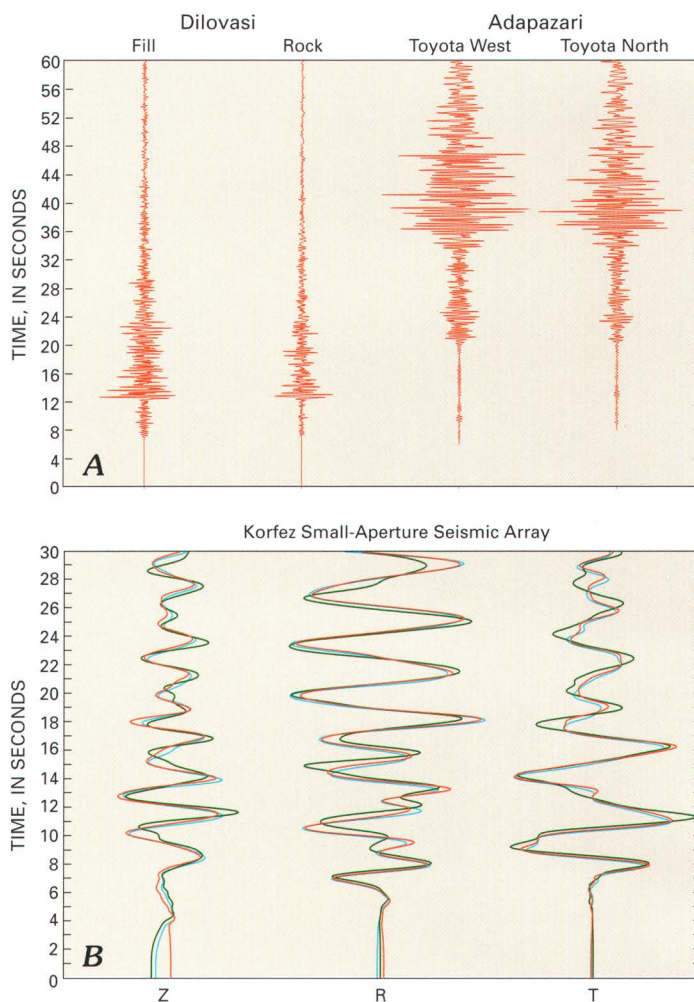
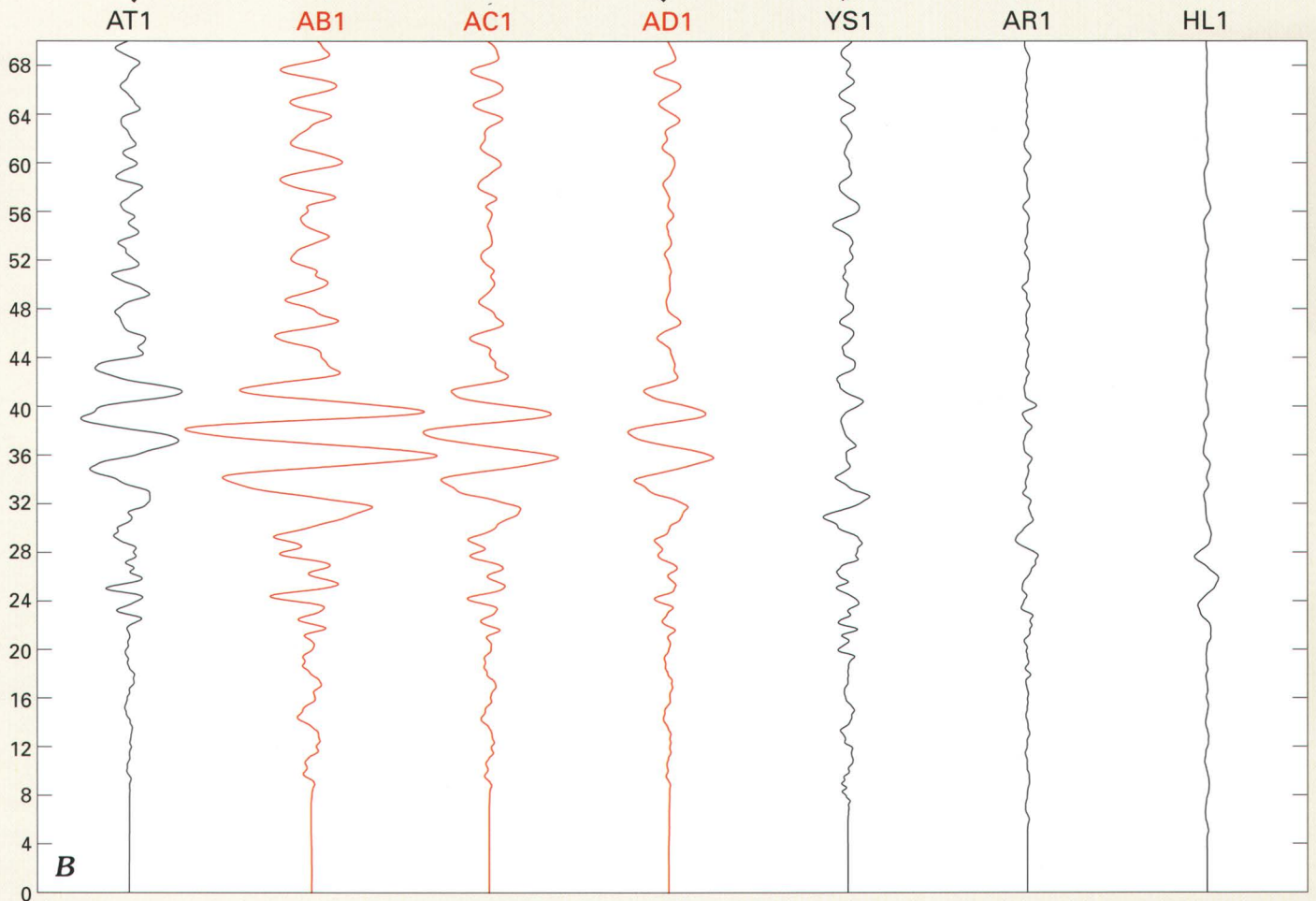
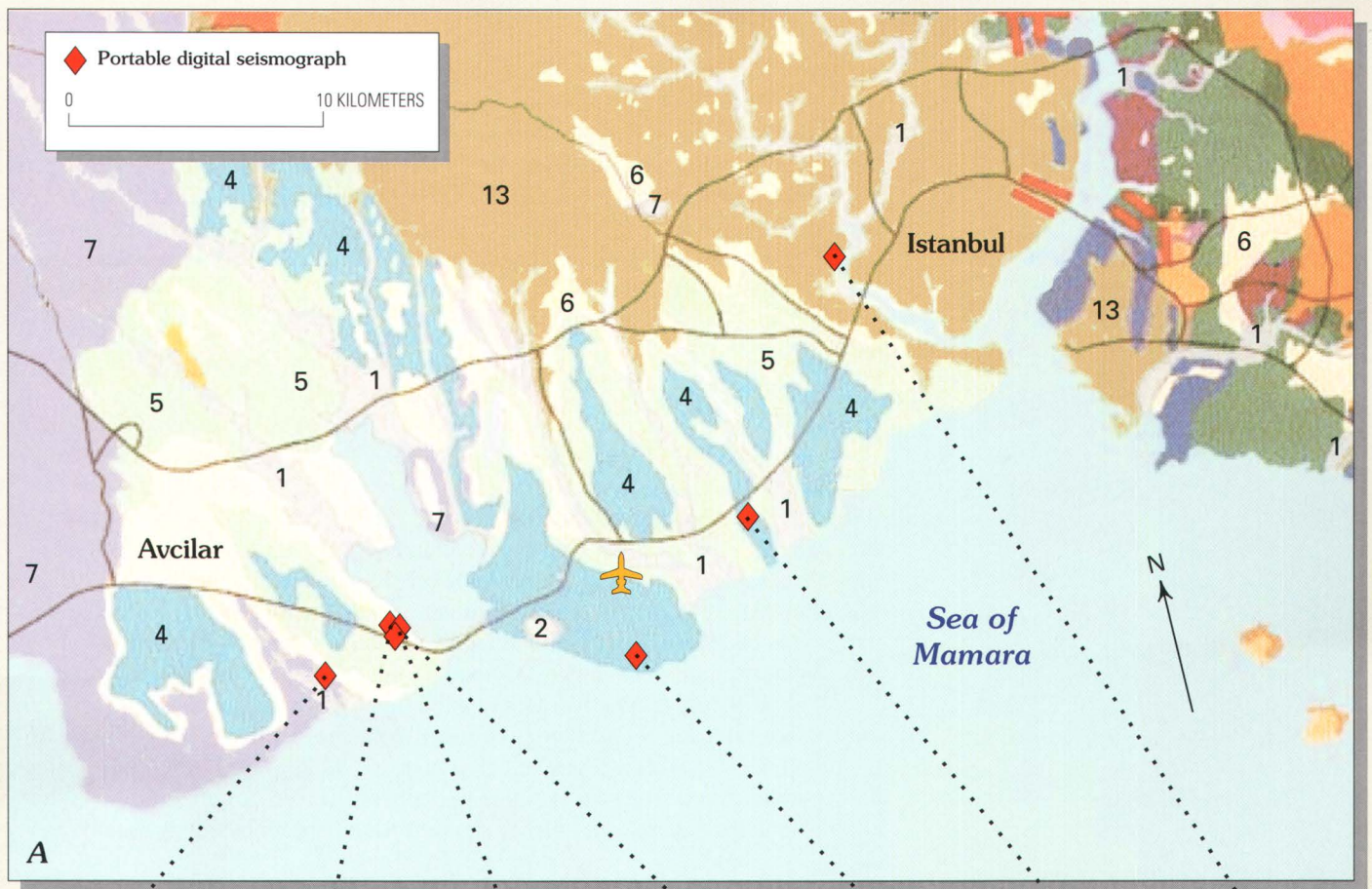


Figure 32. A, Pseudo-record section of ground motions from two pairs of stations at Dilovasi and Adapazari plotted on the same amplitude and time scales. Note the S-minus-P time of the first pair is approximately 5 s and that of the second is approximately 16 s. B, Overlay of Z, R, T components of closely spaced North, South, West stations at Korfez, all traces plotted on the same amplitude and time scales. *Illustration by Edward Cranswick.*

Figure 33 (facing page). A, Geotechnical surface map of Avcilar district and West Istanbul. 1-3, alluvium with low-loading capacities where load capacity increases from 1 to 3 (3 not mapped in this area); 4, alluvium with good loading capacity with weak zones locally; 5, alluvium with low-loading capacity with increase probability of landslides on slopes reaching 14-15°; 6, alluvium with high-loading capacity but landslides may occur where ground water accumulates at bottom of slopes; 7, alluvium with low-loading capacities with known damage to structures; 13, rock with high-loading capacities except on slopes. B, Low-frequency ground motion is amplified at sites in the damage area of the Avcilar district, stations AB1, AC1, and AD1 (in red). Only radial components are displayed. *Illustration by Mark Meremonte.*



Liquefaction



Buildings in several communities, including Adapazari, Gölcük, and Sapanca, sank or settled into the ground during the August 17, 1999, earthquake. In areas where buildings sank, surface manifestations of liquefaction, a process by which shaking during an earthquake causes saturated sandy materials to become fluidlike, were observed. The observed surface manifestations include sandy subsurface materials that vented to the surface, features known as sand boils, and lateral shifting of the ground, a process known as lateral spreading.

Settling of buildings was widespread in the city of Adapazari. Hundreds of buildings were affected; in many city blocks, the majority of buildings sank. Buildings in Adapazari locally sunk as much as 1.5 m (fig. 34). The part of Adapazari in which buildings settled is an area built on young flood-plain deposits of the Sakarya River that has a shallow ground-water table. Although most buildings simply sank upright into the soil, a few were also overturned, which exposed their foundations (fig. 35). The sunken buildings in many cases were less damaged from shaking than adjacent buildings that were on soils that did not liquefy during the earthquake. In addition, items on shelves in many stores in the settled buildings were not even dislodged. This suggests that once the foundation soils liquefied, seismic waves were unable to propagate through the liquefied soil and shake the buildings that settled as violently as adjacent buildings on nonliquefied soil. Sand boils were the primary surface evidence of liquefaction (fig. 36); these sand boils vented onto sidewalks adjacent to buildings and into first floor of buildings that settled. Many sidewalks around the buildings that settled were heaved upward, indicating that liquefied material was pushed outward from beneath buildings as they sank



Figure 34. Building in Adapazari that sank 1.5 m uniformly into the ground when the soil beneath it liquefied and was pushed outward from beneath the building. Magnitudes of sinking were proportional to weight of building. *Upper photograph by Thomas L. Holzer; lower photograph by National Institute of Standards and Technology.*



Figure 35. Buildings in Adapazari that either toppled or partially overturned because soil beneath them liquefied and weakened the foundation. *Upper photograph by Thomas L. Holzer; lower photograph by Richard S. Olsen.*



Figure 36. Sand boil on sidewalk in Adapazari. Sand ejected from underground when sandy soils beneath the ground-water table liquefied during the earthquake. *Photograph by Mehmet Çelebi.*

into the ground. These buildings sank due to soil bearing failure associated with the loss of strength caused by liquefaction. Settling also appears to be proportional to the weight of the building; multistory buildings sank more than adjacent single-story buildings. Delayed building settlements were also reported for foundations of silt that developed high pore pressures, but only experienced marginal liquefaction.

Along the southeast shore of Lake Sapanca, soils also liquefied and the Lake Sapanca Hotel was dramatically affected. The hotel, which was built on an old stream delta that had prograded into Lake Sapanca, sank about 0.3 m into the ground. The regional land surface around the hotel also lowered causing the shoreline to submerge (figs. 37, 38). In addition, the hotel was displaced about 0.5 m toward the lake by a lateral spread along the shoreline of the lake. Large quantities of subsurface sand vented to the surface and covered much of the driveway and the landscaping around the hotel.

Minor sinking of buildings occurred along the shoreline of Izmit Bay in Gölcük. A few multistory buildings sank about 0.1 m. Sand boils and lateral spreading, which caused parts of the coastline to move bayward less than 0.5 m, were observed and provide evidence of liquefaction along the coast. In the eastern part of Gölcük, a broad regional subsidence occurred. The subsidence was believed to be tectonic because it was bounded by the normal fault described previously. The fault-bounded tectonic subsidence caused a 4-km-long section of the coast near Gölcük to submerge about 2 to 3 m.

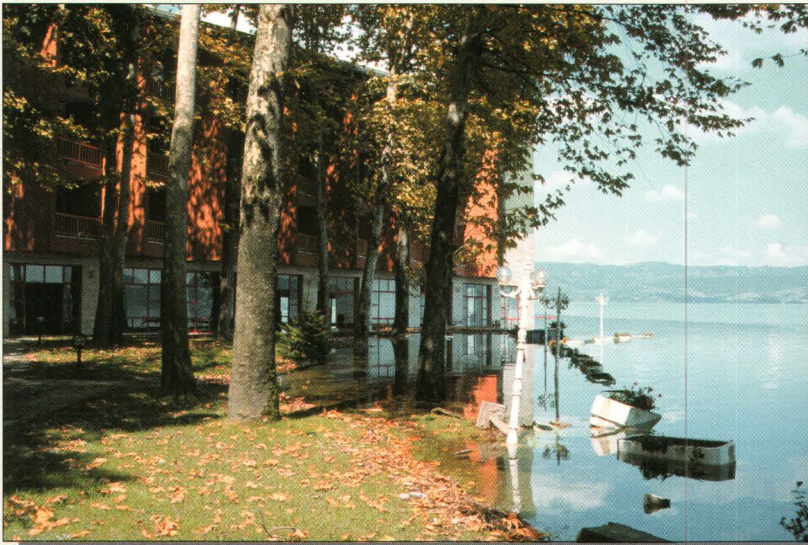


Figure 37. Submergence of shoreline at Lake Sapanca and settlement of Sapanca Hotel. "Moat" adjacent to wall indicates the hotel has sunk into the ground because of liquefaction of underlying sandy soil. *Photographs by Thomas L. Holzer.*





Figure 38. Sunken entryway into Sapanca Hotel created when building sank into liquefied soil. *Photograph by Thomas L. Holzer.*

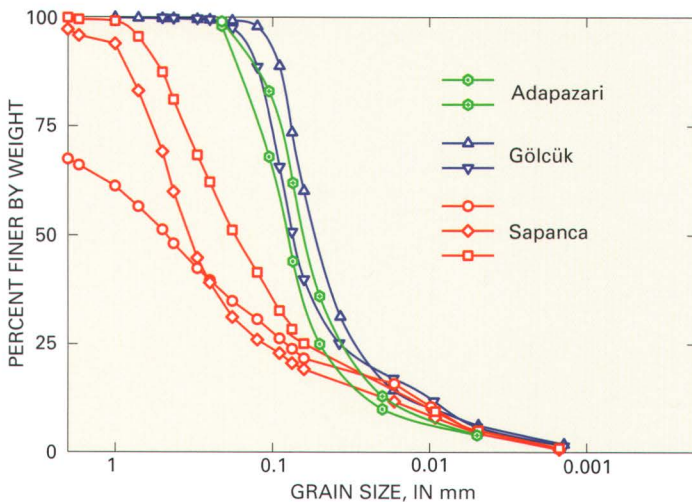


Figure 39. Grain-sized distributions of sand boils sampled near sites of sunken buildings in Adapazari, Gölcük, and Sapanca. Vertical axis is percent of sample by weight finer than the grain size shown on the horizontal axis. *Illustration prepared by Michael J. Bennett. Data from USGS and ERDC.*

Sand boils were sampled at Adapazari, Gölcük, and Sapanca. Liquefied material was predominantly fine grained; grain-size distributions of the material typically ranged from silts to silty sands (fig. 39). The two coarser sand boils sampled at the Sapanca site contained cobbles and other coarse-grained material. These sand boils may have been contaminated with cobbles contained in the base of a driveway. The other sand boil at Sapanca was in an open area and not susceptible to contamination.

Sunken and overturned buildings have been observed in other large, greater than 7, magnitude earthquakes, including the 1964 Niigata, Japan, and 1990 Philippines earthquakes. Magnitudes of sinking of buildings during smaller, less than 7, magnitude earthquakes typically have been small. In general, the duration of strong shaking is proportional to earthquake magnitude. These observations suggest that the magnitude of sinking is dependent not only on the weight of the building but on the duration of strong shaking, which both keeps the liquefied soil in a fluid state and potentially liquefies a greater thickness of soil.

Performance of the Built Environment

Buildings



The region hit by the Kocaeli earthquake is the industrial heartland and one of the most densely populated sections of Turkey. Official government estimates of damaged living and business units (as of October 19, 1999) indicate the magnitude of the human disaster. More than 77,000 living units were heavily damaged, more than 77,000 were moderately damaged, and about 90,000 were lightly damaged. All of the heavily damaged and most of the moderately damaged living and business units are in buildings that are beyond repair and will probably be demolished. The region with heavy damage extends from Yalova, which is 50 km west of the epicenter, to the town of Düzce, which is 100 km east of the epicenter. The majority of the building collapses and deaths occurred in small towns located on the narrow flat shorelines of the Sea of Marmara. There was also heavy damage and loss of life in Adapazari, which is located on the flood plain of the Sakarya River. A small western suburb of Istanbul, Avcilar, located near Istanbul Atatürk airport, suffered about 1000 fatalities from collapsed buildings despite the unusually large distance (about 80 km) from the seismic source zone.

Most residential construction in the affected region of Turkey consists of reinforced concrete frames (column-slab systems) with masonry infill. Multistory residential buildings, as well as buildings containing commercial space on the first floor and residential units above, use this type of construction. The reinforced concrete frame buildings that suffered severe structural damage or complete collapse were typically four to eight stories in height. Many of the collapsed buildings appeared to be relatively new and indeed some were either under construction or recently completed, but not yet occupied at the time of the earthquake.

Figure 40 shows a building under construction illustrating common construction practice. In most cases of building collapse, there was no evidence of shear walls. Consequently, lateral resistance to the strong ground shaking was provided solely by frame action. Concrete compressive strength was not measured, but honeycombing was observed in similar new construction that did not collapse suggesting somewhat poorer concrete placement practices than typically found in U.S. construction. Furthermore, undeformed reinforcing bars were widely used for both flexural and shear reinforcement, a practice not permitted under U.S. building codes. Most of the reinforced concrete buildings can be characterized as having little or no ductility.

Trans European Motorway (TEM)



Earth Dams

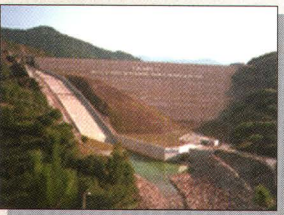




Figure 40. Building in Izmit under construction using reinforced concrete frame construction. Note absence of shear walls. *Photograph by National Institute of Standards and Technology.*

The most common type of structural failure observed throughout the affected regions was shear failure of first-story columns. In many instances, the first story collapsed while the upper stories remained relatively undamaged as seen in the 5-story apartment building in Yalova shown in figure 41. In other instances, shear failure of intermediate columns triggered partial collapse of the buildings as illustrated in figure 42. Hinging of first-story columns was also observed (fig. 43).

In Adapazari, part of which is situated on soils that liquefied during the ground shaking, many buildings sank due to soil failure as previously discussed. Figure 34 shows several commercial buildings that sank and heaved the surrounding brick sidewalk. In other instances, soil failure contributed to overturning of buildings with narrow footprints as seen in figure 35.



Figure 41. Partial building collapse in Yalova as the result of shear failure of first story columns. *Photograph by National Institute of Standards and Technology.*



Figure 42. Partial collapse of building near Izmit as the result of shear failure of intermediate columns. Note various stages of damage despite apparently similar construction. *Photograph by National Institute of Standards and Technology.*



Figure 43. Near collapse of building in Adapazari as the result of formation of column hinges in the first story. *Photograph by National Institute of Standards and Technology.*



Figure 44. Damage to Officer's Club on Turkish Naval Base, Gölcük, which was located directly on the surface fault rupture. *Photograph by National Institute of Standards and Technology.*

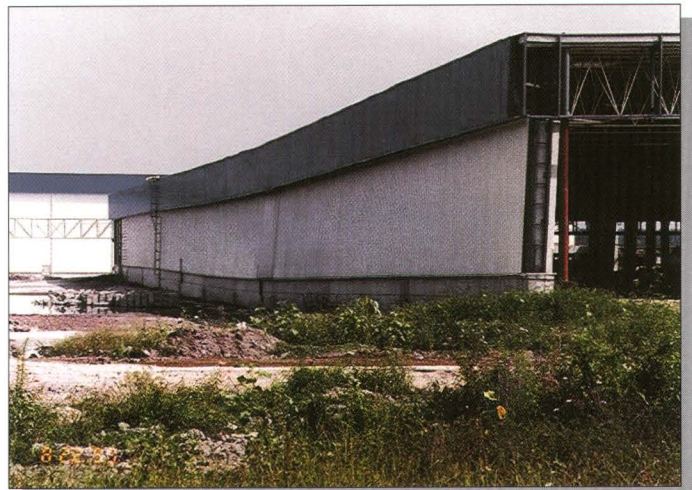


Figure 45. Industrial building damaged by near-fault ground movements east of Gölcük. Building is on downthrown block of normal fault and near a major change of strike in the surface fault scarp. *Photograph by National Institute of Standards and Technology.*

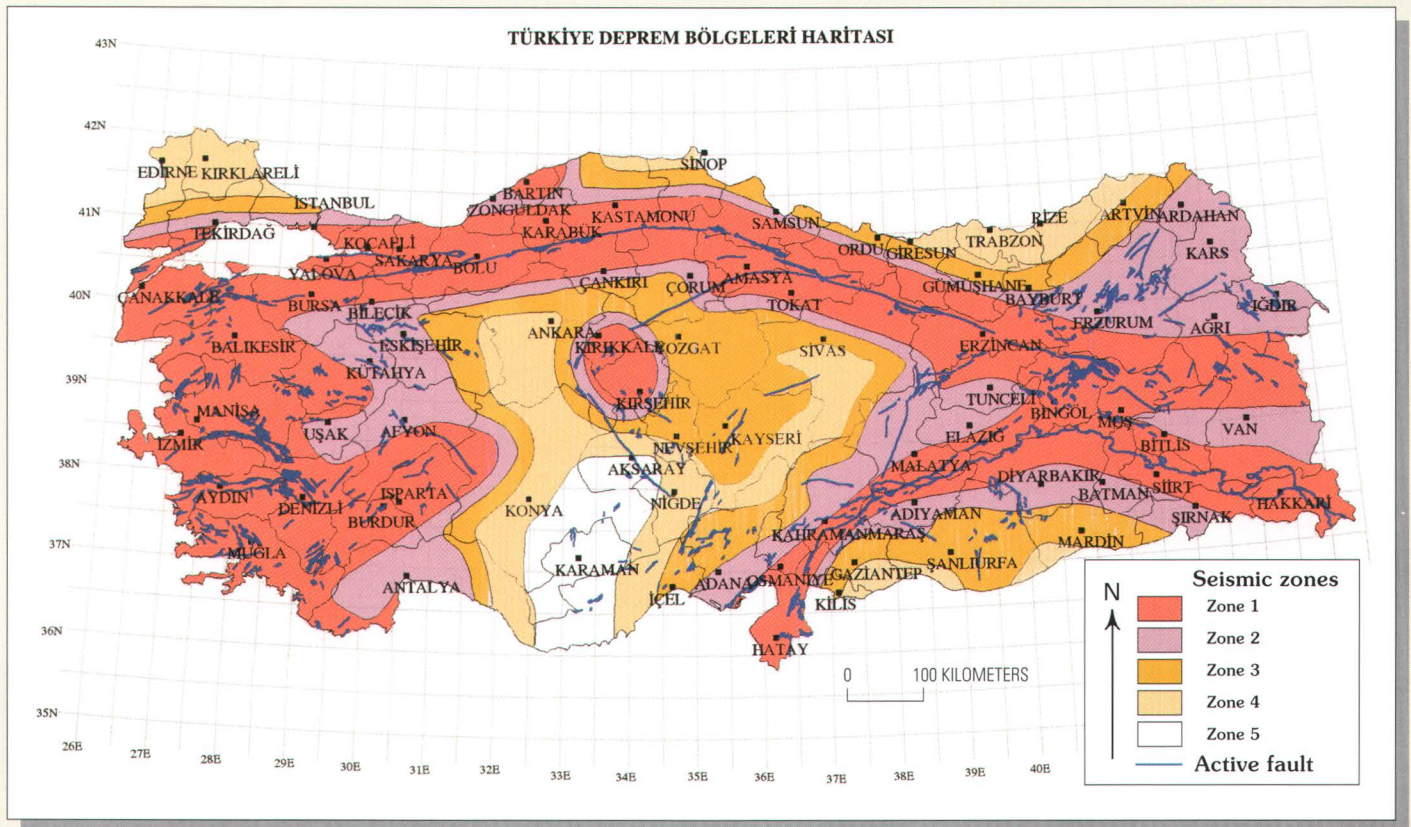


Figure 46. Modified earthquake zoning map of Turkey. Modified from Earthquake Research Department, Directorate for Disaster Affairs, Ministry of Public Works and Settlement.

Locally, surface fault rupture caused collapse of or damage to many structures. The majority of structures directly atop the rupture either collapsed or were seriously damaged. One example of fault damage is the Officer's Club located on the Turkish Navy Base at Gölcük (fig. 44). Lateral displacement of more than 2 m was observed in the portion of the building directly over the fault resulting in significant damage, while adjacent sections of the building fared better exhibiting less damage. Differential ground movement adjacent to fault rupture was also responsible for building damage in a few cases as seen in figure 45. An industrial building under construction was deformed by approximately 0.5 m of differential settling associated with a change in strike of the trace of a normal fault that ruptured during the Kocaeli earthquake.

Turkey has adopted modern building codes with up-to-date seismic design provisions. According to the Turkish seismic zone map, the areas affected by the Kocaeli earthquake are in the zone of highest risk (fig. 46). Although only examples of severe damage and collapse have been reported here, many buildings in the affected areas performed well with little or no apparent damage. Indeed, on figure 42, three buildings, one of which collapsed completely, one of which suffered partial collapse, and one of which appears to be relatively undamaged are visible. The absence of shear walls, deficient detailing around beam-column joints, and use of smooth rather than deformed steel reinforcement may have contributed to the extent of damage and collapse by reducing the ductility of the buildings. However, the heavy

damage or collapse of some buildings where nearby buildings of similar size, configuration, and construction survived relatively intact, suggests that the poor performance of some buildings may be traced to failure to design or construct in compliance with established building codes. The contrasting performance between similar buildings that survived and those that collapsed or were heavily damaged illustrates that modern building codes, when complied with, can help prevent or limit disaster.

The Kocaeli earthquake also demonstrated the hazard posed by aftershocks to buildings following a large earthquake. Figure 47 shows a building in Gölcük before and after it collapsed during a M_W 5.9 aftershock on September 13. This aftershock, which was the largest magnitude aftershock at that time to follow the August 17 earthquake, killed 7 people, injured at least 239 people, and caused dozens of buildings to collapse in three cities near the epicenter.

Figure 47 (pages 45–46). Multistory residential building in Gölcük. Tectonic subsidence associated with faulting in the main shock caused the inundation of the first floor of the building. Upper photograph shows building standing after the August 17 main shock and before it collapsed in an aftershock; photograph by Thomas L. Holzer. Lower photograph shows building collapsed by M_W 5.9 aftershock four weeks after the main shock; copyrighted photograph by AP/Wide World Photos, used with permission.





Performance of the Built Environment

Buildings



Trans European Motorway (TEM)



In 1985, Turkey initiated an ambitious national motorways program along its most heavily used transport corridors. This program has cost more than \$13 billion and included planned construction of 1,900 km of motorway. Approximately 1,600 km of motorway have been completed. The Trans European Motorway (TEM) is an important part of the motorway system, which connects Asia to Europe. The TEM runs westward from Ankara, the capital city of Turkey, to Turkey's border with Bulgaria and Greece, where it connects to other European highways.

The TEM was constructed following a modern construction code similar to the American Association of State Highway and Transportation Officials (AASHTO) standard. As such, its performance during the Kocaeli earthquake may provide some insight into how American highway systems will perform in similar situations.

Immediately following the August 17, 1999, earthquake, the section of the TEM east of Izmit was closed because large cracks and areas of settlement on the roadway, one collapsed overpass, and the need to inspect all of the bridges. Temporary repairs were made and the TEM was reopened to the traffic after three days. In some areas, however, traffic was limited to two-way traffic on one side and speed limits were imposed while repairs continued (fig. 48). Most repair work was completed within 18 days following the earthquake and the TEM returned to normal operation.

Statistics for damage sustained along the TEM between Camlica, Istanbul and Gumusova, Bolu are summarized in table 2. Although a significant portion of the TEM is in the area strongly shaken by the Kocaeli earthquake, damage to bridges along the motorway was restricted to the section between 5 km west of Izmit and the Sakarya River. Densification of dry roadway fills and bridge and culvert approaches locally caused settlements of the roadway surface in the section extending from about Izmit to 50 km east of Izmit. At several locations, surface faulting along the North Anatolian fault offset the TEM (fig. 49). The TEM runs parallel to the North Anatolian Fault on the south side of Lake Sapanca.

Earth Dams

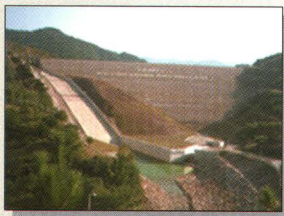


Figure 48. Following the earthquake, road surface repairs forced alternative use of the eastbound and westbound lanes of the Trans European Motorway as a two-way highway with greatly reduced speeds from Izmit to about 50 km east of Izmit. *Photograph by Thomas L. Holzer.*



Figure 49. The North Anatolian fault, which crossed the Trans European Motorway at several locations in Turkey, caused major disruptions to the roadway surface. *Photograph by Robert K. Langridge.*

Strong ground shaking caused slight to moderate damage to bridges and overpasses. The most common types of damage were displacements of girders at seatings, shear key failures, and cover concrete spalling of deck around abutments. For example, at the Cinarlidere viaduct both shear key failure and cover concrete spalling of deck around an elastomeric bearing pad are visible (fig. 50). Additional instances of cover concrete spillings of deck were observed as a result of the deck pounding the abutment.

At the Sakarya River viaduct, bearings were unseated and the bridge carrying the westbound lanes of the TEM over the

Sakarya River had to be closed to traffic for repairs.

The damage was more significant at the east abutment side of the bridge.

Approximately 50 cm of transverse displacement of the span with respect to the east abutment is visible on figure 51. This was the

largest permanent displacement caused by shaking at the TEM bridges. As a result of strong ground shaking, shear keys failed and the span was unseated. The adjacent bridge carrying the east-bound lanes of the TEM sustained less damage and remained fully operational.

Concrete spalling: Pieces breaking off the surface of main concrete structure.

Shear key: Concrete structure at abutments that inhibit transverse and longitudinal seismic movements of girders.

Soil densification: Decrease in volume of a block of granular material.

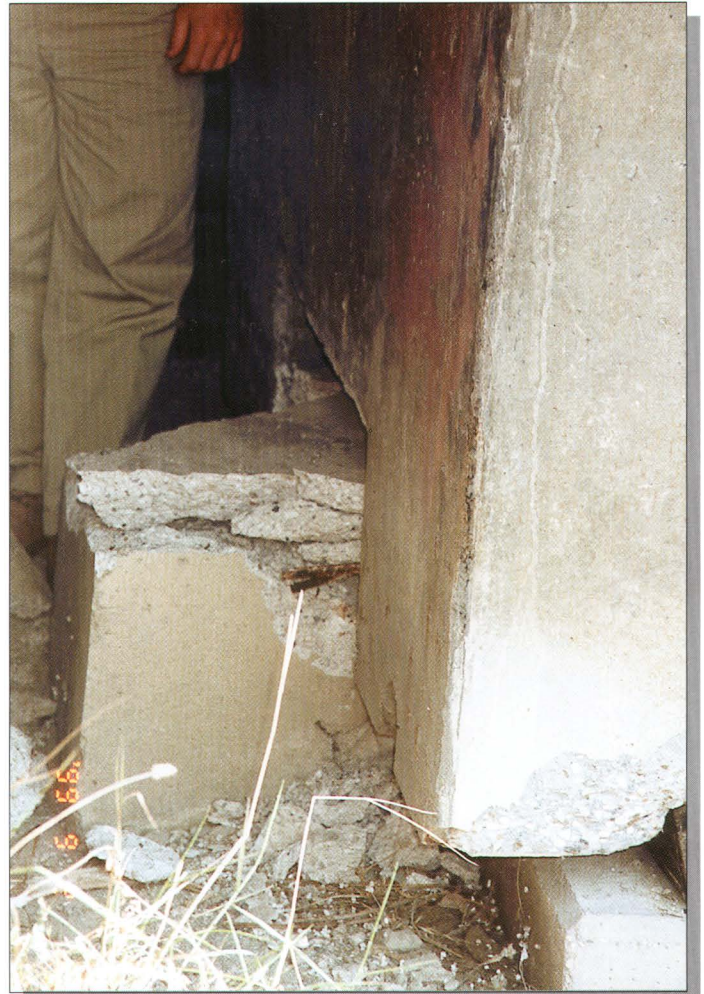


Figure 50. Failure of shear keys was common at bridges of the Trans European Motorway. Shear keys at the end of girders prevent transverse and longitudinal seismic movements. *Photograph by Selcuk Toprak.*

Table 2. Statistics for earthquake damage along Trans European Motorway between Camlica and Gumusova, Turkey.

Motorway feature	Total	Damaged
Roadway	183 km	50 km
Tunnel	4	---
Viaduct	28	4
Overpass, underpass, and stream bridges	143	8
Overpass, underpass, and stream bridge approaches (differential settlement)	143	26

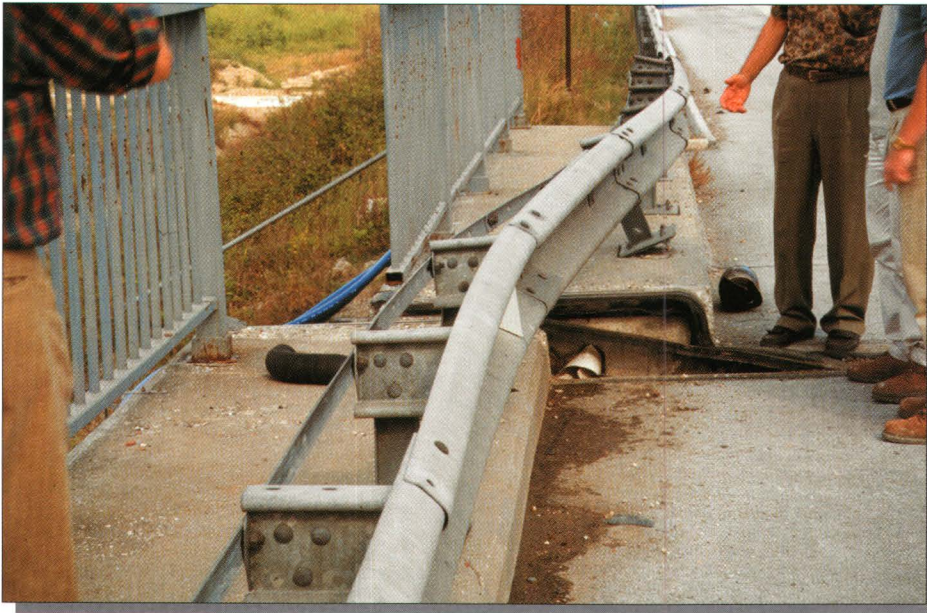


Figure 51. Ground shaking caused the westbound span of the Sakarya River bridge to displace 50 cm relative to the east abutment. This was the largest permanent displacement caused by shaking at any bridge. *Photograph by Selcuk Toprak.*

Figure 52. Densification of dry approach fill adjacent to bridges of the Trans European Motorway was widespread and caused disruption of the roadway. Immediately following the earthquake, Turkish highway engineers placed asphalt ramps on the roadway to reduce the hazard. *Photographs by Thomas L. Holzer.*





Figure 53. The Arifiye overpass collapsed because the surface fault rupture passed directly through its north abutment (foreground). Ten riders of a bus were killed when the bus collided with the collapsed overpass. *Photograph by Thomas L. Holzer.*

Permanent ground displacements, such as extensive cracks and settlement, caused significant damage to the roadway surface. Approximately 50 km of the TEM required resurfacing. Densification of dry fill commonly caused settlements in areas where the motorway approached bridges, viaducts, and culverts; some areas settled as much as 0.3 m. Figure 52 shows one example of settlement.

The surface fault crossed the TEM at several locations and caused the collapse of the Arifiye overpass (fig. 53). Field observations revealed that the fault rupture passed directly beneath the north end of the overpass. Fault displacement along the fault near the overpass was 3.6 ± 0.3 m. This large fault displacement caused the spans to fall to the ground. Immediately after the collapse, a bus crashed into one of the fallen spans killing 10 people.

Performance of the Built Environment

Buildings



Four major dams within 45 km of the fault rupture were visited by the team from the Engineer Research and Development Center of the U.S. Army Corps of Engineers (fig. 54). Two dams north of the Izmit Bay, Omerli Dam and Darlik Dam, were in the area where ground motions were inferred to be less than 0.2 g. Two other major dams south of Izmit Bay, Kirazdere (Yuvacik) Dam and Gokce Dam, were in the area where peak ground accelerations were inferred to be equal to or greater than 0.2 g. Kirazdere Dam is about 4 km from the causative fault. The dam may have experienced peak horizontal motions of 0.3 to 0.4 g. Gokce Dam is in the area of considerable damage and numerous aftershocks in the area of Yalova. Gokce Dam may have experienced motions of at least 0.2 g or greater (table 3).

Omerli Dam holds the primary water reservoir supplying the Asian side of Istanbul, that part of the city that lies on the east side of the Bosphorus. The soil and rock dam is of critical importance for Istanbul. The reservoir at the time of the inspection was 5 m below the spillway invert. The upstream face of the dam is composed of rocks as large as 1 m in diameter. The downstream area of the dam is covered with grass with shrubs as high as 1 m. No cracking was observed during the site visit or by the guard who was at the dam the morning after the earthquake. There may have been water seepage at the downstream toe because the observed type of vegetation requires lots of water. No seepage or effects of seepage were seen at the junctions of the embankment to the valley wall. The upstream slope down to the reservoir level is not uniform. Specifically, just above the reservoir level, the upstream slope had a “bump.” The non-uniform “bump” had an approximate height of 2+ m and a length along the slope of 5 m. It is not known if the feature was caused by shallow slumping during the earthquake.

Darlik Dam is composed of a rock-filled shell with a clay core. The upstream and downstream faces are composed of 1-m-diameter angular rock. The reservoir level during the earthquake appears to be at 60 percent capacity relative to the spillway invert. The access to the crest of the dam was from a road on the downstream slope. No damage or deformation was observed at Darlik Dam. No cracks on either the asphalt crest road or adjacent gravel side were observed during the site visit or reported by the manager of the dam. The upstream and downstream face of the dam appeared to be very uniform when observed from the crest and downstream toe. No movement or cracks were observed on the access road. There was also no evidence of recent water seepage or sand boils near the downstream toe or sidewalls of the dam.

Trans European Motorway (TEM)



Earth Dams

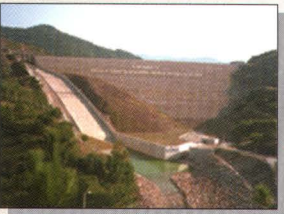




Figure 54. Locations of earth dams visited by U.S. Army Corps of Engineers representatives. *Base map courtesy of BKS Surveys Ltd., N. Ireland.*

Table 3. Descriptions of major earth dams in the epicentral area of the Kocaeli, Turkey, earthquake.

Earth dam	Height from foundation, in m	Height from river bed, in m	Crest length, in m	Reservoir area, in km ²	Reservoir volume, in km ³	Distance from fault, in km
Omerli	54	52	372	23	0.386	43
Darlik	47	45	308	5.56	0.107	45
Gokce	47	50	748	1.28	0.013	36
Kirazdere (Yuvacik)	108	102	390	1.74	0.005	4

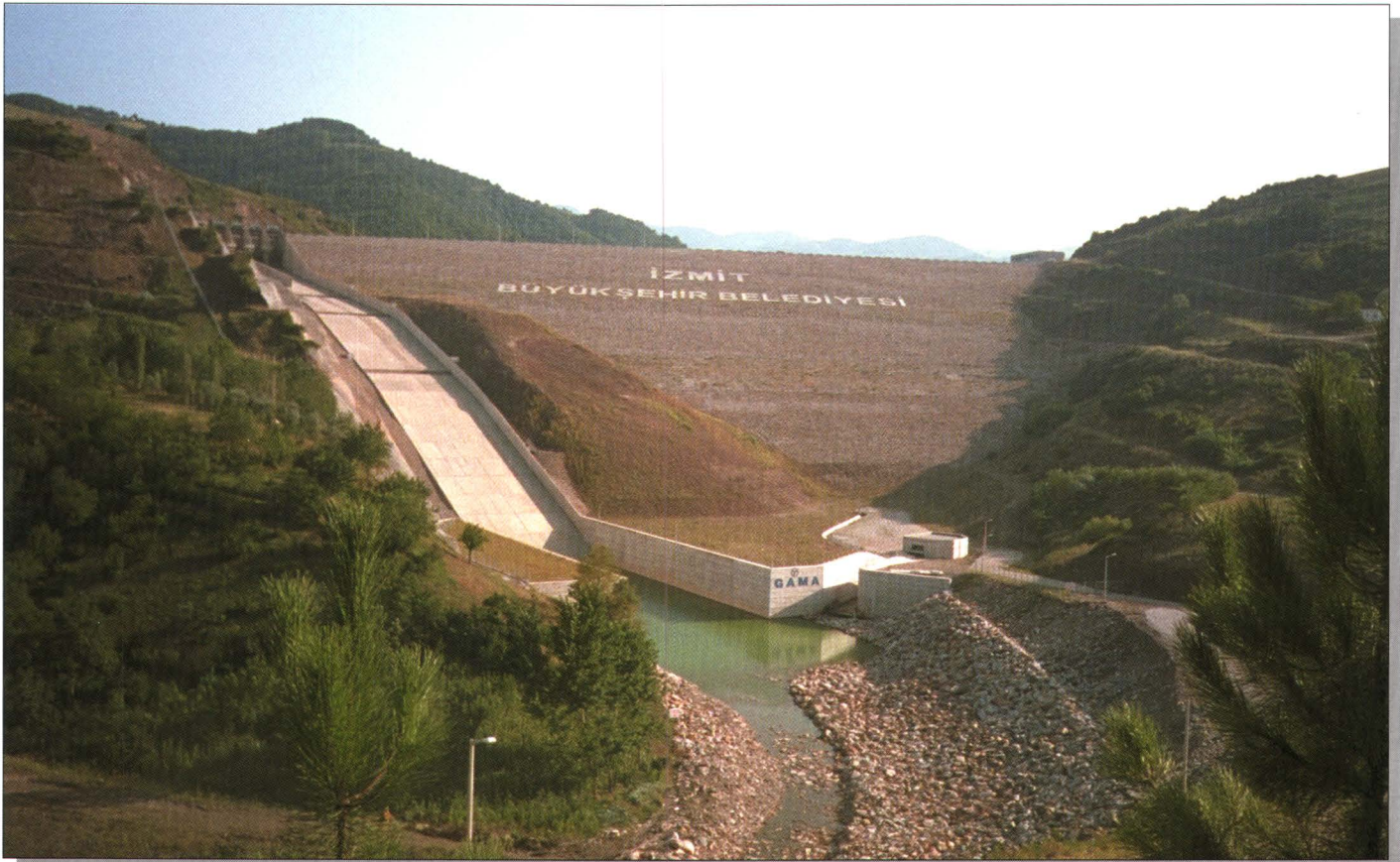


Figure 55. View of Kirazdere (Yuvacik) Dam after the Kocaeli earthquake. The dam was only about 4 km from the surface rupture and did not suffer damage. Photograph by Richard S. Olsen.

Spillway invert: The lowest point on the passage in or about a dam for the escape of surplus water.

The Gokce Dam is composed of a rock-filled shell and a clay core with upstream and downstream sand filters and is founded on bedrock. The reservoir level during the earthquake appears to be at 70 percent in terms of the spillway invert.

Gokce Dam is estimated to have experienced 0.2 g or greater of peak horizontal acceleration. The only observed effect of the earthquake on the dam was a longitudinal crack that developed along the full length of the crest. The crack was located along the upstream side of the gravel road that runs along the crest of the dam. The maximum width of the crack was 7 mm at the middle of the dam and the upstream side of the crack appears to have slightly dropped down. Fine cracks, not affecting the structure, were observed in a concrete pump station building at the dam.

The downstream face of the dam was observed to be somewhat irregular; the irregularity is on the order of 1 to 2 m. There was no evidence that this irregularity was the result of localized slumping and there were no indications of fresh soil movement such as effects on plants or exposures of soil surfaces. The exposed upstream face appears to have a more uniform appearance. There was also no evidence of recent water seepage or sand boils from piping near the downstream toe of the dam. Except for the longitudinal crack at the crest, the dam showed no effects of the earthquake shaking.



İZMİT BÜYÜKŞEHİR BELEDİYESİ

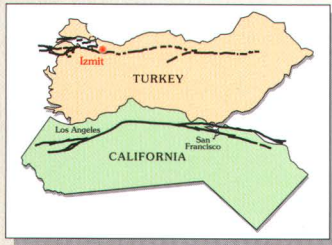
Kirazdere Dam, also known as Yuvacık Dam, is an earth-fill dam with a clay core, sand and gravel filters, and a rock shell (fig. 55). Kirazdere Dam is of particular interest because it is only 4 km from the surface rupture associated with the Kocaeli earthquake. The dam is inferred to have experienced 0.3 to 0.4 g of peak horizontal acceleration, a shaking duration of 30 s with accelerations greater than 0.05 g, and a spectral range of excitations from 0.2 to 6.0 Hz. However, the dam appears to have suffered no damage from the earthquake. The dam manager stated that a few short 2-mm-wide cracks resulted from the earthquake on the gravel road along the crest near the left abutment looking upstream, parallel to the axis of the dam. The lengths of these cracks were not measured. The road on the crest is heavily used and the cracks quickly disappeared. A few hairline cracks were seen in a one-story concrete structure at the dam. No cracks were seen in the concrete of the spillway.

Benches excavated into the left abutment, looking upstream, showed some material that had fallen away from the stepped benches and small accumulations of talus and rockfall debris. The dam manager explained that although some of this material fell during the earthquake, some was there before the earthquake. The cracks and talus on the abutment were extremely minor and the upstream and downstream faces of the

dam were straight and uniform. An underground water supply pipeline from the dam was damaged during the earthquake and was being repaired during the field visit.

The notable observation about earth dam performance during the Kocaeli earthquake is the absence of damage. No dams exhibited any damage other than cracks that opened a few millimeters. Two earth dams on bedrock that were examined experienced earthquake shaking with peak accelerations greater than 0.2 g; these were Gokce Dam where the peak acceleration was approximately 0.2 g, and Kirazdere (Yuvacık) Dam where the peak acceleration was as much as 0.4 g. The behavior of Kirazdere Dam, which is located practically at the epicenter of the Kocaeli earthquake, is of particular interest because the dam experienced a very significant (M_W 7.4) earthquake with no damage. The spectral range of the excitations was extremely broad, from 0.2 to 6.0 Hz. The duration of shaking with accelerations greater than 0.05 g was around 30 s. Gokce Dam is situated in an area of considerable damage and numerous aftershocks and may have experienced motions of at least 0.2 g or greater. The only effect of the earthquake at Gokce Dam was an explainable minor crack along the crest.

Implications for the United States



Earthquakes in urban areas offer special opportunities to evaluate the effect of shaking and secondary effects from earthquakes on the built environment. Although on average, about 19 earthquakes with magnitude greater than 7 occur annually worldwide, few of these occur in or near urban areas where substantial damage occurs to buildings and other civil works. The M_W 7.4 Kocaeli, Turkey, earthquake is one of these few earthquakes. Large earthquakes impact almost all elements of the urban environment and impact large numbers of people making it challenging to single out the most important lessons to be learned. However, some important implications for the United States can be drawn from the Kocaeli earthquake and they are outlined below.

LARGE-SCALE HUMAN DISASTER

Of all natural disasters, large magnitude earthquakes in urban areas are almost unique in their ability to cause large-scale human suffering and property loss. Only hurricanes and typhoons can compare. That the Kocaeli earthquake damaged homes and displaced a quarter of a million people illustrates the scale of the loss (fig. 56). Urban areas in the United States in which potential seismic sources have been recognized include Salt Lake City, Seattle, San Francisco Bay region, greater Los Angeles area, and greater San Diego area. Computer models, such as the Federal Emergency Management Agency HAZUS™ earthquake loss model (National Institute of Building Sciences, 1997), predict that similar tragedies are possible here in the United States. For example, these models predict that a magnitude 7.2 quake on the San Francisco Peninsula would displace more than 100,000 people from their homes while a magnitude 7.3 on the Hayward fault, which passes through Oakland, Calif., would displace about 150,000 people. A magnitude 6.6 on the northern part of the Hayward fault would probably displace more than 30,000 people.

BUILDING COLLAPSE HAZARD

The large number of collapsed buildings in Turkey was the principal cause of the large death toll in the Kocaeli earthquake. More than 20,000 buildings are estimated to have collapsed. Nearly all of these buildings, in addition to the ones that were damaged beyond repair, are made of reinforced concrete, a common construction style both in the United States and worldwide (fig. 57). Although modern engineering design of reinforced concrete buildings, particularly in areas of high seismic risk, incorporates ductility that permits new buildings to withstand the oscillatory motions imposed by earthquakes, much of the building stock in the United States was constructed before the importance of ductility was fully appreciated. In the Eastern United States most reinforced concrete structures, including both buildings and bridges, have little or no ductility. This leaves the United States vulnerable to the catastrophic collapse of large numbers of buildings and bridges when they are shaken by the oscillatory motion of large earthquakes. The collapse of the Cypress Street viaduct in Oakland, which killed 42 people during the 1989 Loma Prieta, Calif., earthquake, is a recent example in the United States of the seismic failure of a concrete structure with little or no ductility.



Figure 56. On November 16, 1999, President Clinton greets a displaced Turkish family living in a temporary tent city near Izmit since the August 17 Kocaeli earthquake. *Copyrighted photograph by J. Scott Applewhite, AP/Wide World Photos, used with permission.*

EARTHQUAKE MONITORING SYSTEMS

A belated reaction by government emergency response officials in Turkey to the earthquake disaster may have been due in part to the inability of the local seismic monitoring network to determine a reliable seismic magnitude and shaking intensities for the Kocaeli earthquake. Near real-time warnings using modern digital technology are now available and can identify precisely both the size and location of a large earthquake within minutes of its occurrence as well as the distribution of shaking

intensities. This was most recently demonstrated in Taiwan, where governmental officials were alerted within two minutes of the occurrence of the M_W 7.6 Chi-Chi earthquake of September 21, 1999. Most regional seismic networks in the United States rely on old analog technology and await modernization.





Figure 57. Street scene in Adapazari following the Kocaeli, Turkey, earthquake. Extensive damage to concrete structures with little or no ductility displaced more than a quarter of a million people from their homes in the epicentral region. *Photograph by Thomas L. Holzer.*

EARTHQUAKE FORECASTING

The details of how the ground ruptured along the North Anatolian fault will be useful in the understanding of how faults in the United States may rupture in future earthquakes. Of particular interest is where and how the surface ruptures started and stopped in relation to geometric changes in the North Anatolian fault, the amount of slip, and the length of rupture. Field studies of surface ruptures from major earthquakes permit geoscientists to better understand the faulting process and the characteristics of segmented faults. Identification of fault segments likely to rupture in an earthquake is an important step in the forecasting of both magnitude and location of future earthquakes in the United States.

The North Anatolian fault system is a close analog of the San Andreas fault system in California. Both are boundaries between tectonic plates and have similar slip rates, total length and straightness (fig. 58). The systematic westward progression of earthquakes along 1000 km of the North Anatolian fault since 1939 suggests that each of the earthquakes in the progression in Turkey has triggered the next one. It is likely that the November 12, 1999, M_w 7.1 earthquake near Düzce was triggered because it occurred in an area where stress was increased by the August 17, 1999, main shock. Understanding this process may be useful for improving probabilistic earthquake forecasts in the United States. Such forecasting is increasingly being applied to the San Andreas fault system, where recent forecasts indicate a 70 percent probability of an $M_w > 6.7$ in the San Francisco Bay region in the next 30 years. The probability of an earthquake with a magnitude greater than or equal to that of the M_w 7.4 Kocaeli earthquake is 13 percent.

PERMANENT GROUND DEFORMATION HAZARDS

While earthquake shaking typically causes more than 90 percent of the loss associated with earthquakes, permanent deformation of the ground locally can be more devastating to structures. Few structures are built to withstand large permanent ground movement. Three causes of permanent ground deformation were noteworthy in the Kocaeli earthquake: liquefaction, surface faulting, and densification of dry soil.

The buildings that sunk in Adapazari and other communities because of liquefaction demonstrate one effect of long duration shaking associated with larger magnitude earthquakes. Numerous multistory buildings in Adapazari suffered the dramatic consequence of foundation liquefaction and the resulting loss of strength. These buildings experienced massive foundation-bearing failures resulting in buildings either sinking vertically into the ground or overturning.

Liquefaction of silts observed in the city of Adapazari has important implications for earth dams founded on alluvial foundations around the world. Low-strength silt and soil mixture foundations beneath earth dams can liquefy and cause the embankment to sink or rotate into the foundation. The consequence could be large deep cracks near or through the clay core with the potential for release of the reservoir. Historically, silts have been observed to liquefy during earthquakes, however, many believed that the consequences would be less severe than where clean sands liquefied. The performance of buildings founded on weak silts in Adapazari during the Kocaeli earthquake has advanced our understanding of liquefaction effects and has shown how earth dams founded on weak silts could deform and fail. Settlement during the earthquake of properly compacted earth dams founded on rock foundations in Turkey, however, was minimal.

The bearing capacity failures associated with the sunken buildings may also be relevant to the response of levee systems in the United States when they are shaken by earthquakes. Levees typically are built in flood plains, where the soils are highly susceptible to liquefaction when shaken strongly. Levee systems along the Mississippi River in the New Madrid seismic region of the Central United States are potentially vulnerable. Liquefaction during a repeat of the 1811-12 earthquake sequence could result in widespread lowering of levees along the entire Mississippi River system. The stability of the levee system in the Sacramento-San Joaquin River delta, California is likewise threatened. This hazard compounds the existing challenge of dealing with the extensive potential for static failures of levee systems in the United States.

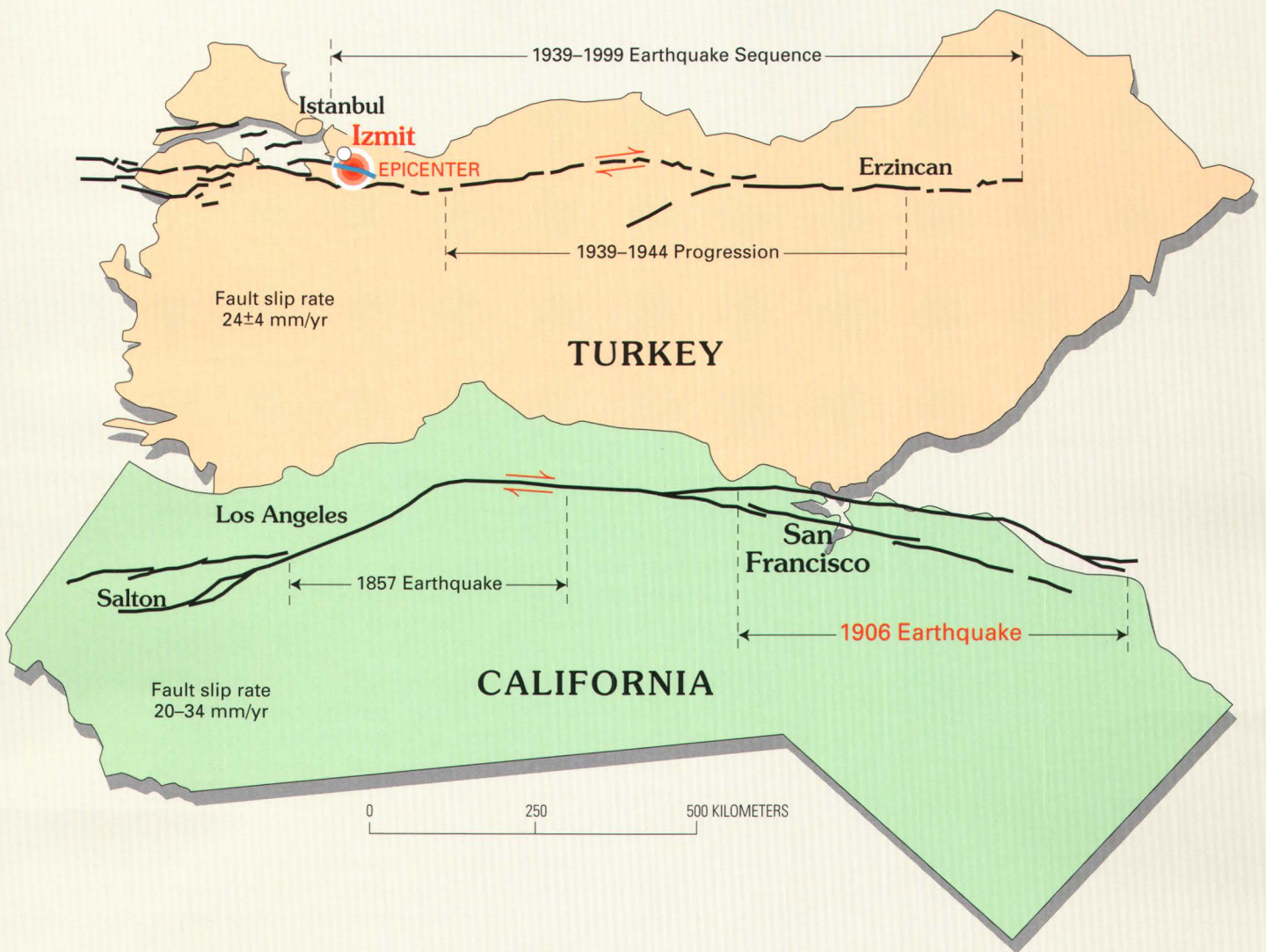


Figure 58. The striking resemblance of the San Andreas and North Anatolian fault systems is visible in this comparison. This suggests that understanding of fault mechanics from one fault system may be applied directly to the other. *Illustration prepared by Ross S. Stein.*

The 110-km-long surface fault rupture associated with the earthquake was particularly damaging because it intersected many developed regions. Although California has implemented an effective program through the Alquist-Priolo Act, which was enacted after the 1971 San Fernando, Calif., earthquake, to prevent significant new construction on active surface faults, older construction and lifelines continue to be at risk. Other parts of the country with mapped active faults have yet to regulate development on fault lines. For example, on the western front of the Wasatch Mountains in Utah, development on well known active faults is left to the option of and regulated by individual cities, which has left some populated areas at risk.

The Turkish segment of the Trans European Motorway (TEM), which was built to the standards of the American Association of State Highway and Transportation Officials (AASHTO), was seriously disrupted by permanent ground deformation. The kinds of deformation that affected the TEM, which included both faulting and densification of dry soils, are not addressed in the AASHTO code. Operation of the TEM was impacted when approaches to bridges that settled required extensive resurfacing and at one location when surface faulting through an overpass caused its collapse and temporarily halted traffic during the critical period just after the earthquake. The implications to the highway system in the United States are profound.

Acknowledgments



Kandilli Observatory and Earthquake Research Institute (KOERI) of Bogazici University in Istanbul, Turkey, was the USGS host and collaborator for the post-earthquake investigations and aftershock monitoring. We thank Professor Ahmet Mete Isikara, the Director of the Observatory, and Professor Mustafa Erdik, the Head of the Institute, for their hospitality and help, and all the researchers and graduate students who participated in our investigations, instrument deployment, and data analysis.

The USGS fault rupture investigation was coordinated through Istanbul Technical University. It received generous guidance and assistance from Professor Aykut Barka as well as Professors Serder Akyuz and Erhan Altunel of Osmangazi University.

Many people generously assisted the investigation of earth dams by the Engineer Research and Development Center of the U.S. Army Corps of Engineers. Professor Mustafa Erdik furnished strong motion instrumental data and background for understanding the earthquake processes in the region. He also provided contacts with Turkish officials for permission to visit dams. Assistance in making contacts was also provided by Ms. Juana Alsace and Ms. Mary Ann Whitten of the U.S. Consulate in Istanbul. The Operations Disaster Center at the Istanbul International Airport where many Turkish governmental agencies were represented was visited. Major Bill Pitts, U.S. Army, put the group in touch with Dr. Tanay Sidki Vyar, Technical Advisor for State Affairs of Water, Turkey, and Mr. Mehmet Duman, Istanbul Director of Foreign Relations. Meetings were arranged with Mr. Halil Tanir, head of the Water Construction Department, Istanbul Water Administration (ISKI), Mr. Cemaletti Yicher, geologist with ISKI, and Mr. Ahmet Otblu, civil engineer with ISKI. Further meetings were held with Mr. Lutfi Aydin, Director of Administration, ISKI, and Dr. Veysel Eroglu, Director General of the Istanbul Water Administration. Field visits were arranged for the dams.

The investigation of structural damage by the National Institute of Standards and Technology was assisted by the reconnaissance team of the Earthquake Engineering and Research Institute. Many individuals shared information and provided transportation and access to sites of damage in Turkey. They included Professor T. Leslie Youd (Brigham Young University), Professor Mark Ascheim (University of Illinois at Urbana/Champaign), Professor John Mander (SUNY at Buffalo), Professor Mete Sozen (Purdue University), Gayle Johnson and Peter Yanev (EQE International, Inc.), Professor Bill Mitchell (Baylor University), and Professor Emre Otay (Bogazici University).



The following people at Directorate of Highways, District 1, provided highway damage information and escorted U.S. researchers to Trans European Motorway bridge sites: Yalcin Yumrukcalli, Tarcan Atay, Dogan Akgun, Yavuz Oktay, Mesut Korukluoglu, and Unal Anakok. We especially thank Yavuz Oktay for excellent feedback to follow-up questions. Professor Kutay Ozaydin of Yildiz Technical University arranged the meeting at Directorate of Highways, District 1.

We gratefully acknowledge the following people who provided either information or assistance in the field: Gulum Birgoren, Muzaffer Gul, Mehmet Cem Ozbey, Kemal Beyen, Seref Polat, Hafez Keypour (all from KOERI), Mohammad R. Zolfaghari (Applied Insurance Research, Ltd.), Gerzel Sunal, Aynur Dikbas, Zya Cakir, M. Kaya, B. Yerli (all from Istanbul Technical University), Professor James Dolan, Ross Hartleb, Shari Christofferson, Alan Tucker (all from University of Southern California and Southern California Earthquake Center), Dr. R. Armijo, Dr. B. Meyer, Dr. J. B. de Chabaliere (all from Institut de Physique du Globe de Paris), Professor Atilla Ansal (Istanbul Technical University), Professor Polat Gulkan (Middle East Technical University, Ankara), Mr. Engin Inan and Mr. Huseyin Guler (Earthquake Research Department, Directorate for Disaster affairs, Ministry of Public Works and Settlement), Mr. Ruchan Yilmaz (Director for Directorate for Disaster affairs, Ministry of Public Works and

Settlement), Oktay Ergunay (Ministry of Public Works and Settlement), Professor Dogan Altinbilek (Director General, Public Water Works, Ankara), and Professor Cetin Yilmaz (Middle East Technical University, Ankara).

Robert D. Brown, Jr., and James W. Dewey reviewed early drafts of the circular and made many constructive suggestions. Michael J. Bennett, Joel Robinson, Selcuk Toprak, and Nancy Shock created drafts of illustrations. The base map used in figures 22 and 54 was provided courtesy of BKS Surveys Ltd., N. Ireland.

The Circular was edited by S.J. Kropschot and coordination of graphics, layout, and design was by Carol A. Quesenberry.

References



- Ambraseys, N.N., 1970, Some characteristic features of the Anatolian fault zone: *Tectonophysics*, v. 9, p. 143–165.
- Ambraseys, N.N., and Finkel, C.F., 1995, The seismicity of Turkey and adjacent areas, A historical review, 1500–1800: Istanbul, Muhittin Salih Eren, 240 p.
- Ambraseys, N.N., and Zatopec, A., 1969, The Mudurnu Valley, West Anatolia, Turkey, Earthquake of 22 July 1967: *Seismological Society of America Bulletin* v. 59, no. 2, p. 521–589.
- Armijo, R., Meyer, B., Hubert, A., and Barka, A., 1999, Westward propagation of the North Anatolian Fault into the northern Aegean—Timing and kinematics: *Geology*, v. 27, p. 267–270.
- Aydinoglu, N., trans., 1998, Specification for structures to be built in disaster areas: Ministry of Public Works and Settlement Government of Republic of Turkey, Issued on 2.9.1997, Official Gazette no.23098, effective from 1.1.1998; amended on 2.7.1998, Official Gazette no.23390.
- Barka, A., 1992, The North Anatolian fault zone: *Annales Tectonicae*, v. 6, suppl., p. 164–195.
- Barka, A., 1996, Neotectonics of the Marmara region—Selected papers on the North Anatolian fault, field trip to the North Anatolian fault, August 1–15, 1997: Istanbul, Istanbul Technical University and Eurasia Earth Science Institute, 56 p.
- Barka, A., 1999, The 17 August 1999 Izmit earthquake: *Science*, v. 285, p. 1858–1859.
- Barka, A., Akyuz, S., Altunel, E., Sunal, G., Cakir, Z., Dikbas, A., Yerli, B., Rockwell, T., Dolan, J., Dawson, T., Hartleb, R., Tucker, A., Fumal, T., Langridge, R., Stenner, H., Christofferson, S., Armijo, R., Meyer, B., and Chabaliere, J., 1999, 17 August 1999 Izmit Earthquake, Northwestern Turkey [abs.]: *Eos*, in press.
- Boore, D.M., Joyner, W.B., and Fumal, T.E., 1994, Estimation of response spectra and peak accelerations from western North American earthquakes—An interim report; Part 2: U.S. Geological Survey Open-File Report 94–127, 40 p.
- Federal Emergency Management Agency, 1998, 1997 edition, NEHRP recommended provisions for seismic regulations for new buildings and other structures, Part 1—Provisions: Washington, D.C., Building Seismic Safety Council, FEMA 302, 337 p.
- Fumal, T.E., Langridge, R.M., Stenner, H.D., Christofferson, S., Dolan, J.F., Hartleb, R., Tucker, A.Z., Rockwell, T., Dawson, T., Çakir, Z., Dikbas, A., Yerli, B., and Barka, A., 1999, Slip distribution and geometry of the Sakarya section of the 1999 Izmit earthquake ground rupture, Western Turkey [abs.]: *Eos*, in press.
- Hartleb, R., Dawson, T., Tucker, A., Dolan, J., T., Rockwell, J., Yerli, B., Dikbas, A., Çakir, Z., Gurer, T., Uslu O., and Barka, A., 1999, Surface rupture and slip distribution along the Düzce strand of the 17-August-1999 Izmit, Turkey earthquake [abs.]: *Eos*, in press.
- Ikeda, Y., Suzuki, Y., Herece, E., Saroglu, F., Isikara, A.M., and Honkura, Y., 1991, Geological evidence for the last two faulting events on the North Anatolian fault zone in the Mudurnu Valley, western Turkey: *Tectonophysics*, v. 193, p. 335–345.
- Nalbant, S.S., Hubert, A. and King, G.C.P., 1998, Stress coupling between earthquakes in northwest Turkey and the north Aegean Sea: *Journal of Geophysical Research*, v. 103, p. 24,469–24,486.
- National Institute of Building Sciences, 1997, HAZUS97—Users Manual: Washington, D.C., unnumbered pages; available from National Institute of Building Sciences, 1201 L St. NW, Suite 400, Washington, D.C., 20005.
- National Institute of Standards and Technology, 1996, The January 17, 1995 Hyogoken-Nanbu (Kobe) earthquake: National Institute of Standards and Technology Special Report 901, 538 p.

- O'Rourke, T.D., ed., *The Loma Prieta, California, earthquake of October 17, 1989—Marina district*: U. S. Geological Survey Professional Paper 1551-F, 215 p.
- Rockwell, T., Barka, A., Dawson, T., Thorup, K., and Akyuz, S., in press, Paleoseismology of the Gazikoy-Saros segment of the North Anatolia fault, northwestern Turkey—Comparison of the historical and paleoseismic records, implications of regional seismic hazard, and models of earthquake recurrence: *International Journal of Seismology*.
- Stein, R.S., Barka, A.A., and Dieterich, J.H., 1997, Progressive failure on the North Anatolian fault since 1939 by earthquake stress triggering: *Geophysical Journal International*, v. 128, p. 594–604.
- Straub, C.S., and Kahle, H., 1995, Active crustal deformation in the Marmara Sea region, NW Anatolia, inferred from GPS measurements: *Geophysical Research Letters*, v. 22, no. 18, p. 2533–2536.
- Trifunac, M.D., and Brady, A.G., 1975, A study on the duration of strong earthquake ground motion: *Seismological Society of America Bulletin* v. 65, no. 3, p. 581–626.
- U.S. Geological Survey, 1989, *Lessons learned from the Loma Prieta, California, earthquake of October 17, 1989*: U.S. Geological Survey Circular 1045, 48 p.
- U.S. Geological Survey, 1996, *USGS response to an urban earthquake*: U.S. Geological Survey Open-File Report 96-263, 78 p.
- Wood, H.O., and Neumann, F., 1931, Modified Mercalli intensity scale of 1931: *Bulletin of the Seismological Society of America*, v. 21, no. 4, p. 277–283.





Manuscript approved for publication November 22, 1999
Published in the Central Region, Denver, Colorado
Graphics coordinated by *Carol A. Quesenberry*
Design and photocomposition by *Carol A. Quesenberry*
Edited by *S.J. Kropschot*

